

ISSN = 1980-993X (Online)

<http://www.ambi-agua.net>

EDITORIAL BOARD

Editors

Getulio Teixeira Batista (Emeritus Editor) Universidade de Taubaté - UNITAU, BR

Nelson Wellausen Dias (Editor-in-Chief), Fundação Instituto Brasileiro de Geografia e Estatística - IBGE, BR

Associate Editors

Ana Aparecida da Silva Almeida

Marcelo dos Santos Targa

Universidade de Taubaté (UNITAU), BR

Universidade de Taubaté (UNITAU), BR

Editorial Commission

Andrea Giuseppe Capodaglio

Arianna Callegari

Antonio Teixeira de Matos

Apostol Tiberiu

Claudia M. dos S. Cordovil

Dar Roberts

Giordano Urbini

Gustaf Olsson

Hélio Nobile Diniz

Ignacio Morell Evangelista

János Fehér

Julio Cesar Pascale Palhares

Luis Antonio Merino

Maria Cristina Collivignarelli

Massimo Raboni

Petr Hlavínek

Richarde Marques da Silva

Stefan Stanko

Teresa Maria Reyna

Yosio Edemir Shimabukuro

Zhongliang Liu Beijing

University of Pavia, ITALY

Università degli Studi di Pavia, ITALY

Universidade Federal de Minas Gerais (UFMG), BR

University Politechnica of Bucharest, România

Centro de estudos de Engenharia Rural (CEER), Lisboa, Portugal

University of California, Santa Barbara, United States

University of Insubria, Varese, Italy

Lund University, Lund, Sweden

Inst. Geológico, Sec. do Meio Amb. do Est. de SP (IG/SMA), BR

University Jaume I- Pesticides and Water Research Institute, Spain

Debrecen University, Hungary

Embrapa Pecuária Sudeste, CPPSE, São Carlos, SP, BR

Institute of Regional Medicine, National University of the Northeast, Corrientes, Argentina

University of Pavia, Depart. of Civil Engineering and Architecture, Italy

LIUC - University "Cattaneo", School of Industrial Engineering, Italy

Brno University of Technology República Tcheca

Universidade Federal da Paraíba (UFPB), BR

Slovak Technical University in Bratislava Slovak, Eslováquia

Universidad Nacional de Córdoba, Argentina

Instituto Nacional de Pesquisas Espaciais (INPE), BR

University of Technology, China

Text Editor

Theodore D'Alessio, **FL, USA**, Maria Cristina Bean, **FL, USA**

Reference Editor

Liliane Castro, **Bibliotecária - CRB/8-6748, Taubaté, BR**

Peer-Reviewing Process

Marcelo Siqueira Targa, **UNITAU, BR**

System Analyst

Tiago dos Santos Agostinho, **UNITAU, BR**

Secretary and Communication

Luciana Gomes de Oliveira, **UNITAU, BR**

Library catalog entry by Liliane Castro CRB/8-6748

Revista Ambiente & Água - An Interdisciplinary Journal of Applied Science / Instituto de Pesquisas Ambientais em Bacias Hidrográficas. Taubaté. v. 17, n.4 (2006) - Taubaté: IPABHi, 2022. Quadrimestral (2006 – 2013), Trimestral (2014 – 2016), Bimestral (2017), Publicação Contínua a partir de Janeiro de 2018.

Resumo em português e inglês.

ISSN 1980-993X

1. Ciências ambientais. 2. Recursos hídricos. I. Instituto de Pesquisas Ambientais em Bacias Hidrográficas.

CDD - 333.705

CDU - (03)556.18

TABLE OF CONTENTS

COVER:

This series of maps shows the enrichment, geoaccumulation, potential ecological risk, and distribution of metals results in the Aguada Blanca Reservoir in southern Peru. This reservoir is the main source of drinking water for more than one million people in the city of Arequipa. It can be observed that most of the elements present an increase in their concentrations as they approach the reservoir outlet, which could indicate water quality problems due to inappropriate sediment removal in the last 30 years. Source: ESPIRILLA, A.T. *et al.* Distribution and assessment of the environmental risk of heavy metals in Aguada Blanca reservoir, Peru. *Rev. Ambient. Água, Taubaté*, vol. 17 n. 4, p. 1-16, 2022. [doi:10.4136/ambi-agua.2838](https://doi.org/10.4136/ambi-agua.2838)

ARTICLES

01	Effect of humic acid on the growth of seedling tomato (<i>Solanum lycopersicum</i>) and melon <i>Cucumis melo</i>) doi:10.4136/ambi-agua.2808 Arnulfo Antonio Tarón Dunoyer; Fredy Colpas Castillo; Jairo Mercado Camargo Andrade	1-11
02	Investigation of new natural coagulant - cationic hemicellulose associated with cationic tannin - for coagulation/dissolved air flotation (C/DAF) in the treatment of industrial effluent doi:10.4136/ambi-agua.2824 Ana Gabriela Tomé Alves; Ingrid da Silva Pacheco; Amanda Bessa Freitas; Elaine Angélica Mundim Ribeiro; Sheila Cristina Canobre; Fábio Augusto do Amaral	1-17
03	Panorama of the water supply in the Campinas region and a brief comparison with other regions in the Southeast of Brazil doi:10.4136/ambi-agua.2835 Maria Isabel Andrekowisk Fioravanti; Paulo Henrique Leutevilier Pereira; Laila Martins Camargo; Gleize Villela; Elaine Marra de Azevedo Mazon	1-10
04	Distribution and assessment of the environmental risk of heavy metals in Aguada Blanca reservoir, Peru doi:10.4136/ambi-agua.2838 Alfonso Torres Espirilla; Trinidad Betty Paredes de Gómez	1-16
05	Water scarcity footprint of cocoa irrigation in Bahia doi:10.4136/ambi-agua.2840 Kelly Félix Olegário; Edilene Pereira Andrade; Ana Paula Coelho Sampaio; Joan Sanchez Matos; Maria Cléa Brito de Figueirêdo; José Adolfo de Almeida Neto	1-9
06	Analyzing the impact of agricultural water-demand management on water availability in the Urubu River basin – Tocantins, Brazil doi:10.4136/ambi-agua.2847 Nicole John Volken; Ricardo Tezini Minoti; Conceição Maria de Albuquerque Alves; Fernán Enrique Vergara	1-23



Effect of humic acid on the growth of seedling tomato (*Solanum lycopersicum*) and melon *Cucumis melo*)

ARTICLES doi:10.4136/ambi-agua.2808

Received: 25 Oct. 2021; Accepted: 02 May. 2022

Arnulfo Antonio Tarón Dunoyer^{1*}; Fredy Colpas Castillo²
Jairo Mercado Camargo²

¹Faculty of University of Cartagena. Avenue Del Consulado, Calle 30 # 48-152, 130011, Cartagena, Colombia

²Exact and Natural Sciences Faculty. Chemistry program. University of Cartagena, Street 50, n° 24120, 130014, Zaragocilla, Cartagena, Colombia. E-mail: fcolpasc1@unicartagena.edu.co, jmercadoc@unicartagena.edu.co

*Corresponding author. E-mail: atarond@unicartagena.edu.co

ABSTRACT

This study evaluated the effect of HS extracted from mineral coal on the growth of tomato (*Solanum lycopersicum*) and melon (*Cucumis melo*) plants to determine the role that humic substances (HS) play as promoters of plant growth. Three concentrations of HS were evaluated in 200 grams of soil. The fertilizer (urea 0.3%) and humic acid in concentrations of 0.05%, 0.1%, and 0.2% were added directly and at the same time to the amount of soil, using a control sample without the addition of humic acid. Increase measurements were made at three-day intervals up to 45 days. Plants treated with high concentrations of HS demonstrated a significant increase in roots ($p > 0.05$). In both plants, the concentration of 0.2% in HS showed the greatest increase in growth, with the melon plant showing the greatest variation as time passed, with its highest peak in 36 days (13.1 ± 0.05 cm) of the experiment, while in the tomato plant the maximum growth occurred in 30 days (9.2 ± 0.01 cm). The Dunnett test showed that there was no statistically significant difference between the control and the concentrations of 0.05% and 0.1% ($p > 0.05$), while among the control and the soil sample with a concentration of 0.2% there was a statistically significant difference ($p < 0.05$). The results show a notable influence of humic acid on the growth of the studied plants, especially at high concentrations.

Keywords: fertilizer, horticulture, humic acid, soils.

Efeito do ácido húmico no crescimento de mudas de tomate (*Solanum lycopersicum*) e melão (*Cucumis melo*)

RESUMO

Para determinar o papel que as substâncias húmicas (HS) desempenham como promotores do crescimento vegetal, foi avaliado o efeito do HS extraído do carvão mineral no crescimento de plantas de tomate (*Solanum lycopersicum*) e melão (*Cucumis melo*). Três concentrações de HS foram avaliadas em 200 gramas de solo. O fertilizante (uréia 0,3%) e ácido húmico nas concentrações de 0,05%, 0,1% e 0,2% foram adicionados diretamente e ao mesmo tempo na quantidade de solo, utilizando uma amostra controle sem adição de ácido húmico. As medições de aumento foram feitas em intervalos de três dias até 45 dias. Plantas tratadas com altas concentrações de HS demonstraram um aumento significativo nas raízes ($p > 0,05$). Em ambas



as plantas, a concentração de 0,2% no HS apresentou o maior aumento de crescimento, com o melão apresentando a maior variação com o passar do tempo, com seu maior pico nos 36 dias ($13,1 \pm 0,05\text{cm}$) do experimento, enquanto no no tomateiro o máximo crescimento ocorreu em 30 dias ($9,2 \pm 0,01\text{ cm}$). O teste de Dunnett mostrou que não houve diferença estatisticamente significativa entre o controle e as concentrações de 0,05% e 0,1% ($p > 0,05$), enquanto entre o controle e a amostra de solo com concentração de 0,2% houve diferença estatisticamente significativa ($p < 0,05$). Os resultados obtidos mostram uma notável influência do ácido húmico no crescimento das plantas estudadas, principalmente em altas concentrações.

Palavras-chave: ácido húmico, fertilizante, horticultura, solos.

1. INTRODUCTION

Humification is the chemical and microbiological process that transforms the dead remains into humic substances. It is the second-most extensive process on earth after photosynthesis, involving from 20 to 75 gigatons of carbon each year (Bacilio *et al.*, 2017; Marschner *et al.*, 2008). Humic substances are found in soils, sediments and natural waters like rivers, lakes and oceans (Wu *et al.*, 2017)

They also represent a large proportion of the organic matter in peat swamps, carbonaceous shales, dark coals (lignites), and sewage. Humic materials contribute to the yellow and brown colors of leaf litter and composts, the dark brown or black colors of topsoil, and when in high concentrations, the brown stain in freshwater creeks and lakes (Khorasaninejad *et al.*, 2018). They have even been detected on the Antarctic continent. The understanding of humic substances and the way they work are both substantially more sophisticated than the basic knowledge of fertilizers. Generally, humic substances are considered as a series of relatively high-molecular-weight, brown to black colored substances formed by secondary synthesis reactions. The term is employed as a generic name to describe the colored material or its fractions obtained based on solubility characteristics (Kipton *et al.*, 1992).

The fraction called humic acid is not soluble in water under acidic conditions ($\text{pH} < 2$) but is soluble at higher pH values (Morozesk *et al.*, 2017). Many experts currently believe that all dark-colored humic substances are part of a system of closely related but not completely identical, high-molecular-weight polymers. According to this concept, differences between humic and fulvic acids can be explained by variations in molecular weight, the number of functional groups (carboxyl, phenolic OH), and the extent of polymerization. Among the humic substances are the humic acids, which are formed by nuclei of aromatic and polyaromatic compounds. Humic acids have different functional groups in their structure that give them the capacity to exercise various functions in the soil-plant relationship (Pantoja *et al.*, 2016; Canellas *et al.*, 2010).

These substances are formed by the decomposition of plant and animal material deposited in the soil (Wu *et al.*, 2017; Maji *et al.*, 2017). The organic matter is initially degraded, then depolymerized, and finally by the action of microorganisms produces new components with a high degree of dark-colored polymerization (Canellas and Olivares, 2014). Humic substances (HS) can cause changes in the root and architecture and can increase dynamics, which result in a larger root size, better branching, and/or a higher density of root hair with a greater surface area, for this reason, they have been widely recognized as promoters of plant growth (Brown *et al.*, 2013).

The study of Trevis *et al.* (2010) found that humic substances (SH) stimulate the growth of the stem, root, leaves, fresh, and dry mass, size, and quality of the fruits; as well as crop yields. In support of this, a previous study showed that the dry mass of herbaceous plant shoots and roots increased by about 22% in response to the exogenous application of humic and fulvic

acid (Rose *et al.*, 2014). Humic compounds such as humic acid and fulvic acid have been shown to stimulate plant growth in terms of increasing plant height and dry or fresh weight as well as enhancing nutrient uptake (Felle, 2002). These effects seem to depend on the concentration and source of the substance and the plant species (Quaggiotti *et al.*, 2004).

Humic substances are classified depending on the separation process used; among the major components of humus are acids soluble in the acid medium, known as fulvic acids (AF), and insoluble in acid medium, called humic acids (AH) (Canellas *et al.*, 2015). In many studies, humic and fulvic acid preparations were reported to increase the uptake of mineral elements. Due to the positive effect of humic substances on the visible growth of plants, these chemicals have been widely used by growers instead of other substances such as pesticides, etc. This, however, has led to growers using higher amounts of these substances. The carboxylic, phenolic, carbonyl, methoxide, and aliphatic groups present in the structure of the humic substances make this a highly complex structural matrix, which has uniformity in each of its units, conformed by condensed aromatic rings containing carboxylic groups (Gomes De Melo *et al.*, 2016).

It is estimated that approximately a quarter of the molecular weight of the humic substances is due to the oxygenated groups, mainly carboxylic groups that increase with the degree of humification of the organic matter and that can form carboxylates with metals present in the medium, phenolic groups that they form in the initial stages of humification and carbonyls groups that by oxidation reactions form carboxylic groups (Fischer, 2017; Gomes De Melo *et al.*, 2016; Cantero *et al.*, 2015; Pédrot and Mélanie, 2010). Humic substances play a very important role in nature; this is due to their present oxygenated functional groups, and they can participate in cation retention processes that are essential for plants as well as retaining heat on the surface due to their dark color (Pédrot and Mélanie, 2010). These substances can be used as fertilizers, given their ability to retain metals useful for agriculture; they can also be used in the removal of toxic substances in aqueous effluents (Nardi *et al.*, 2016; Sun *et al.*, 2015; Tang *et al.*, 2014; Kalina *et al.*, 2013).

A significant source of humic substances in the low range carbons, which have a high content of oxygenated groups and a part of their structure quite similar to that of humic acids (Motta and Santana, 2013). This allows being able to perform the extraction with alkaline solutions of the humic material of this type of coal. Moderate oxidation reactions in mineral carbons may increase the content of humic substances in their structure, which also leads to higher percentages of extraction of this type of materials (Zhiyuan *et al.*, 2012).

This research assessed the effect of humic acid obtained from low-grade coal from the Montelíbano mine (Córdoba-Colombia) on tomato and melon plants grown in low-fertility soils.

2. MATERIAL AND METHODS

2.1. Mineral material

In this research, low-grade coal from the mine located in the rural area of Montelíbano (7°58'45.0" N -75°25'12.7" W) in the department of Córdoba-Colombia is used as the starting mineral material. All the experiments were carried out at the facilities of the Faculty of Engineering, Food Engineering Program of the University of Cartagena.

2.2. Preparation of the carbon sample

The sample was first crushed and sieved to a particle size between 3.1 and 7.1 mm through a sieve with a mesh number of 6. A portion of 100 g of the material was demineralized for 1 hour at room temperature with hydrochloric acid 0.5 M. Before the oxidation process, the mineral starting sample was subjected to a debitumization process using an ethanol-benzene mixture (1:1 v/v) at reflux for 24 hours. The solvent was removed by distillation in Soxhlet and

vacuum filtration with distilled water. The remaining moisture was removed by drying at 80°C for 12 hours (Anillo *et al.*, 2013). Subsequently, oxidation was carried out in an aqueous medium with 30% hydrogen peroxide and concentrated acetic acid. This system was heated to a temperature of 60°C with continuous agitation for a space of 12 hours (Anillo *et al.*, 2013).

2.3. Production of the humic acid

A volume of 100 mL of 0.1 M NaOH was added to 5 g of oxidized carbon; this system was maintained at 60°C for 1 h in continuous agitation. The resulting solution was filtered under vacuum and then 100 mL of 0.1 M HCl was added. This system was kept at rest for 24h and was subsequently centrifuged at 3600 rpm for 10 minutes. The colloid obtained after the centrifugation was washed with ethanol and heated to a temperature of 100°C for one hour and subsequently analyzed. The percentage of humic acids extracted was quantified to the mass of extracted acids obtained from the initial weight of the oxidized carbon samples (Anillo *et al.*, 2013).

2.4. Soil strengthening

The soils were fortified with humic acid and urea. Two hundred g of soil was added directly to fertilizer and humic acid at a concentration of 0.05%, 0.1%, and 0.2% directly concerning the amount of soil, using a sample control, containing urea (0.3%) as fertilizer, without the addition of humic acid. The amount of irrigation water for the tomato seedlings was 1 to 1.5 L/day by sprinkling and for the melon it was 3 liters with 4 irrigations per week, which was done by drip irrigation, taking into account a good distribution of irrigation throughout the crop cycle, avoiding subjecting the crop to deficiencies or excess of water. The soils were enriched with nitrogen, phosphorus, potassium, magnesium and calcium.

2.5. Agronomic management

The tomato and melon seeds were supplied by farmers in the northern part of the department of Bolivar, Colombia. They were grayish in color, flattened oval in shape, and ranged in size from 2-6 mm in diameter and 2 mm in length. In the case of melon, these seeds were white to brown to orange-yellowish, smooth morphology with some flattening, elongated, small and pointed at one end, with a dimension of ¼ to ¾ inch long.

The seeds were sown uniformly in an open space. The temperature during the seedling growth period was between 26 (minimum) and 31°C (maximum), with an average relative humidity of 80%. The soil pH range for tomato seedling development was 5.9 to 6.5 and for melon seedlings between 6 and 7.

2.6. Experimental design

In this research, a unifactorial experimental design was used, complemented at random with three repetitions, where the tomato (*Solanum lycopersicum*) plants and melon (*Cucumis melo*) seeds were planted in the strengthened soils and the control. After the first day of planting, a growth measurement was made at a time interval of 3 days to complete a total of 45 days. All soil samples were hydrated by irrigation.

2.7. Statistical analysis

The results were statistically analyzed, taking as a response variable the measure of plant growth. The analyses included one-way ANOVA (unidirectional), using measurements of the growth of the plants to determine statistically significant differences ($P < 0.05$) between the samples. The multiple comparison tests of Dunnett were used with the purpose of making comparisons of plant growth in the presence of humic acid and the control, in this case, urea, at a confidence level of 95%.

3. RESULTS AND DISCUSSION

The growth of tomato and melon plants was significantly influenced by each of the different concentrations of humic acids in the fertilizer medium. The tomato plant presented a similar behavior in a study carried out by Rodríguez (2019, reported by Cantero *et al.*, 2015). Various studies demonstrate the importance of the use of bioactive substances. For example, humic substances can directly affect the metabolism of plants by exerting an influence on the transport of ions, facilitating their absorption, increasing respiration and the speed of enzymatic reactions. This leads to greater energy production, increases the chlorophyll content, increases the synthesis of nucleic acids, the selective effect on protein synthesis and the increase or inhibition of various enzymes, resulting in a positive effect on plant growth (Reyes-Pérez *et al.*, 2020; Shah *et al.*, 2018; You *et al.*, 2018).

These structures are capable of chelating metals, being able to influence the physico-chemical structure of the protoplasm of plants, thereby increasing the permeability of plant membranes, which increases plants' assimilation of nitrogen, phosphorus, potassium and other microelements present in the soil.

3.1. Tomato plant growth behavior

Current evidence suggests that the biostimulant effects of humic substances are characterized by both structural and physiological changes in roots and shoots related to absorption, assimilation and distribution of nutrients (efficiency traits in the use of nutrients). In addition, they can induce changes in the primary and secondary metabolism in the tomato plant related to tolerance to abiotic stress that participates in the modulation of plant growth (Canellas *et al.*, 2015).

Figure 1 shows the growth of the tomato plants (*Solanum lycopersicum*) versus the concentration of humic acid in the soil, with the concentration of 0.2% showing a considerable increase in the growth of the plant compared to the control and the other two concentrations (average growth of 6.88 ± 2.99 cm).

The analysis of ANOVA shows that at the concentration of 0.2% the statistically significant difference with the control is evidenced ($p < 0.05$), while at the concentrations of 0.05% and 0.1% with the control there is no significant difference ($p > 0.05$).

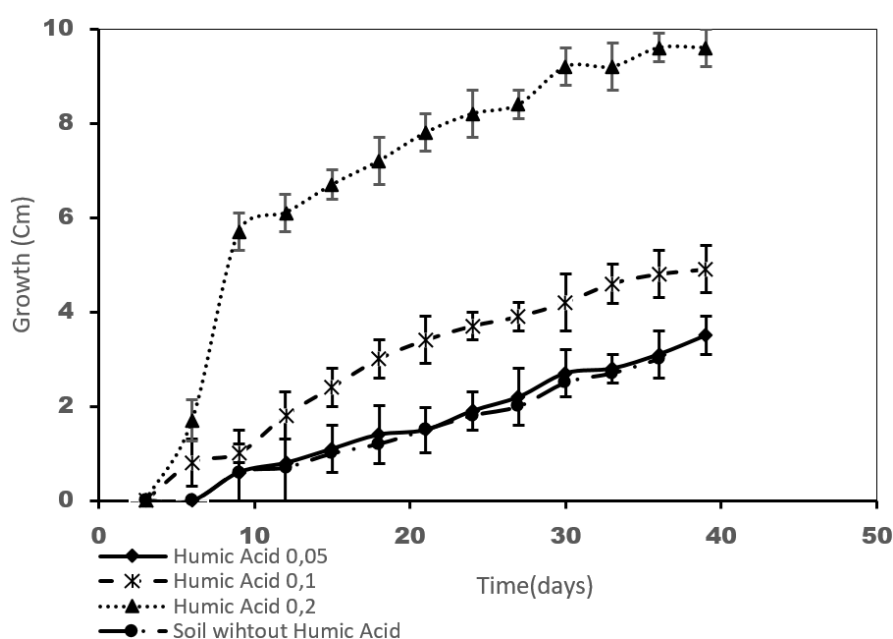


Figure 1. Growth rate of *Solanum lycopersicum* (tomato) using different concentrations of humic acid.

This growth can be noticed as the days passed, with an increase in plant growth appearing on Day 9 (Table 1). Figure 3a shows the growth of the plant at the 0.05% concentration is very similar to the control plants (mean growth of 1.66 ± 1.15 cm and 1.41 ± 1.01 cm, respectively); while the concentration of 0.1% at 12 days begins a significant growth compared to the control at the concentration of 0.05%. However, as shown in Figure 3a, at the humic acid concentration of 0.2%, abrupt growth of the plant occurs 9 days after sowing, causing a large, statistically significant difference between the control and the other concentrations (Colpas *et al.*, 2018).

According to the results, the tomato plant presents growth dependent on the concentration of humic acid, reaching a maximum peak (9.20 ± 0.01 cm) on Day 30 and then attaining a steady state.

Table 1. Tomatoes (*Solanum lycopersicum*) grown in soils fertilized with urea and different concentrations of humic acid.

Days of growth	Soils fertilized with urea and fortified with humic acid (%)			
	0.05%	0.1%	0.2%	Control
3	-	-	-	-
6	-	0.8 ± 0.02^a	1.7 ± 0.04^c	-
9	0.6 ± 0.019^a	1.0 ± 0.02^b	5.7 ± 0.02^c	0.6 ± 0.06^a
12	0.8 ± 0.019^a	1.8 ± 0.03^b	6.1 ± 0.08^c	0.7 ± 0.02^a
15	1.1 ± 0.015^a	2.4 ± 0.01^b	6.7 ± 0.21^c	1.0 ± 0.01^a
18	1.4 ± 0.022^a	3.0 ± 0.02^b	7.2 ± 0.01^c	1.2 ± 0.02^b
21	1.5 ± 0.018^a	3.4 ± 0.01^b	7.8 ± 0.03^c	1.5 ± 0.05^a
24	1.9 ± 0.030^a	3.7 ± 0.03^b	8.2 ± 0.02^c	1.8 ± 0.03^a
27	2.2 ± 0.023^a	3.9 ± 0.05^b	8.4 ± 0.02^c	2.0 ± 0.03^d
30	2.7 ± 0.005^a	4.2 ± 0.03^b	9.2 ± 0.01^c	2.5 ± 0.01^d
33	2.8 ± 0.027^a	4.6 ± 0.11^b	9.2 ± 0.03^c	2.7 ± 0.01^a
36	3.1 ± 0.009^a	4.8 ± 0.01^b	9.6 ± 0.01^c	3.0 ± 0.01^a
39	3.5 ± 0.002^a	4.9 ± 0.01^a	9.6 ± 0.03^c	-
42	-	-	-	-
45	-	-	-	-

Different letters in the same row differ significantly ($p < 0.05$). The values represent the mean \pm S.E. ($n = 3$). The growth of the plant is expressed in centimeters (Cm). The - denotes absence of growth.

3.2. Melon plant growth behavior

Initial concentrations of 0.05 and 0.1% are similar to the control only at 18 days (Figure 2), corroborated with the Dunnett multiple comparison test, where no statistically significant differences are found between these concentrations and the control (Figure 3b). At a concentration of 0.2 as shown, there are differences in the control. It is interesting to note that the growth of the melon plant at a concentration of 0.2% increases as time goes on, observing an almost exponential growth starting on the ninth day, reaching a maximum length on Day 36 (average of 8.04 ± 4.08 cm), where a slight steady state is noticeable (Table 2).

The variance analysis shows that there is a statistically significant difference ($p < 0.05$) as the concentration of humic acid increases. Thus, favoring the growth of the melon. The Dunnett test shows that there is a statistically significant difference between the control and the 0.2% concentration. It can be highlighted that the growth of the melon plant is favored when the

humic acid concentrations increase in the soil. While at low concentrations, this growth is similar when this plant grows in soil without humic acid. The results of the humic acid (HS) application test show that all treatments cause significant increases in the total surface area of roots. The increase in leaf area and total root surface caused by treatments with different types of humic acid contributes to the hypothesis of a biostimulant action in plant development (Nebbioso and Piccolo. 2012). Numerous studies have been conducted on the effects of humic substances and commercial humic products on the growth and yield of plants. The reviewed articles demonstrated a positive response to germination and seedling growth, root initiation and shoot growth and development to a variety of humic extracts from a variety of sources.

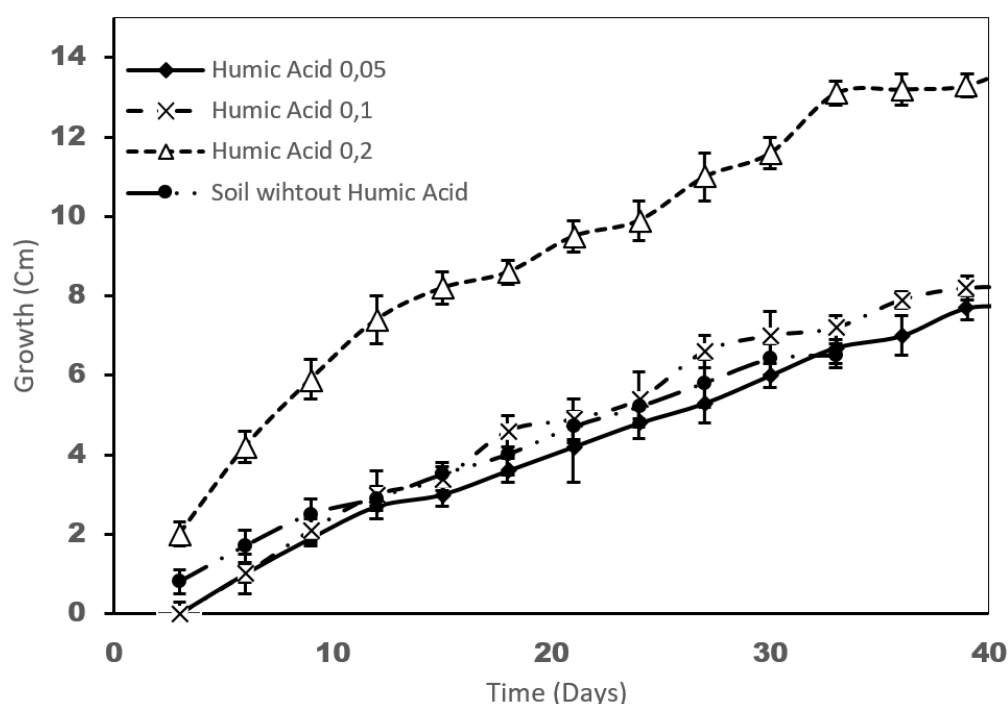


Figure 2. Growth rate of *Cucumis melo* (melon) using different concentrations of humic acid.

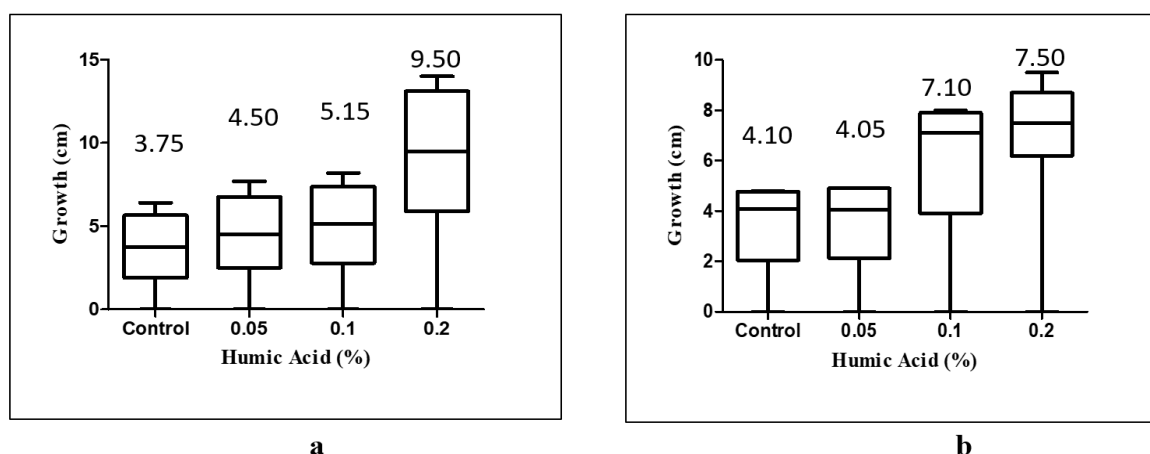


Figure 3. Growth variations in the presence of different concentrations of humic acids compared to the control (without humic acid). a) *Solanum lycopersicum* (tomato) and b) *Cucumis melo* (melon).

Table 2. Melon plant growth (*Cucumis melo*) cultivated in soils fertilized with urea and different concentrations of humic acid.

Days of growth	Soils fertilized with urea and fortified with humic acid (%)			
	0.05%	0.1%	0.2%	Control
3	-	-	-	-
6	1.0 ± 0.01 ^a	1.0 ± 0.03 ^b	2.0 ± 0.03 ^c	0.8 ± 0.01 ^d
9	1.9 ± 0.05 ^a	2.1 ± 0.02 ^b	4.2 ± 0.01 ^c	1.7 ± 0.01 ^d
12	2.7 ± 0.02 ^a	3.0 ± 0.03 ^b	5.9 ± 0.01 ^c	2.5 ± 0.04 ^d
15	3.0 ± 0.03 ^a	3.4 ± 0.06 ^b	7.4 ± 0.06 ^c	2.9 ± 0.03 ^a
18	3.6 ± 0.03 ^a	4.6 ± 0.01 ^b	8.2 ± 0.04 ^c	3.5 ± 0.03 ^a
21	4.2 ± 0.09 ^a	4.9 ± 0.11 ^b	8.6 ± 0.01 ^c	4.0 ± 0.01 ^d
24	4.8 ± 0.01 ^a	5.4 ± 0.07 ^b	9.5 ± 0.02 ^c	4.7 ± 0.01 ^a
27	5.3 ± 0.05 ^a	6.6 ± 0.04 ^b	9.9 ± 0.01 ^c	5.2 ± 0.10 ^a
30	6.0 ± 0.03 ^a	7.0 ± 0.06 ^b	11.0 ± 0.10 ^c	5.8 ± 0.06 ^d
33	6.7 ± 0.01 ^a	7.2 ± 0.01 ^b	11.6 ± 0.17 ^c	6.4 ± 0.04 ^d
36	7.0 ± 0.01 ^a	7.9 ± 0.02 ^b	13.1 ± 0.01 ^c	6.5 ± 0.03 ^d
39	7.7 ± 0.01 ^a	8.2 ± 0.03 ^b	13.2 ± 0.01 ^c	-
42	7.7 ± 0.01 ^a	8.2 ± 0.03 ^b	13.3 ± 0.10 ^c	-
45	-	-	14.0 ± 0.01	-

Different letters in the same row differ significantly ($p < 0.05$). The values represent the mean \pm S.E. ($n = 3$). The growth of the plant is expressed in centimeters (Cm). The - denotes absence of growth.

Water absorption, respiration and germination were increased in a variety of seeds including winter wheat, maize and barley. The germination rate responded to the humic treatments but not to the percentage of viable seeds (Nardi *et al.*, 2016). There were positive responses from the treatment with humic products for tomatoes, cotton, grapes and sweet potatoes. Many authors have suggested mechanisms by which humic products could stimulate the growth of plants. The possibility of improving the availability and absorption of nutrients.

Metal chelation, increased water efficiency, improved permeability of the cell membrane, antioxidant and hormone-like effects and improved microbial metabolism were discussed (Arancon *et al.*, 2006).

The mechanism by which humic substances could promote the growth of plants is through the induction of the activity of H^+ -ATPase, promoting the transport of secondary ions and the absorption of other nutrients. These channels facilitate the transport of nitrates through an electrochemical gradient of protons that induce the activity of this enzyme, the humic acid, when in contact with the cellular reticular cells (Sloboda *et al.*, 2017)

Humic substances promote plant growth through the acid growth of the root by proton increase, using the H^+ -ATPase, pumping the apoplast, acidifying the cell wall, making it more flexible, which facilitates root elongation (Canellas and Olivares, 2014; Canellas *et al.*, 2015; Gomes De Melo *et al.*, 2016).

4. CONCLUSIONS

Humic acids stimulate growth in tomato (*Solanum lycopersicum*) and melon (*Cucumis melo*) plants. Considerable changes occur in the morphology of the plant. In the melon plant, growth is well known when the concentration of humic acid is increased above 0.1%, which did not happen with the tomato plants due to the lower increase at low concentrations, although higher concentrations of humic acid ($>0.1\%$) accentuated the growth curve when compared against the control. This type of research can assist in the understanding of how humic

substances influence plant biology and aid in the development of new technologies to increase the growth of plants based on humic material.

5. REFERENCES

- ANILLO, R.; COLPAS, F.; MEZA, E. Increase in the content of humic acids in a low-range carbon through oxidation with air and with hydrogen peroxide or nitric acid. **Química Nova**, v. 36, n. 3. p. 387-392, 2013. <https://doi.org/0.1590/S0100-40422013000300007>
- ARANCON, N.; EDWARDS, C.; ROBERT, S. Effects of humic acids from vermicomposts on plant growth. **European Journal of Soil Biology**, v. 42, n. 1, p. 65-69, 2006. <https://doi.org/10.1016/j.ejsobi.2006.06.004>
- BACILIO, M.; MORENO, M.; LOPEZ-AGUILAR, R.; BASHANA, Y. Scaling from the growth chamber to the greenhouse to the field: Demonstration of diminishing effects of mitigation of salinity in peppers inoculated with plant growth-promoting bacterium and humic acids. **Applied Soil Ecology**, v. 119, p. 327-338, 2017. <https://doi.org/10.1016/j.apsoil.2017.07.002>
- BROWN, L. K.; GEORGE, T. S.; DUPUY, L. X.; WHITE, P. J. A conceptual model of root hair ideotypes for future agriculture environments: what combination of traits should be targeted to cope with limited P availability? **Annals of Botany**, v. 112, p. 17-330, 2013. <https://doi.org/10.1093/aob/mcs231>
- CANELLAS, L. P.; OLIVARES, F. L.; AGUILAR, N. O.; JONES, D. L.; NEBBIOSO, A.; MAZZEI, P. *et al.* Humic and fulvic acids as biostimulants in horticulture. **Scientia Horticulturae**, n. 196, p. 15-27, 2015. <https://doi.org/10.1016/j.scienta.2015.09.013>
- CANELLAS, L. P.; PICCOLO, A.; DOBBSS, L. B.; SPACCINI, R.; OLIVARES, F. L.; ZANDONADI, D. B. *et al.* Chemical composition and bioactivity properties of size-fractions separated from a vermicompost humic acid. **Chemosphere**, v. 78, n. 4, p. 457-466, 2010. <https://doi.org/10.1016/j.chemosphere.2009.10.018>
- CANELLAS, L. P.; OLIVARES, F. L. Physiological responses to humic substances as plant growth promoter. **Chemical and Biological Technologies in Agriculture**, v. 1, n. 1, p. 1-11, 2014. <https://doi.org/10.1186/2196-5641-1-3>
- CANTERO, J.; ESPITIA, L.; CARDONA, C.; VERGARA, C.; ARAMÉNDIZ, H. Efectos del compost y lombriabono sobre el crecimiento y rendimiento de berenjena *Solanum melongena* L. **Revista de Ciências Agrícolas**, v. 32, n. 2, p. 56-67, 2015. <https://doi.org/10.22267/rcia.153202.13>
- COLPAS, F.; TARÓN, A.; MERCADO, J. Agricultural soils strengthening employing humic acids and its effect on plant growth chili pepper and eggplant. **Emirates Journal of Food and Agriculture**, v. 30, n. 11, p. 941-945, 2018. <https://doi.org/10.9755/ejfa.2018.v30.i11.1845>
- FELLE, H. pH as a signal and regulator of membrane transport. In: RENGEL, Z. (ed.). **Handbook of Plant Growth pH as the Master Variable**. New York: Marcel Dekker, 2002. p. 118-14.
- FISCHER, T. Humic supramolecular structures have polar surfaces and unpolar cores in native soil. **Chemosphere**, v. 183, p. 437-443, 2017. <https://doi.org/10.1016/j.chemosphere.2017.05.125>

- GOMES de MELO, B.; LOPES, L.; ANDRADE, M. Humic acids: Structural properties and multiple functionalities for novel technological developments. **Materials Science & Engineering**, v. 62, n. 1, p. 967-974, 2016. <https://doi.org/10.1016/j.msec.2015.12.001>
- KALINA, M.; KLUČÁKOVÁ, M.; SEDLÁČEK, P. Utilization of fractional extraction for characterization of the interactions between humic acids and metals. **Geoderma**, v. 207-208, n. 1, p. 92-98, 2013. <https://doi.org/10.1016/j.geoderma.2013.04.031>
- KHORASANINEJAD, S.; AHMADABADI, A.; HEMMATI, H. The effect of humic acid on leaf morphophysiological and phytochemical properties of *Echinacea purpurea* L. under water deficit stress. **Scientia Horticulturae**, v. 239, p. 314-323, 2018. <https://doi.org/10.1016/j.scienta.2018.03.015>
- KIPTON, H.; POWELL, J.; TOWN, R. Solubility and fractionation of humic acid; effect of pH and ionic medium. **Analytica Chimica Acta**, v. 267, n. 1, p. 47-54, 1992. [https://doi.org/10.1016/0003-2670\(92\)85005-Q](https://doi.org/10.1016/0003-2670(92)85005-Q)
- MOROZESK, M.; MARQUES, M.; DA COSTA SOUZA, I.; DORSCH, L.; DRUMOND, I.; OLIVEIRA, I. *et al.* Effects of humic acids from landfill leachate on plants: An integrated approach using chemical, biochemical and cytogenetic analysis. **Chemosphere**, v. 184, p. 309-317, 2017. <https://doi.org/10.1016/j.chemosphere.2017.06.007>
- MOTTA, F.; SANTANA, M. Production of humic acids from oil palm empty fruit bunch by submerged fermentation with *Trichoderma viride*: Cellulosic substrates and nitrogen sources. **Biotechnology Progress**, v. 29, p. 31-637, 2013. <https://doi.org/10.1002/btpr.1715>
- MAJI, D.; MISRA, P.; SINGH, S.; KALRA, A. Humic acid rich vermicompost promotes plant growth by improving microbial community structure of soil as well as root nodulation and mycorrhizal colonization in the roots of *Pisum sativum*. **Applied Soil Ecology**, v. 110, p. 97-108, 2017. <https://doi.org/10.1016/j.apsoil.2016.10.008>
- MARSCHNER, B.; BRODOWSKI, S.; DREVES, A.; GLEIXNER, G.; GUDE, A.; GROOTES, P. M. *et al.* How relevant is recalcitrance for the stabilization of organic matter in soils? **Journal of plant nutrition and soil science**, v. 171, n. 1, p. 91-110, 2008. <https://doi.org/10.1002/jpln.200700049>
- NARDI, S.; PIZZEGHELLO, D.; SCHIAVON, M.; ERTANI, A. Plant biostimulants: physiological responses induced by protein hydrolyzed-based products and humic substances in plant metabolism. **Scientia Agricola**, v. 73, n. 1, p. 18-23, 2016. <https://doi.org/10.1590/0103-9016-2015-0006>
- NEBBIOSO, A.; PICCOLO, A. Advances in Humeomic: enhanced structural identification of humic molecules after size fractionation of a soil humic acid. **Analytical Chimica Acta**, v. 720, p. 77-90, 2012. <https://doi.org/10.1016/j.aca.2012.01.027>
- PANTOJA, M.; ALMANZA, Y.; VALERO, N. Evaluación del efecto auxin-like de ácidos húmicos en maíz mediante análisis digital de imágenes. **Revista U.D.C.A Actualidad & Divulgación Científica**, v. 19, n. 2, p. 361-369, 2016. <https://doi.org/10.31910/rudca.v19.n2.2016.9>
- PÉDROT, M.; MÉLANIE, M. Dynamic structure of humic substances: Rare earth elements as a fingerprint. **Journal of Colloid and Interface Science**, v. 345, p. 206-213, 2010. <https://doi.org/10.1016/j.jcis.2010.01.069>







- QUAGGIOTTI, S.; RUPERTI, B.; PIZZEGHELLO, D.; FRANCIOSO, O.; TUGNOLI, V.; NARDI, S. Effect of low molecular size humic substances on nitrate uptake and expression of genes involved in nitrate transport in maize (*Zea mays* L.). **Journal of Experimental Botany**, v. 55, p. 803–813, 2004. <https://doi.org/10.1093/jxb/erh085>
- REYES-PÉREZ, J. J.; ENRÍQUEZ-ACOSTA, E. A.; RAMÍREZ-ARREBATO, M. Á.; RODRÍGUEZ-PEDROSO, A. T.; FALCÓN-RODRÍGUEZ, Y. A. Efecto de ácidos húmicos, micorrizas y quitosano en indicadores del crecimiento de dos cultivares de tomate (*Solanum lycopersicum* L.). **Terra Latinoamericana Número Especial**, v. 38, n. 3, p. 653–666, 2020. <https://doi.org/10.28940/terra.v38i3.671>
- ROSE, M. T.; PATTI, A. F.; LITTLE, K. R.; BROWN, A. L.; JACKSON, W.; CAVAGNARO, T. R. A meta-analysis and review of plant-growth response to humic substances: practical implications for agriculture. In: SPARKS, D. L. (ed.). **Advances in Agronomy**. Elsevier, 2014. V. 124. p. 37–89. <https://doi.org/10.1016/B978-0-12-800138-7.00002-4>
- SHAH, Z. H.; REHMAN, H. M.; AKHTAR, T.; ALSAMADANY, H.; HAMOOH, B. T.; MUJTABA, T. *et al.* Humic substances: Determining potential molecular regulatory processes in plants. **Frontiers in Plant Science**, v. 9, p. 263, 2018. <https://doi.org/10.3389/fpls.2018.00263>
- SLOBODA, E.; XAVIER, S.; RIBEIRO de AZEVEDO, E.; DI BERNARDO, A.; VIEIRA, E. Comparative characterization of humic substances extracted from freshwater and peat of different apparent molecular sizes. **Revista Ambiente & Água**, v. 12, n. 5, p. 776–788, 2017. <https://doi.org/10.4136/ambi-agua.2022>
- TANG, W.; ZENG, G. M.; GONG, J. L.; LIANG, J.; XU, P.; ZHANG, C. *et al.* Impact of humic/fulvic acid on the removal of heavy metals from aqueous solutions using nanomaterials: A review. **Science of the Total Environment**, v. 468–469, p. 1014–1027, 2014. <https://doi.org/10.1016/j.scitotenv.2013.09.044>
- TREVISAN, S.; FRANCIOSO, O.; QUAGGIOTTI, S.; NARDI, S. Humic substances biological activity at the plant-soil interface: From environmental aspects to molecular factors. **Plant Signaling & Behavior**, v. 5, n. 6, p. 635–43, 2010. <https://doi.org/10.4161/psb.5.6.11211>
- SUN, Z.; TANG, B.; XIE, H. Treatment of Waste Gasses by Humic Acid. **Energy & Fuels**, v. 29, n. 3, p. 269–1278, 2015. <https://doi.org/10.1021/ef502299k>
- WU, J.; ZHAO, Y.; QI, H.; ZHAO, X.; YANG, T.; DU, Y. *et al.* Identifying the key factors that affect the formation of humic substance during different materials composting. **Bioresource Technology**, v. 244, n. 1, p. 1193–1196, 2017. <https://doi.org/10.1016/j.biortech.2017.08.100>
- YOU, W.; LIU, H. C.; CAO, J. W.; SHEN, Y. L.; CHEN, W. Removal of humic acid from water by magnetic chitosan-grafted polyacrylamide. **Huan Jing Ke Xue**, v. 39, n. 12, p. 5532–5540. 2018. <https://doi.org/10.13227/j.hjhx.201803074>
- ZHIYUAN, Y.; LIANG, G.; PAN, R. Preparation of nitric humic acid by catalytic oxidation from Guizhou coal with catalysts. **International Journal of Mining Science and Technology**, v. 22, p. 75–78, 2012. <https://doi.org/10.1016/j.ijmst.2011.06.006>



Investigation of new natural coagulant - cationic hemicellulose associated with cationic tannin - for coagulation/dissolved air flotation (C/DAF) in the treatment of industrial effluent

ARTICLES doi:10.4136/ambi-agua.2824

Received: 23 Dec. 2021; Accepted: 18 Apr. 2022

Ana Gabriela Tomé Alves^{1*} ; **Ingrid da Silva Pacheco¹** ; **Amanda Bessa Freitas¹** ;
Elaine Angélica Mundim Ribeiro¹ ; **Sheila Cristina Canobre²** ;
Fábio Augusto do Amaral² 

¹Instituto de Ciências Agrárias. Universidade Federal de Uberlândia (UFU), Rua Acre, n° 1004, CEP: 38405-325, Uberlândia, MG, Brazil. E-mail: ingridspache@gmail.com, amandabessa2803@gmail.com, eamundim@yahoo.com.br

²Instituto de Química. Universidade Federal de Uberlândia (UFU), Avenida João Naves de Ávila, n° 2121, CEP: 38400-902, Uberlândia, MG, Brazil. E-mail: scanobre@yahoo.com.br, fabioamaral@yahoo.com.br

*Corresponding author. E-mail: anagabriela_tome@hotmail.com

ABSTRACT

The use of plant-based coagulants (natural coagulants) in wastewater treatments has potential advantages over the inorganic coagulants used commercially. This study evaluated organic coagulants cationic hemicelluloses (CH) synthesized from peanut shell and associated with commercial cationic tannin (TSG) for use as the primary coagulation/flocculation treatment, followed by solid-liquid separation via sedimentation/flotation by dissolved air (DAF). The assay was carried out in a jar test on effluent from a multinational industry in the grain processing sector, located in the city of Uberlândia-MG. Coagulation diagrams were determined using the data spatial interpolation method of the Kriging regression model and the Tukey test was used to assess the difference in the results obtained. The optimum removal points of turbidity removal efficiency (TRE), greater than 98%, were achieved for the TSG/CH association with 200 mg L⁻¹ (pH 10.72), 350 mg L⁻¹ (pH 9.72), 500 mg L⁻¹ (pH 9.56) in sedimentation. For the separation by DAF, the association of TSG/CH resulted in TRE values greater than 95% at dosages of 350 mg L⁻¹ (pH 9.59) and 500 mg L⁻¹ (pH 7.92). Furthermore, the results indicate that the associated use of TSG/CH, a coagulation aid, favored the coupling of the DAF bubble-particle, resulting in a smaller volume of sludge. In addition, CH expanded the action of TSG to the basic region.

Keywords: agroindustry residue, natural organic coagulants, primary physical chemical treatment.

Investigação de um novo coagulante natural - hemicelulose catiônica associada ao tanino catiônico – na coagulação/flotação por ar dissolvido (C/DAF) no tratamento de efluente industrial

RESUMO

O uso de coagulantes à base de plantas (coagulante natural) em tratamentos de efluentes tem potencial contra coagulantes inorgânicos utilizados comercialmente. Este trabalho teve



como objetivo avaliar os coagulantes orgânicos hemiceluloses catiônicas (CH) – sintetizadas a partir da casca de amendoim – associadas ao tanino catiônico (TSG) – comercial – para coagulação/floculação como tratamento primário, seguido de separação sólido-líquido via sedimentação/flotação por ar (DAF). O ensaio foi realizado em *jar test* em efluente de uma indústria multinacional do setor de beneficiamento de grãos, localizada na cidade de Uberlândia-MG. Os diagramas de coagulação foram determinados pelo método de interpolação espacial de dados do modelo de regressão de *Kringing* e o teste de Tukey foi utilizado para avaliar a diferença nos resultados obtidos. Os pontos ótimos de eficiência de remoção de turbidez (TRE), superiores a 98%, foram alcançados para a associação TSG/CH com 200 mg L⁻¹ (pH 10,72), 350 mg L⁻¹ (pH 9,72), 500 mg L⁻¹ (pH 9,56) na sedimentação. Para a separação por DAF, a associação de TSG/CH resultou em valores de TRE superiores a 95% nas dosagens de 350 mg L⁻¹ (pH 9,59) e 500 mg L⁻¹ (pH 7,92). Além disso, os resultados obtidos indicam que o uso associado de TSG/CH como auxiliar de coagulação, favoreceu o acoplamento bolha-partícula, resultando em menor volume de lodo, além disso, o CH expandiu a ação do TSG para a região básica.

Palavras-chave: coagulantes orgânicos naturais, resíduo agroindustrial, tratamento primário físico-químico.

1. INTRODUCTION

Effluent treatment technologies to better preserve the quality of water resources and conserve aquatic ecosystems have been developed and improved in recent decades. In general, effluent treatment can be divided into physical (sedimentation, flotation, filtration, membrane, adsorption), chemical (coagulation, oxidation, catalytic reduction, ion exchange) and biological (bioreactors, microbial biodegradation, phytoremediation) processes. Furthermore, the application of joint technologies for the purpose of obtaining better water quality parameters is common, resulting in the following treatment stages: primary, secondary and tertiary (Pioltine and Reali, 2015; Ang and Mohammad, 2020).

Coagulation is one of the oldest treatment technologies and continues to be constantly investigated and improved. The commonly used coagulants are inorganic and non-biodegradable, such as aluminum sulfate (Al₂(SO₄)₃), iron chloride (FeCl₃) and polyaluminium chloride (Al_n(OH)_mCl_{3n-m}). Despite their proven chemical efficiency, when dosed incorrectly these inorganic coagulants can cause residual concentrations of aluminum, iron, sulfate and chlorides that remain in the treated water, thus impacting aquatic ecosystems. Furthermore, there are reports that the increase in aluminum concentration in treated water, due to the use of coagulants containing aluminum, contributes to the increase in cases of diseases such as: Alzheimer's, Parkinson's and Down's syndrome (Shak and Wu, 2015; Silva, 1999).

In view of the consequences associated with the use of inorganic coagulants, natural coagulants have been introduced as alternatives having safety advantages for human health and ecosystems (Shak and Wu, 2015; Franco *et al.*, 2017). When compared to the aforementioned inorganic coagulants, these have lower toxicity and higher biodegradability, thus following the principles of green chemistry (Lima Júnior and Abreu, 2018).

There are several authors who report the use of biopolymers with natural coagulant, tannins (Justina *et al.*, 2018; Ribeiro *et al.*, 2017a), oil moringa (Ntibrey *et al.*, 2020), chitosan (Jagaba *et al.*, 2021), okra and passion fruit seeds (Muniz *et al.*, 2020a). One of the advantages of natural coagulants is that their synthesis reactants may come from agro-industrial residues, as in the case of cellulosic derivatives such as Cationic Hemicellulose (Ren *et al.*, 2006; Landim *et al.*, 2013; Ribeiro *et al.*, 2017a; 2017b).

Agro-industrial production stands out as one of the main economic activities in the country, mainly for promoting the production of food, fibers, bioenergy, among other products and by-

products. In this sector, the production of peanuts is attracting attention and, according to the National Supply Company (CONAB), 165.1 thousand hectares were planted in the country's first crop. Brazil currently occupies the 12th position in the world ranking of largest peanut producers and reached record levels of production in 2020 (CONAB, 2021). As for the total Brazilian production, again according to CONAB (2021), the 2020/21 crop corresponded to 574.4 thousand tons, representing a productivity of 3,479 kg/ha. Furthermore, the foreign market purchases from 60% to 70% of the total amount of peanuts produced in Brazil, with Russia, Holland and Algeria being its main buyers.

Considering the size of production, one of the biggest concerns of the agro-industrial sector is the generation of enormous residues. As an example of the dimension of this activity, according to data from Vaz Junior (2020) it is estimated that world agricultural production is around 7.26 Gt and that the volume of dry residue from plant biomass reaches the equivalent of 140 Gt. This huge amount of waste becomes an aggravating environmental factor. According to Ribeiro (2017), peanut shells are tailings consisting mainly of cellulose (from 20% to 30%), hemicelluloses (from 10% to 15%) and lignin (from 40% to 45%), presenting itself as source of biomass for the obtaining of natural coagulants.

Furthermore, the association of coagulation by natural biopolymers, followed by solid-liquid separation via dissolved air flotation (C/DAF) has been highlighted as a more sustainable method, as it allows both the formation of smaller volumes of sludge in shorter separation times and Biochemical oxygen demand (BOD) reduction. The use of dissolved air flotation (DAF) occurred in the mid-1920s and there are records of it being used in two factories located in Sweden as early as the 1970s (Pioltione and Reali, 2015). Subsequently, its use was extended to several other European countries and today it is widely used in countries such as the United States, (Creamer *et al.*, 2010), Canada (Gudmundur *et al.*, 2020), China (Wang *et al.*, 2021), South Korea (Oh *et al.*, 2019), New Zealand (Okoro *et al.*, 2017), Iran (Behin and Bahrami, 2012), Malaysia (Rozainy *et al.*, 2014), Brazil (Muniz *et al.*, 2020b), among others.

The main objective of the present study was to carry out the C/DAF with a natural organic coagulant obtained by the association of cationic hemicellulose, extracted and synthesized from the agroindustrial residue of peanut shell by the authors, and commercial cationic tannin in the treatment of effluent generated by a multinational in the grain processing sector, located in the city of Uberlândia, Minas Gerais, in order to obtain a more sustainable and effective technology.

2. MATERIAL AND METHODS

2.1. Synthesis of cationic hemicelluloses (CH) from agroindustrial peanut shell residue

The holocellulose was extracted from the lignocellulosic agroindustrial residue of peanut shells according to the procedure described by Vieira *et al.* (2012), in which the peanut shells were mixed with distilled water at a ratio of 1:20 (g mL⁻¹) and heated at 75°C for 30 min. Then, acetic acid and sodium chlorite were added to the system in a ratio of 1:1.5 (mL g⁻¹) and kept under stirring for 1 h. This process was repeated 3 times and every 1 hour the same amount of these reagents was added to the system, adding up to a digestion period of 4h. Then, the reaction mixture was cooled to 10°C and filtered. The fibrous residue, composed of holocellulose, was washed with distilled water at 5°C for 20 min, at which point it displayed a whitish color. At the end of the washing step, it was dried in an oven at 75°C for 6 h.

The procedure established by Morais *et al.* (2010) was followed for the isolation of natural hemicelluloses, in which a 17.5% (m v⁻¹) NaOH solution was added to the holocelluloses in a proportion of 15:1 (mL g⁻¹). The material was then ground for 8 min and the mixture filtered in a nylon strainer to separate the celluloses, the fibrous residue of the hemicelluloses (liquid part). Acid solution 1:1 (v v⁻¹) ethanol/acetic acid (CH₃COOH/Ethanol (C₂ H₅OH)) was added to the liquid part to precipitate the material which, after 12 h, was filtered in a porous plate funnel and

dried in an oven at 75°C for 6 h.

Cationic hemicelluloses were synthesized according to procedures adapted from Ren *et al.* (2006; 2007) and Landim *et al.* (2013), in which a 10% (w v⁻¹) solution of hemicelluloses was kept under stirring at 60°C for 30 min. Subsequently, a NaOH solution was added to the reaction medium in a proportion of 14% (m v⁻¹) and kept under stirring for 20 min. After this time, a solution of (2,3-Epoxypropyl) trimethylammonium chloride 6.8% (v v⁻¹) was added and again the reaction medium was kept under stirring for 30 min. Afterwards, a 2.2% NaOH solution (m v⁻¹) was added and the reaction medium was kept under stirring at 60°C for 5 h. The resulting mixture was cooled in an ice bath and neutralized with HCl solution. Then, the Cationic Hemicelluloses were precipitated with 98% ethanol and filtered in a porous plate funnel. The final material was oven dried at 75°C for 6 h.

2.2. Determination of the degree of substitution (DS) of CH by elementary analysis

The synthesized CH was previously dried at a temperature of 60°C for 24 h. The determination of carbon (C), hydrogen (H), nitrogen (N) and sulfur (S) was performed by elemental analysis in an EA 1110-CHNS/O equipment from CE Instruments. The degree of substitution (DS) of CH was calculated using Equation 1 (Ren *et al.*, 2006; 2007).

$$DS = \frac{60\% N}{14\% C - 72\% N} \quad (1)$$

In which:

%N = percentage of nitrogen determined by elemental analysis;

%C = percentage of carbon determined by elemental analysis;

60 = molar mass of carbons of the xylose molecule;

14 = molar mass of nitrogen present in the cationic substituent group; and

72 = molar mass of carbons of the cationic substituent group.

2.3. Analytical characterization of industrial effluent

The raw effluent was collected in a composite sample in a grain processing (corn and soybean) plant of a multinational food industry, located in the city of Uberlândia, Minas Gerais. For the analytical characterization of the effluent, the turbidity index/NTU was measured in an Ap 2000 Policontrol turbidimeter, the initial pH in a Hanna instruments[®] pHmeter and the sedimentable solids in an *Imhoff* Cone[®] (mL L⁻¹) for 45 min. These control parameters were adopted as standards of comparison for the evaluation of the treatment effectiveness and for the determination of the turbidity removal (%) efficiency. Another aim was to analyse the volume of sludge formed after sedimentation and solid-liquid separation by DAF.

2.4. Preparation of natural organic coagulant solutions

The coagulant studied in this work, based on cationic tannin, was TANFLOC SG (TSG), a commercial organic-cationic polymer, from black Acassia bark, provided by the company TANAC S/A. Considering that TANFLOC SG has a non-volatile content between 30-34%, an average of 32% was considered for the amount of cationic tannin in this solution (31.25 g), the solution was diluted to 10%.

The coagulant for the TSG/CH association was obtained at the ratio of 3:1 (v v⁻¹), adapted from Ribeiro (2017), by mixing 75 mL of a 10% TANFLOC SG solution (v v⁻¹) with 25 mL of a 10% CH solution (m v⁻¹), resulting in TSG/CH 3:1 (v v⁻¹). Assays were performed for TANFLOC SG and TANFLOC SG/Cationic Hemicellulose (TSG/CH) with the following dosage variations: 200; 350 and 500 mg L⁻¹.

2.5. Grain processing effluent treatability tests

The physical-chemical treatment tests were carried out at the Laboratory of Energy Storage and Effluent Treatment (LAETE/UFU) in jar tests (PolyControl brand Jartest) for coagulation/flocculation, followed by sedimentation. Assays were performed for TANFLOC SG and TANFLOC SG/Cationic Hemicellulose (TSG/CH) with the following dosage variations: 200; 350 and 500 mg L⁻¹. The variation of the coagulation pH was carried out by the addition of a 1 mol L⁻¹ sodium hydroxide solution. Jar tests were carried out with the following steps: (i) 1 L of effluent was added to each jar; (ii) rapid agitation in a mean agitation gradient (G_{mr}) of 300 s⁻¹ (250 rpm) for 30 s, where a 40 mL sample was collected from each jar and the coagulation pH was measured; (iii) a slow mixing occurred in a mean flocculation gradient (G_f) of 35 s⁻¹ (30 rpm) for 15 min; (iv) the treated effluent was transferred to *Imhoff* Cones[®] after 30 min of decantation, the volume of sludge formed by sedimentation was measured and the remaining turbidity was measured.

After selecting the points with TRE greater than 98%, the points were repeated in triplicate using the solid-liquid separation method by C/DAF, through a stainless steel saturation chamber and modified jars for flotation. The treatment was carried out for 1 L of effluent and the water went through a saturation time of 20 min. Thus, the saturated water was injected at a pressure of 5.0 Kgf cm⁻² and administered in the effluent in a 25%/75% (saturated water/effluent) proportion. Finally, the turbidity measurements of the raw effluent were compared with those obtained after sedimentation or DAF, using Equation 2.

$$\text{turbidity removal efficiency (TRE \%)} = \left(1 - \frac{\text{final turbidity}}{\text{initial turbidity}}\right) \times 100 \quad (2)$$

2.6. Determination of coagulation diagrams

The coagulation diagrams were determined in 18 tests for 10% TSG (v v⁻¹) (dosages: 200, 350 and 500 mg L⁻¹) and 18 tests for 10% TSG/CH (v v⁻¹) (dosages: 200, 350 and 500 mg L⁻¹), by design 3 dosages and 3 repetitions. For each batch with 6 jars (in each jar 1 L of effluent were added), the coagulant dosage was maintained in all jars, the pH was varied by the addition of HCl (1 mol L⁻¹), as acidifier, or NaOH (1 mol L⁻¹), as alkalinizing, in different volumes to obtain the desired pH values, between 4 at 12 (for each dosage studied, pH tests were performed that were near 4, 5, 7, 9, 11 and 12).

The records of coagulation pH readings, coagulant dosage and the respective percentages of apparent color removal were tabulated in electronic spreadsheets in Microsoft Excel and later transferred to the computer program Surfer[®] (Golden Software, 2018). The aim was to estimate percentages in non-sampled points and draw the curves of the same removal efficiency, called the “coagulation diagram”.

The Kriging regression method was selected as a mathematical model for the spatial interpolation and estimation of the mean turbidity removal percentages. The model is characterized by isolines, which represent the removal percentage level curves. In this study, ordinary Kriging was used, so the estimate to determine an average value in a non-sampled region was made from neighboring points.

In addition, Figure 1 schematically shows the effluent treatment carried out by sedimentation or DAF from the use of coagulant synthesized from agro-industrial residues. The cationic hemicellulose has a dark brown visual color, the intrinsic viscosity corresponds to viscosity 8.06 mL g⁻¹ (Ribeiro, 2017), solubility 20.00 g L⁻¹ (Ribeiro *et al.*, 2017a) and density 0,1 g mL⁻¹.

2.7. Selection of optimal points

To select the best points of the coagulation diagram, the conditions (dosage and pH) resulting from the percentages of turbidity removal (> 98%) associated with a lower sludge

formation were chosen. Therefore, 3 points were selected for TSG coagulant and 3 points when TSG/HC was applied. These same points were used in DAF.



Figure 1. Schematic representation of coagulant synthesis from agro-industrial waste and effluent treatment.

2.8. Statistical analysis

The statistical treatment of the results obtained in this study was developed using the computer program Sivar and Rbio. To verify the existence of significant differences between different treatments, the analysis of variance (ANOVA) was applied. When identifying the occurrence of significant difference between treatments, the Tukey was applied, with a significance level of 5% and 95% confidence for analyses.

3. RESULTS AND DISCUSSION

3.1. Determination of the degree of replacement of cationic hemicelluloses

Peanut shells have xylan as their main sugar, which makes the hemicellulose from peanut shells contain, mostly, two hydroxyls per unit of xylose available to be etherified (Martin *et al.*, 2007). Thus, according to Ribeiro *et al.* (2017a), for the molar ratio calculation, the hemicellulose was considered to only be constituted of xylose ($MM=132 \text{ g mol}^{-1}$).

Cationic hemicelluloses were synthesized from hemicellulose extracted from the agro-industrial residue of peanut shells. Elemental analysis data and the DS calculation are shown in Table 1 for the duplicates. From Equation 1, it was possible to estimate a DS of 0.410 ± 0.06 , similar to that obtained by Ribeiro (2017) (0.410), which was extracted from the same agro-industrial waste. Furthermore, Ren *et al.* (2006), who studied the effect of the variation of NaOH/ETA molar ratio from 0.1 to 3 on this synthesis, obtained materials with DS for cationic hemicelluloses that ranged from 0.01 to 0.52. These values are similar to those obtained by Ribeiro *et al.* (2017a), Castro (2020) and Landin *et al.* (2013), materials were obtained by the same synthesis method, as shown in Table 2.

3.2. Grain processing effluent treatability tests

The coagulation/flocculation tests were carried out to evaluate the effect of the coagulant dosages on the turbidity removal efficiency from the raw effluent, in order to determine the most appropriate coagulation concentration and pH for the two studied coagulants (TSG and association of TSG/CH 3:1 v v⁻¹). Firstly, dosages were investigated in order to assess the range of values in which the coagulants had the greatest turbidity removal, and then which of these

points provided the smallest amount of sedimentable solids (sludge volume). The analytical characterization of the raw effluent from grain processing presented the following results, shown in Table 3. These were adopted as the standards of comparison for the analysis of the treatment efficiency, which was based on the removal of turbidity and the amount of sludge volume.

Table 1. Percentages and DS obtained from the elemental analysis of CH.

Sample	%C	%H	%N	DS
Cationic Hemicelluloses (CH 1)	14.17	2.97	0.92	0.410 ± 0.06
Cationic Hemicelluloses (CH 2)	14.03	3.02	0.87	

Table 2. Comparison of the Degree of Substitution of Cationic Hemicellulose calculated in the present work and from other residue sources.

Reference	Source	Degree of substitution (DS)
Landim <i>et al.</i> (2013)	Corn straws	0.430
Ribeiro <i>et al.</i> (2017a)	Corn straws	0.520
Ren <i>et al.</i> (2006)	Peanut Shells	0.540
Ribeiro (2017)	Peanut Shells	0.410
Castro (2020)	Peanut Shells	0.295
Present work	Peanut Shells	0.410 ± 0.06

Table 3. Analytical characterization of the raw effluent collected from the grain processing food industry before carrying out the treatability test.

Parameter Analyzed	Value ± standard deviation	Equipment	Procedure
Visual Color	Opaque Dark Gray	-	-
Turbidity (NTU)	196 ± 10.11	Turbidimeter Ap 2000 Policontrol	APHA <i>et al.</i> (2017) nephelometric method (2130 B)
Sedimentable Solids (mL L ⁻¹)	2 ± 1.00	Imhoff Cone®	NBR 10561/1988 (ABNT, 1988)
pH	3.91 ± 0.58	pHmeter Hanna instruments	APHA <i>et al.</i> (2017) electrometric method (4500 H ⁺ B)
Temperature (°C)	23.00 ± 1.50	pHmeter Hanna instruments	APHA <i>et al.</i> (2017) (2550 B)

The coagulation diagrams map the effectiveness of turbidity removal, considering the pH range from 4 to 12. The coagulation diagrams (Figure 2) were determined for both tested coagulants, TSG (a) and TSG/CH (b) using the Kriging method for interpolation of points. On the abscissa axis are the coagulation pH values measured after 30 seconds of rapid mixing (250 rpm), on the ordinate axis are the coagulant dosages in mg L⁻¹, and the curves indicate isoefficiency points for turbidity removal (%). A color scale of similar hue has been adopted to simplify viewing, with the lighter areas having the highest turbidity removal efficiency values.

Figure 2a shows the results of applying only TSG. In the pH 6 to 10 region, there is a predominance of high turbidity removals (90 to 100%) for the application of coagulant dosages of 200 mg L⁻¹ up to 500 mg L⁻¹ of TSG 10%. For these pHs, the turbidity removal index appears to have been more effective. Furthermore, it is observed that at pHs greater than 10, removals were not satisfactory (from 40% to 70%) with the increase of the effluent basicity, showing that high pHs may not be appropriate for the performance of TSG in the studied effluent.

For the application of the TSG/CH 3:1 (v v⁻¹) coagulant, the results presented in Figure 2b show that the most effective coagulation pH range occurred between 8 and 12 for the entire dosage range analysed, with turbidity removals between 90% and 100%. Thus, it is inferred that the association with CH expanded the range of action of TSG in basic environments. These data corroborate those observed by Ribeiro *et al.* (2017b), that the performance range of tannin associated with cationic hemicelluloses, when applied in dosages above 400 mg L⁻¹, led to an increase in turbidity removals in basic pHs. The performance of tannin as a primary coagulant in that region was limited, so being able to achieve turbidity removals above 95% suggests a synergistic effect between the coagulants. Furthermore, the coagulant TSG/CH 3:1 (v v⁻¹) proved to be more efficient when compared to TSG, resulting in turbidity removals greater than 80% for all investigated dosages.

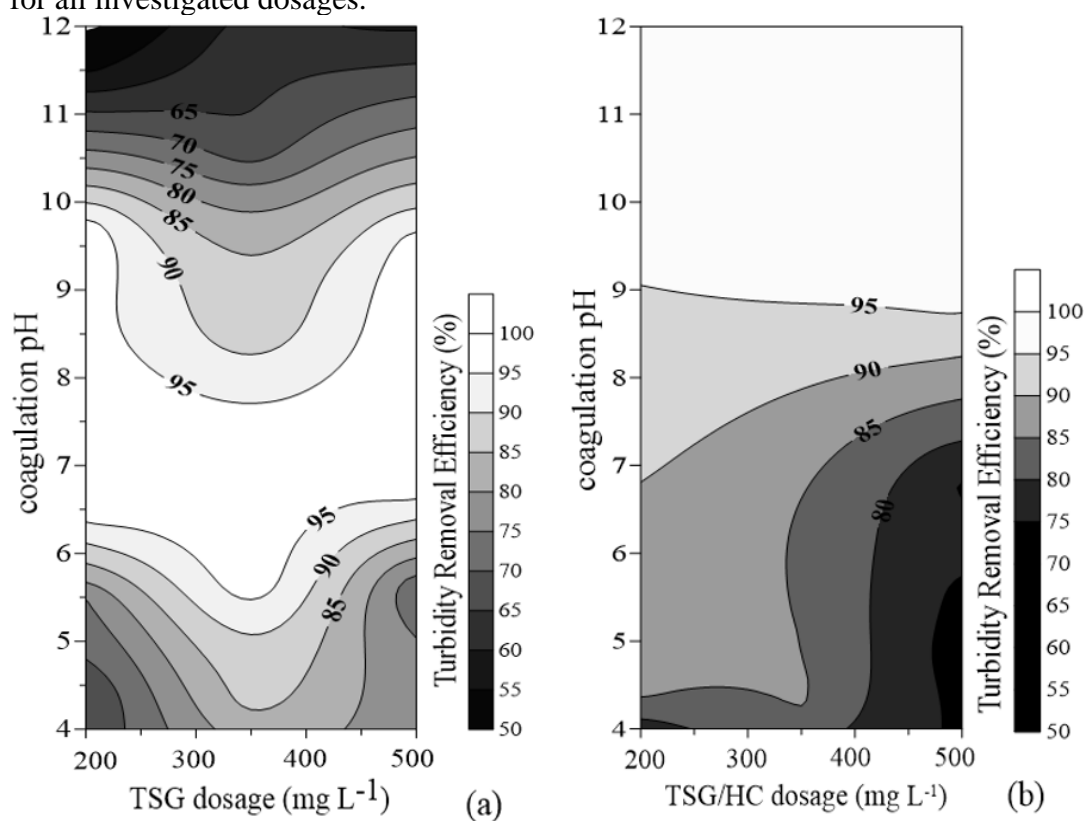


Figure 2. Coagulation diagrams for turbidity removal (%) from the industrial grain processing effluent using the coagulant: (a) TSG and (b) Tanfloc SG associated with Cationic Hemicellulose (TSG/CH 3:1 (v v⁻¹)).

The efficiency of tannins as a primary coagulant has been studied in the physicochemical treatment of various types of industrial effluents, such as those from industrial laundry companies (Ribeiro *et al.*, 2017a), dairy products (Justina *et al.*, 2018) and breweries (Tonhato Junior *et al.*, 2019), as can be seen in Table 4. The treatability efficiencies achieved in this study, either by applying TSG or the TSG/CH association, are comparable to values found in the literature and demonstrate a progress towards promoting greater efficiency for the entire pH range investigated.

Table 4. Main studies selected in the bibliographic survey on the application of Cationic Tannin in Effluent and Water Treatment.

References	Nature of Coagulant	Type of Effluent	Effluent Turbidity (NTU)	Coagulant Dosage (mg L ⁻¹)	pH	Sedimentation Time (min)	Turbidity Removal Ef. (%)
Ribeiro <i>et al.</i> (2017a)	Tannin (TANFLOC SL)	Industrial laundry	>1100	3000	5	-	82
Justina <i>et al.</i> (2018)	Tannin extracted from <i>Acacia Mearnsii</i> (TANFLOC)	Dairy industry	763.84	600	-	60	92
Ribeiro <i>et al.</i> (2017a)	Tannin and cationic hemicellulose	Industrial laundry	>1100	3200	5	-	95
Pacheco <i>et al.</i> (2022)	Tannin (TANFLOC SG)	Synthetic dairy wastewater	553	400	7.38	30	98.67
Present work	Tannin (TANFLOC SG)	Grain processing	391	350	5.65	30	100
Present work	Tannin (TANFLOC SG) and cationic hemicellulose (3:1 v v ⁻¹)	Grain processing	391	200	10.72	30	100

Turbidity has been studied as one of the main previous parameters for comparing efficiency after physicochemical treatment. In the study by Ribeiro *et al.* (2017a) the physicochemical treatment enabled 82% of turbidity removal in an industrial laundry effluent, when 3000 mg L^{-1} at pH 5 was applied. Justina *et al.* (2018) reported removals of 92% from a dairy effluent, for a dosage of 600 mg L^{-1} . Tonhato Junior *et al.* (2019) reported turbidity removal of 99% for the application of 0.23 mL L^{-1} of vegetable tannin at pH 4.9. Pacheco *et al.* (2022) reported turbidity removal of 94.79 and 98.67%, for the dosage of 400 mL L^{-1} (coagulation pH 9 and 7.35) for Cationic Hemicellulose and TANFLOC SG, respectively.

The results showed that the association between tannin and cationic hemicelluloses (3:1 v v⁻¹) achieved turbidity removals greater than 80% for the investigated coagulation pH ranges, including the alkaline regions. To choose the best treatment efficiency point, the volume of sludge formed after the flocculation process was also analysed by sedimentation. The 3 points selected were the ones where removals greater than 98% were achieved with the use of both coagulants and at the same time with the smallest amount of sludge volume formation (mL L^{-1}) in an *Imhoff* Cone®. The results are shown in Figure 3; it can be seen that there are different points (coagulation pH x dosage) for each coagulant (TSG and TSG/CH). The points with the greatest removal were selected for analysis and to proceed with the studies for DAF.

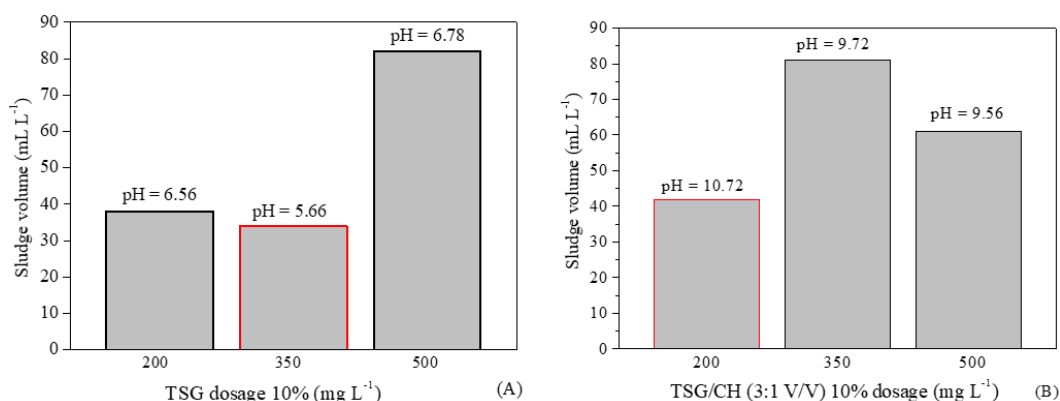


Figure 3. Sludge volume formation (mL L^{-1}) after solid-liquid separation by physical-chemical treatment of the industrial effluent with sedimentation, for TSG and TSG/CH coagulants, respectively.

As can be seen in Figure 3, from the 3 points with the highest TRE for TSG and TSG/CH, the one with the smallest volume of sludge formed was when 350 mg L^{-1} (pH 5.66) was applied. The amount of sludge formed was 34 mL L^{-1} showing the best performance. For TSG/CH 3:1 (v v⁻¹), it was noted that the lowest volume of sedimentable solids occurred after treatment with dosage 200 mg L^{-1} (pH 10.72), forming a sludge volume of 60 mL L^{-1} . With the association of CH with TSG, there was a significant reduction in the dosage used. Therefore, it is noted that when TSG/CH is applied at a higher pH above 10, there was a reduction in dosage compared to when only TSG is applied, which does not have an efficient action at basic pH.

In the work of Pacheco *et al.* 2022, the sludge was analyzed by energy dispersive X-ray spectroscopy indicating a pattern in elemental composition. When CH is applied to the treatment of a dairy effluent, the sludge presented the following elements: carbon ($92.16 \pm 1.13\%$), followed by oxygen (6.23 ± 0.91), Na (0.53 ± 0.04) and P (0.39 ± 0.02). The order of TSG elements is Carbon (75.36 ± 4.57), Oxygen (20.31 ± 4.27), P (1.06 ± 0.01) and Na (0.53 ± 0.04). The sludge composition provides organic coagulants such as cationic hemicelluloses and Tanfloc SG, a potential application in agriculture as a fertilizer.

3.3. Solid-Liquid Separation by Dissolved Air Flotation

From the results obtained with sedimentation, the separation by DAF was performed in

triplicate for the points with the greatest turbidity removals (99.00, 98.10 and 98.27% of TRE). They were reached for TSG with: 200 mg L⁻¹ (pH 6.56), 350 mg L⁻¹ (pH 5.66), 500 mg L⁻¹ (pH 6.78), for dosages and coagulation pH, respectively. For the TSG/CH association, the TREs (97.08, 98.20 and 97.90%) were achieved with 200 mg L⁻¹ (pH 10.72), 350 mg L⁻¹ (pH 9.72), 500 mg L⁻¹ (pH 9.56), for dosages and pH respectively. The results are shown in Figure 4.

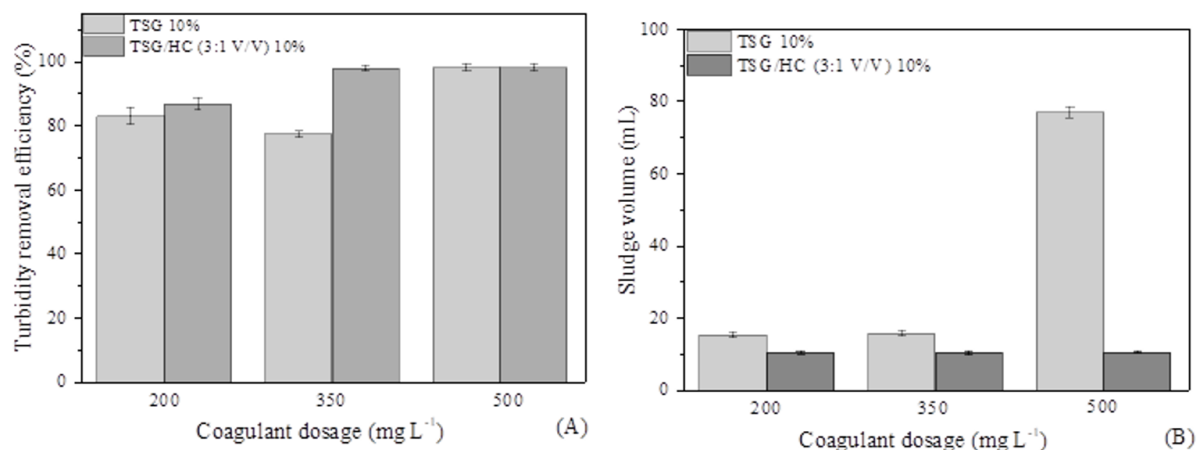


Figure 4. Turbidity removal efficiency (A) and Sludge volume formed (mL L⁻¹) (B) for dissolved air flotation (DAF) applied after coagulation by TSG 10% and TSG/CH (3:1 v v⁻¹) 10%.

In order to assess whether the results obtained in C/DAF from the use of TSG and TSG/CH presented significant differences, the Tukey statistical test was performed. First the Analysis of Variance (ANOVA) was performed. It is shown in Table 5 with a significance level of 95%.

Table 5. Test of Variance (ANOVA) with two factors and repetition applied to the turbidity removal efficiency and sludge volume data when applied: TSG and TSG/CH.

ANOVA						
Source of variation	<i>SQ</i>	<i>gl</i>	<i>MQ</i>	<i>F</i>	<i>P-value</i>	<i>Critical F</i>
Sample	4782.857	5	956.5713	236.0435	1.38508E-19	2.620654148
Columns	46206.55	1	46206.55	11401.93	1.19007E-33	4.259677273
Interactions	2388.104	5	477.6208	117.8577	4.42675E-16	2.620654148
Inside	97.2605	24	4.052521			
Total	53474.77	35				

With the ANOVA test it was possible to infer that there were significant differences between the analysed variables. From Tukey Test, was calculated the minimum significant difference (MSD) resulting in a value of 5.0790 at 95% significance level with a total studentized amplitude (*q*) of 4.37 (tabled variable obtained from the studies carried out by Snedecor, 1934), the description of the statistic from the Tukey Test was attached as supplementary material.

Regarding the sludge volume, when only the Cationic Tannin (TSG) was applied at a dosage of 500 mg L⁻¹, it resulted in the formation of the largest sludge volume, while 350 mg L⁻¹ of TSG resulted in the smallest volume (Figure 4 (b)), which represents an amplitude of 51 mL. However, the same did not occur when varying the dosages of the association between TSG/CH. There was no significant difference, or tendency, between the sludge volumes since the results obtained had very similar values, with a variation of ± 0.031 mL. When comparing

the TSG and TSG/CH variations, only the dosage of TSG 350 mg L⁻¹ did not differ significantly from the results obtained for the association of cationic hemicelluloses with cationic tannin.

Regarding the turbidity removal efficiency, the TSG dosage variations resulted in a significant difference between all points, and only the TSG 500 mg L⁻¹ provided a turbidity removal greater than 95%. Furthermore, the use of TSG in comparison to the TSG/CH association, the dosage of TSG 500 mg L⁻¹ did not result in a significant difference to: TSG/CH 350 mg L⁻¹ and TSG/CH 500 mg L⁻¹. The dosage of TSG 200 mg L⁻¹ did not differ significantly when compared only to TSG/CH 350 mg L⁻¹. Finally, when analysing the dosage variation of the association between TSG/CH, only the dosage of 200 mg L⁻¹ differed from the others. Thus, the association of TSG/CH enabled a greater TRE at lower dosages when compared to cationic tannin acting alone.

The results suggest that CH in association with TSG, influenced the formation of flakes resulting in a better bubble-particle coupling. That is because when TSG alone was used with dosages of 200 and 350 mg L⁻¹, not only were turbidity removals below 85%, but there were sediment flakes at the bottom of the jar, evidencing a low bubble-particle interaction.

The efficiency of natural coagulants has been studied together with dissolved air flotation for various types of industrial effluents, such as those from dairy industry (Muniz *et al.*, 2020a), laundry effluents, bus washing (Araujo, 2017), effluents from the paper industry (Miranda *et al.*, 2013) and even for spring water (Balbinoti, 2018). Table 6 shows the main comparative studies using C/DAF.

Muniz *et al.* (2020b) used mature okra (*Abelmoschus esculentus*) as a natural *organic* coagulant in dissolved air coagulation/flotation (C/DAF) experiments treating synthetic dairy wastewater. The optimal conditions found for turbidity removal (91.1%) was an okra dosage of 2.0 g L⁻¹ at pH 9.00, indicating that okra seed is a promising source for obtaining the coagulating agent.

Araujo (2017) used the commercial natural *organic* coagulant AQUAFLOC/LS in laundry and bus washing effluent using C/DAF. The optimal conditions found were a dosage of 260 mg L⁻¹ at pH 7, resulting in a turbidity removal of 94%. At the same time, Balbinoti (2018) using *Moringa Oleifera* in spring water obtained an optimal dosage of 40 mg L⁻¹ at pH 7.5 providing 85% of turbidity removal. Both studies showed that the use of natural coagulants associated with dissolved air flotation is promising for different types of effluents, including water from springs.

Miranda *et al.* (2013) investigated Chitosan associated with DAF for the treatment of effluent from paper production, resulting in a removal of 89% with an optimal dosage of 100 mg L⁻¹ at pH 7.5. The emergence of new natural coagulants is also observed in the literature. Muniz *et al.* (2020b) proposed the use of “mutamba” (*Guazuma ulmifolia*) as a coagulant agent. The results obtained by the authors demonstrated the material's potential for treatment via C/DAF when applied to dairy effluent at an ideal dosage of 775.8 mg L⁻¹ at pH 5.

The results obtained by the aforementioned authors corroborate this study, indicating that CH associated with TSG favours DAF both in relation to the dosage of coagulant to obtain better treatability and in relation to the volume of sludge. Furthermore, as they are natural coagulants, the sludge formed from this effluent is biodegradable and can undergo simple decomposition processes. Thus, the association between CH and TSG is promising for the treatment by C/DAF for grain processing effluent.

Table 6. Main studies selected in a literature review on the application of DAF after the use of natural coagulants.

References	Coagulant	Effluent	Effluent Turbidity (NTU)	Dosage (mg L ⁻¹)	Ph	Turbidity Removal (%)
Miranda <i>et al.</i> (2013)	Chitosan	Effluent from paper production	89	100	7.5	89
Araujo (2017)	AQUAFLOC/LS	Effluent from laundry and bus washing	194	260	7	94
Balbinoti (2018)	Moringa oil	Spring water	30	40	7.5	85
Muniz <i>et al.</i> (2020a)	Okra <i>Abelmoschus esculentus</i>	Dairy Effluent	698	2000	9	91.1
Muniz <i>et al.</i> (2020b)	Guazuma ulmifolia	Dairy Effluent	698	775.8	5	95.8
Present work	Tannin (TANFLOC SG)	Grain processing	391	500	5.65	98
Present work	Tannin (TANFLOC SG) and cationic hemicellulose (3:1 v v ⁻¹)	Grain processing	391	500	10.72	98

4. CONCLUSIONS

The use of TSG coagulant showed greater turbidity removal (98.10%) when applied to industrial effluent from grain processing in the pH range of 5 to 10. The sludge formation, when applied at a dosage of 350 mg L⁻¹ and coagulation pH of 5.65, was of 34 mL L⁻¹. For the association of TSG/CH, the largest range of action occurred for more basic pHs (pH 9 and 10) promoting 97.90% of TRE. With a dosage of 500 mg L⁻¹ and pH 10, there was a sludge formation of 60 mL L⁻¹.

In the separation by DAF, only the dosage of 500 mg L⁻¹ and coagulation pH of 6.78 promoted turbidity removal greater than 95.00% for TSG. The use of TSG associated with CH, however, resulted in a turbidity removal greater than 95.00% for both 9.72 (350 mg L⁻¹) and 7.92 (500 mg L⁻¹) coagulation pH and dosage, respectively, suggesting a greater bubble-particle interaction. The separation by DAF applied to the effluent from the grain processing industry showed a good performance when evaluated as a function of the turbidity removed and volume of sludge formed. The results of the study indicate that CH as a coagulation aid favours C/DAF, resulting in a smaller volume of sludge, in addition to having an optimal pH range in the basic region.

5. ACKNOWLEDGEMENTS

The authors thank FAPEMIG [grant numbers: APQ-02249-14 and APQ-03219-14], CNPq, CAPES and Rede Mineira de Química for the financial aid and scholarships.

6. REFERENCES

- ABNT. **NBR 10561/1988**: Águas - Determinação de resíduo sedimentável (sólidos sedimentáveis) - Método do cone de Imhoff. Rio de Janeiro, 1988.
- ANG, W. L.; MOHAMMAD, A. W. State of the art and sustainability of natural coagulants in water and wastewater treatment. **Journal of Cleaner Production**, v. 262, p. 01-15, 2020. <https://doi.org/10.1016/j.jclepro.2020.121267>
- APHA; AWWA; WEF. **Standard Methods for the examination of water and wastewater**. 23rd ed. Washington, 2017. 1504 p.
- ARAUJO, A. P. C. S. **Tratamento de efluentes de lavagem de ônibus e de lavanderia por flotação por ar dissolvido e filtração visando o reúso de água**. 2017. 196 f. Dissertação (Mestrado) - Universidade Tecnológica Federal do Paraná, Londrina, 2017.
- BALBINOTI, J. R. **Aplicação de extrato de sementes de Moringa oleifera na remoção de matéria orgânica por flotação por ar dissolvido**. 2018. 96f. Dissertação (Mestrado) - Universidade Tecnológica Federal do Paraná, Curitiba, 2018.
- BEHIN, J.; BAHRAMI, S. Modeling an industrial dissolved air flotation tank used for separating oil from wastewater. **Chemical Engineering and Processing: Process Intensification**, v. 59, p. 1-8, 2012. <https://doi.org/10.1016/j.cep.2012.05.004>
- CASTRO, J. N. S. **Síntese de Hemiceluloses catiônicas por indução de micro-ondas para utilização como coagulante em tratamento de efluentes industriais**. 2020. 76 f. Trabalho de Conclusão de Curso (Graduação em Engenharia Ambiental) - Universidade Federal de Uberlândia, Uberlândia, 2020.

- CONAB (Brasil). Acompanhamento da safra brasileira: grãos: safra 2020/21 4º levantamento. **Boletim Grãos**, v. 8, n. 4, p. 1-85, 2021.
- CREAMER, K. S.; CHEN, Y.; WILLIAMS, C.M.; CHENG, J.J. Stable thermophilic anaerobic digestion of dissolved air flotation (DAF) sludge by co-digestion with swine manure. **Bioresource Technology**, v. 101, p. 3020-3024, 2010. <https://doi.org/10.1016/j.biortech.2009.12.029>
- FRANCO, C. S.; BATISTA, M. D. A.; OLIVEIRA, L. F. C. D.; KOHN, G. P.; FIA, R. Coagulação com semente de moringa oleífera preparada por diferentes métodos em águas com turbidez de 20 a 100 UNT. **Engenharia Sanitária e Ambiental**, v. 22, n. 4, p. 781-788, 2017. <https://doi.org/10.1590/S1413-41522017145729>
- GOLDEN SOFTWARE. **Surfer**. Versão 16.0.3.330 - Surface mapping system. Golden, 2018.
- GUDMUNDUR, H. J.; CROLLA, A.; LAUZON, J. D; BRANDON, H. Estimation of biogas co-production potential from liquid dairy manure, dissolved air flotation waste (DAF) and dry poultry manure using biochemical methane potential (BMP) assay. **Biocatalysis and Agricultural Biotechnology**, v. 25, 2020. <https://doi.org/10.1016/j.bcab.2020.101605>
- JAGABA, A. H.; KUTTY, S. R. M.; HAYDER, G.; BALOO, L.; GHALEB, A. A. S., I. M.; LAWAL, S. *et al.* Degradation of Cd, Cu, Fe, Mn, Pb and Zn by Moringa-oleífera, zeolite, ferric-chloride, chitosan and alum in an industrial effluent. **Ain Shams Engineering Journal**, v. 12, n. 1, p. 57-64, 2021. <https://doi.org/10.1016/j.asej.2020.06.016>
- JUSTINA, M. D.; MUNIZ, B. R. B.; BRÖRING, M. M.; COSTA, V. J.; SKORONSKI, E. Using vegetable tannin and polyaluminium chloride as coagulants for dairy wastewater treatment: A comparative study. **Journal of Water Process Engineering**, v. 25, p. 173-181, 2018. <https://doi.org/10.1016/j.jwpe.2018.08.001>
- LANDIM, A. S; RODRIGUES FILHO, G; SOUSA, R. M. F.; RIBEIRO, E. A. M.; SOUZA, F. R. B.; VIEIRA, J. G. *et al.* Application of cationic hemicelluloses produced from corn husk as polyelectrolytes in sewage treatment. **Polímeros**, v. 23, n. 4, p. 468-472, 2013. <https://Dx.Doi.Org/10.4322/Polimeros.2013.054>
- LIMA JÚNIOR, R. N.; ABREU, F. O. M. S. Produtos Naturais Utilizados como Coagulantes e Floculantes para Tratamento de Águas: Uma Revisão sobre Benefícios e Potencialidades. **Revista Virtual de Química**, v. 10, n. 3, p. 709-735, 2018. 10.21577/1984-6835.20180052
- MARTIN, C.; ALRIKSSON, B.; SJODE, A.; NILVEBRANT, N. O.; JONSSON, L. J. Dilute sulfuric acid pretreatment of agricultural and agro-industrial residues for ethanol production. **Applied Biochemistry and Biotechnology**, v. 137, p. 339–352, 2007. <https://doi.org/10.1007/s12010-007-9063-1>
- MIRANDA, R.; RALUCA, N.; LATOUR, I.; LUPEI, M.; BOBU, E.; BLANCO, A. Efficiency of chitosans for the treatment of papermaking process water by dissolved air flotation. **Chemical Engineering Journal**, v. 231, p. 304-313, 2013. <https://doi.org/10.1016/j.cej.2013.07.033>
- MORAIS, J. P. S, ROSA, M. F. R, MARCONCINI, J. M. **Procedimento para Análise Lignocelulósica**. Campina Grande: Embrapa, 2010. 36 p.

- MUNIZ, G. L.; BORGES, A. C.; DA SILVA, T. C. F. Performance of natural coagulants obtained from agro-industrial wastes in dairy wastewater treatment using dissolved air flotation. **Journal of Water Process Engineering**, v. 37, p. 101453, 2020a. <https://doi.org/10.1016/j.jwpe.2020.101453>
- MUNIZ, G. L.; DA SILVA, T. C. F.; BORGES, A. C. Assessment and optimization of the use of a novel natural coagulant (*Guazuma ulmifolia*) for dairy wastewater treatment. **Science of The Total Environment**, v. 744, p. 140864, 2020b. <https://doi.org/10.1016/j.scitotenv.2020.140864>
- NTIBREY, R. A. K.; FRANCIS, A. K.; GYASI, S. F. Antimicrobial and coagulation potential of *Moringa oleifera* seed powder coupled with sand filtration for treatment of bath wastewater from public senior high schools in Ghana. **Heliyon**, v. 6, n. 8, p. e04627, 2020. <https://doi.org/10.1016/j.heliyon.2020.e04627>
- OH, H. S.; KANG, S. H.; NAM, S.; KIM, E.; HWANG, T. CFD modelling of cyclonic-DAF (dissolved air flotation) reactor for algae removal. **Engineering Science and Technology, an International Journal**, v. 22, n. 2, p. 477-481, 2019. <https://doi.org/10.1016/j.jestch.2018.12.003>
- OKORO, V. O.; SUN, Z.; BIRCH, J. Meat processing dissolved air flotation sludge as a potential biodiesel feedstock in New Zealand: A predictive analysis of the biodiesel product properties. **Journal of Cleaner Production**, v. 168, p. 1436-1447, 2017. <https://doi.org/10.1016/j.jclepro.2017.09.128>
- PACHECO, I. S.; ALVES, A. G. T.; SANTANA, L. C.; RIBEIRO, E. A. M.; CANOBRE, S. C. C.; AMARAL, F. A. Performance of cationic hemicelluloses arising from peanut shell residue from agroindustry in application as primary coagulant in physical-chemical treatment of dairy wastewater. **Journal of Water Process Engineering**, v. 47, 2022. <https://doi.org/10.1016/j.jwpe.2022.102661>
- PIOLTINE, A.; REALI, M. A. P. Influência do tamanho dos flocos e da concentração de ar dissolvido na eficiência da flotação. **Engenharia Sanitária e Ambiental**, v. 20., n. 3, p. 513-523, 2015. <https://doi.org/10.1590/S1413-41522015020000090030>
- REN, J. L.; SUN, R. C.; LIU, C. F.; CHAO, Z. Y.; LUO, W. Two-Step Preparation and Thermal Characterization of Cationic 2-Hydroxypropyltrimethylammonium Chloride Hemicellulose Polymers from Sugarcane Bagasse. **Polymer Degradation**, v. 91, p. 2579–2587, 2006. <https://doi.org/10.1016/J.Polyimdegradstab.2006.05.008>
- REN, J. L.; SUN, R. C.; LIU, C. F.; LIN, L.; HE, B. H. Synthesis and characterization of novel cationic SCB hemicelluloses with a low degree of substitution. **Carbohydrate Polymers**, v. 67, p. 347–357, 2007. <https://doi.org/10.1016/j.carbpol.2006.06.002>
- RIBEIRO, E. A. M. **Lignocelulósicos nos processos de purificação de biodiesel por via úmida utilizando flocculantes de fontes renováveis e processo de separação com membranas de celulose regenerada**. 2017. Tese (Mestrado em Biocombustível) - Universidade Federal de Uberlândia, Uberlândia, 2017.
- RIBEIRO, E. A. M.; RODRIGUES FILHO, G.; ROZENO, N. S.; NOGUEIRA, J. M. B. A.; RESENDE, M. A.; THOMPSON JUNIOR, J. P. *et al.* Polymeric polyelectrolytes obtained from renewable sources for biodiesel wastewater treatment by dual-flocculation. **Express Polymer Letters**, v. 11, 2017b. <https://doi.org/10.3144/expresspolymlett.2017.47>

- RIBEIRO, E. A. M.; SOUZA, F. R. B.; AMARAL, F. A.; RODRIGUES FILHO, G.; SOUSA, R. M. F.; VIEIRA, J. G. *et al.* Utilização de hemiceluloses catiônicas, obtidas a partir do aproveitamento da palha de milho, associadas com tanino para o tratamento de efluentes de lavanderia industrial. **Química Nova**, v. 40, n. 1, p. 17-24, 2017a. <https://doi.org/10.21577/0100-4042.20160147>
- ROZAINY, M. M. R.; HASIF, M.; SYAFALNY; PUGANESHWARY, P.; AFIFI, A. Combination of Chitosan and Bentonite as Coagulant Agents in Dissolved Air Flotation. **APCBEE Procedia**, v. 10, p. 229-234, 2014. <https://doi.org/10.1016/j.apcbee.2014.10.044>
- SHAK, K. P. Y.; WU, T. Y. Optimized use of alum together with unmodified Cassia obtusifolia seed gum as a coagulant aid in treatment of palm oil mill effluent under natural pH of wastewater. **Industrial Crops and Products**, v. 76, p. 1169-1178, 2015. <https://doi.org/10.1016/J.Indcrop.2015.07.072>
- SILVA, T. **Estudo de Tratabilidade Físico-Química com uso de Taninos Vegetais em Água de Abastecimento e de Esgoto**. 1999. 85f. Dissertação (Mestrado) – Escola de Saúde Pública, Fundação Oswaldo Cruz, Rio de Janeiro, 1999.
- SNEDECOR, G. W. Cálculo e interpretação da análise de variância e covariância. Collegiate Press. 1934. **APA PsycBooks**. <https://doi.org/10.1037/13308-000>
- TONHATO JUNIOR, A.; HASAN, S. D. M.; SEBASTIEN, N. Y. Optimization of Coagulation/Flocculation Treatment of Brewery Wastewater Employing Organic Flocculant Based on Vegetable Tannin. **Water, Air & Soil Pollution**, v. 230, n. 8, 2019. <https://doi.org/10.1007/s11270-019-4251-5>
- VAZ JUNIOR, S. **Aproveitamento de resíduos agroindustriais: uma abordagem sustentável**. Brasília, DF: Embrapa, 2020. 26 p.
- VIEIRA, J. G.; RODRIGUES, G.; MEIRELES, C.; FARIA, F. A. C.; GOMIDE, D.; PASQUINI, D. *et al.* Synthesis and characterization of methylcellulose from cellulose extracted from mango seeds for use as a mortar additive. **Polímeros**, v. 22, n. 1, p. 80-87, 2012. <http://Dx.Doi.Org/10.1590/S0104-14282012005000011>
- WANG, Y.; SUN, W.; DING, L.; LIU, W.; TIAN, L.; ZHAO, Y. *et al.* A study on the feasibility and mechanism of enhanced co-coagulation dissolved air flotation with chitosan-modified microbubbles. **Journal of Water Process Engineering**, v. 40, p. 101847, 2021. <https://doi.org/10.1016/j.jwpe.2020.101847>



Panorama of the water supply in the Campinas region and a brief comparison with other regions in the Southeast of Brazil

ARTICLES doi:10.4136/ambi-agua.2835

Received: 09 Feb. 2022; Accepted: 06 Jun. 2022

Maria Isabel Andrekowisk Fioravanti* ; **Paulo Henrique Leutevilier Pereira** ;
Laila Martins Camargo ; **Gleize Villela** ; **Elaine Marra de Azevedo Mazon** 

Núcleo de Ciências Químicas e Bromatológicas. Centro de Laboratório Regional de Campinas III.

Instituto Adolfo Lutz (IAL), Rua São Carlos, n° 720, CEP: 13035-420, Campinas, SP, Brazil.

E-mail: paulo.pereira@ial.sp.gov.br, laila.camargo@ial.sp.gov.br, gleize.villela@ial.sp.gov.br,

elaine.mazon@ial.sp.gov.br

*Corresponding author. E-mail: maria.fioravanti@ial.sp.gov.br

ABSTRACT

Access to drinking water is one of the most important factors for health. The lack of access to safe drinking water results in a high prevalence of infections, such as bacterial gastroenteritis and outbreaks of diarrhea. This study evaluated the quality of the public water supply in 42 municipalities located in the eastern region of the State of São Paulo, Brazil, from 2016 to 2020. Physical, chemical, and microbiological parameters were investigated. Sample collection, preservation and analyses were carried out in accordance with national and international standards. The results demonstrated non-compliance with Brazilian legislation for apparent color (1.1%), turbidity (0.4%), fluoride content (14.2%), total coliforms (4.4%) and *Escherichia coli* (*E. coli*) (0.4%). In a brief comparison with other studies in the southeastern region of Brazil, the highest percentage of unsatisfactory samples is due to the fact that fluorine is below the minimum of <0.6 ppm, demonstrating the need for training in the fluoridation process. The need to invest in the training of health surveillance teams to carry out field analyses (chlorine and pH) was also observed. This study can inform future actions, guiding the adoption of preventive and corrective measures and demonstrating the importance of monitoring water-supply quality.

Keywords: drinking water, public health, water quality.

Panorama da água de abastecimento da região de Campinas e uma breve comparação com outras regiões do Sudeste do Brasil

RESUMO

O acesso à água potável é um dos fatores mais importantes para a saúde. A falta de acesso à água potável resulta em alta prevalência de infecções, como gastroenterite bacteriana e surtos de diarreia. Este estudo teve como objetivo avaliar a qualidade da água de abastecimento público em 42 municípios, localizados na região Leste do Estado de São Paulo, Brasil, durante os anos de 2016 a 2020. Os parâmetros investigados incluíam físicos, químicos e microbiológicos. A coleta de amostras, preservação e análises foram realizadas de acordo com as normas nacionais e internacionais. Os resultados obtidos demonstraram não conformidade com a legislação brasileira para cor aparente (1,1%), turbidez (0,4%), fluoreto (14,2%),



This is an Open Access article distributed under the terms of the Creative Commons Attribution License, which permits unrestricted use, distribution, and reproduction in any medium, provided the original work is properly cited.

coliformes totais (4,4%) e *Escherichia coli* (*E. coli*) (0,4%). Em uma breve comparação com outros estudos, o maior percentual de amostras insatisfatórias se deve ao fato de o flúor estar abaixo do mínimo de <0,6 ppm, demonstrando a necessidade de treinamento no processo de fluoretação. A necessidade de investir na capacitação das equipes de vigilância sanitária para realizar análises de campo (cloro e pH) também foi observada. O presente estudo pode ser um guia para ações futuras, orientando a adoção de medidas preventivas e corretivas, demonstrando a importância do monitoramento da qualidade da água de abastecimento.

Palavras-chave: água potável, qualidade da água, saúde pública.

1. INTRODUCTION

Access to safe drinking water is one the most important socioeconomic determinants of the health of a community and is considered one of the main characteristics of a developed country (Tolentino *et al.*, 2019). Consumption of untreated or inadequately treated water remains a major public health burden and can expose the community to the risk of outbreaks of intestinal and other infectious diseases (WHO, 2022).

According to the Guidelines for Drinking Water Quality (WHO, 2022), the safety of drinking water is guaranteed by implementing a Water Safety Plan (WSP), which includes monitoring and verification of quality drinking water, which can be carried out by the supplier, surveillance agencies or a combination of the two. The WHO also emphasizes that the microbial water quality is based on the analysis of faecal indicator microorganisms, the organism of choice being *E. coli*, as it provides conclusive evidence of recent faecal pollution and should not be present in drinking water. The chemical quality of water involves many compounds and contaminants and judicious choices for monitoring and an analysis must be completed before starting an assessment (WHO, 2022).

In Brazil, the quality of drinking water is regulated by the Ministry of Health, which defines the organoleptic, physical, chemical, and bacteriological parameters (Brasil, 2004; 2021). To ensure water quality, three indicators specifically related to compliance with the National Directive are evaluated monthly in the water supplied to a population: Turbidity, Total Coliforms and Residual Disinfectant Agent (Brasil, 2016; 2020). In 1992, the State Program for the Surveillance of Water Quality for Human Consumption (PROÁGUA) was initiated in the State of São Paulo, Brazil, aimed at developing actions to improve the sanitary conditions of the systems and alternative solutions for the water supply and, as a result, to reduce mortality from waterborne diseases (São Paulo, 1992).

In general, even after treatment, the public water supply samples analyzed in several studies in Brazil were exposed to several conflicting factors that could affect their quality, resulting in one or more physicochemical and microbiological parameters in disagreement with the potability standards established and/or recommended by the legislation in force in the country (Palmeira *et al.*, 2019; Douvidauskas *et al.*, 2017a; Freitas *et al.*, 2002; Tolentino *et al.*, 2019; Anversa *et al.*, 2019; Romani *et al.*, 2018; Faria *et al.*, 2021; Scalize *et al.*, 2018). This study therefore evaluated the quality of the public water supply in 42 cities located in the eastern region of the State of São Paulo, Brazil, during the years from 2016 to 2020, and conducted a brief comparison with other studies in the southeastern region of Brazil. The parameters investigated included apparent color, turbidity, fluoride content and the presence of total coliforms and *E. coli*.

2. MATERIAL AND METHODS

2.1. Data collection and sampling

From 2016 to 2020, during the activities of the PROÁGUA Program, the Adolfo Lutz

Institute - Campinas Regional Laboratory Center (IAL-CLR Campinas) received approximately 16,500 samples of treated drinking water obtained from water supply systems and alternative supply solutions in the cities included in the XVII Sanitary Surveillance Group - Campinas (GVS XVII), which comprises 42 cities located in the Eastern region of the State of São Paulo, Brazil. The GVS XVII is divided into four Regions: Metropolitan Campinas, Water Circuit, Jundiaí and Bragança Paulista (Figure 1) with a population of approximately 4,500,000 ($\pm 10\%$ of the population of the State of São Paulo) (IBGE, 2022).

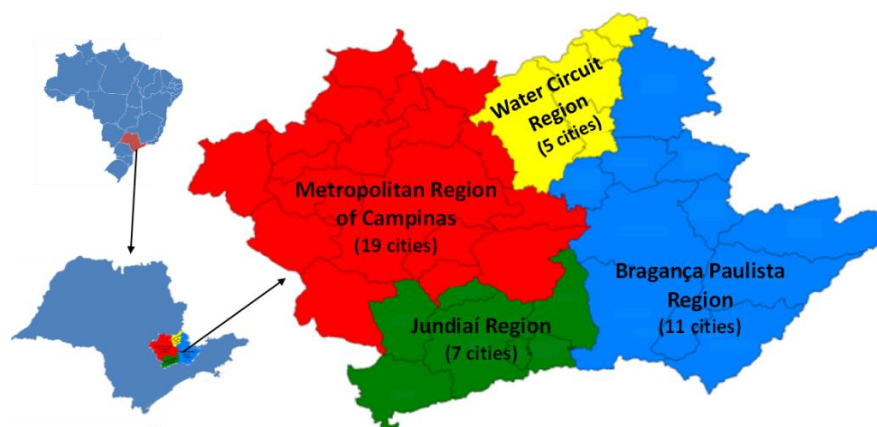


Figure 1. Map according to GVS XVII region.

Source: Elaborated by the authors, 2022.

Regarding the type of water sources evaluated: Amparo, Artur Nogueira, Bom Jesus dos Perdões, Cabreúva, Hortolândia, Itatiba, Jaguariúna, Joanópolis, Lindóia, Monte Mor, Nazaré Paulista, Pedreira, Pinhalzinho, Santo Antônio de Posse, Serra Negra, Valinhos and Vinhedo have mixed water abstraction (surface water and groundwater) offered by water supply systems; Americana, Bragança Paulista, Indaiatuba, Jundiaí, Monte Alegre do Sul, Piracaia, Santa Barbara d'Oeste and Sumaré also have mixed water abstraction, but offered both by water supply systems and alternative supply solutions; Águas de Lindóia, Atibaia, Campinas, Campo Limpo Paulista, Cosmópolis, Holambra, Itupeva, Jarinu, Louveira, Morungaba, Nova Odessa, Paulínia, Socorro, Vargem and Várzea Paulista use surface water and water supply systems; in Pedra Bela and Tuiuti, water is from groundwater and by water supply systems (Brasil, 2022).

The samples were collected by the Municipal Sanitary Surveillance (MSS) teams, according to the basic requirements of the American Public Health Association (APHA *et al.*, 2012) and the sampling plan considered the population density and other criteria, following the criteria established by the National Guideline of the Sampling Plan Surveillance Quality for Drinking Water, defined by the Ministry of Health (Brasil, 2016). The samples were sent to IAL Campinas with a registration form with information concerning the location collected, type of system and data obtained from the analyses carried out in the field (chlorine and pH).

2.2. Analytical methods

To carry out the research, the following physical, chemical, and microbiological parameters were analyzed at the IAL-CLR Campinas. Approximately 200 mL samples of water were collected in sterile, disposable bags. Each sample was analyzed as described in the Standard Methods for The Examination of Water and Wastewater (APHA *et al.*, 2012) for apparent color (visual comparison method 2120 B), turbidity (nephelometric method 2130 B), and fluoride content (ion-selective electrode method 4500-F- C). For the microbiological analyses, 100 mL samples of water were collected in sterile, disposable bags containing sodium thiosulfate. Each sample was evaluated for the presence or absence of total coliforms and *E. coli* by the chromogenic/enzymatic substrate method (Colilert system®, Idexx

Laboratories/USA), method 9223 B as described in APHA *et al.* (2012).

The results were evaluated according to the Decree that establishes the potability standards of water for human consumption (Brasil, 2017; 2011), and Resolution SS-250/1995, which defines the fluoride ion content in water supply systems of the State of São Paulo (São Paulo, 1995).

2.3. Statistical analysis

Statistical analysis was performed with software Jamovi® – Version 1.6.23. For the “satisfactory and unsatisfactory aspects,” the chi-square test was applied. The significance level was set at 5%.

3. RESULTS AND DISCUSSION

Data referring to the field analyses, chlorine and pH, were not considered in this study due to divergences and, frequently, difficulty in understanding the data. Having identified the need for training of MSS teams on how to carry out field analysis.

Most samples from the 42 cities were satisfactory for the parameters analyzed, as can be seen in Table 1. An increase in the number of total samples analyzed over the years is evident. This increase was due to a greater adhesion of cities to the monitoring program over the years and to the increase in the analytical capacity of the laboratory (capacity from 2,928 samples per year in 2016 to 5,460 in 2020).

The number of total samples analyzed did not increase in the year 2020 due to the beginning of the Covid 19 pandemic. With the declaration of the pandemic in April, 2020, many cities required about 2 months to adapt to the new reality according to the sanitary protocols and reorganization of the field teams.

Statistical analysis showed no significant differences between the different years for the parameters of turbidity, total coliforms and *E. coli* in the water samples. However, the percentage of samples that reported the presence of an apparent color and fluoride contents showed significant differences ($p < 0.05$) over the years (Table 1).

For fluoride, the reference value was set by the SES-SP (São Paulo, 1995) value for samples collected in water supply systems and by the Brasil (2017; 2011) legislations (these two legislations did not change the reference values for the parameter analyzed) for samples collected in alternative supply solutions. The unsatisfactory fluoride results obtained in this study were due to values obtained outside the range of 0.6 to 0.8 ppm, as established by SES-SP (São Paulo, 1995).

The number of samples collected in alternative supply solutions correspond to less than 2% of the total samples analyzed, most of them in private systems of closed condominiums in the regions of Jundiaí and Campinas. These samples showed no difference in relation to the water supply systems for the analyzed parameters.

The parameters of apparent color and turbidity (Table 1) showed unsatisfactory values of $1.1 \pm 0.3\%$ and $0.4 \pm 0.1\%$, respectively, percentages lower than those obtained in the study carried out in the same region in the 1990s by Freitas *et al.* (2002), who highlighted that the presence of color and turbidity directly compromised the organoleptic characteristics of the water and, therefore, consumer satisfaction and product suitability.

A total of 2005 (13.5%) water samples analyzed were in disagreement with the legislation for fluoride. This fact was also observed in the study by Freitas *et al.* (2002), but with a much higher percentage of unsatisfactory results (47.8%). It is interesting to note that the parameter of fluoride showed a decrease in the percentage of unsatisfactory samples from 16.5% in 2016 to 11.9% in 2019. This decrease was obtained due to the efforts of cities to adjust the amount of fluorine added after the water treatment. After the declaration of the pandemic in 2020, the percentage of samples showing fluoride outside the recommended range rose again.

Table 1. Analytical results, in numbers of samples (and percentage) per year of the five parameters surveyed.

Parameters	Analytical results ^a	2016 n (%)	2017 n (%)	2018 n (%)	2019 n (%)	2020 n (%)	Total (mean% ± SD)	<i>p</i> ^c
Apparent color	Satisfactory	758 (98.6%)	2943 (99.2%)	3741 (99.1%)	4430 (99.0%)	4427 (98.5%)	16299 (98.9 ± 0.3%)	0.014
	Unsatisfactory	11 (1.4%)	23 (0.8%)	33 (0.9%)	44 (1.0%)	67 (1.5%)	178 (1.1 ± 0.3%)	
Turbidity	Satisfactory	765 (99.5%)	2955 (99.6%)	3758 (99.6%)	4198 (99.5%)	4478 (99.6%)	16154 (99.6 ± 0.1%)	0.843
	Unsatisfactory	4 (0.5%)	11 (0.4%)	16 (0.4%)	21 (0.5%)	16 (0.4%)	68 (0.4 ± 0.1%)	
Fluoride	Satisfactory	632 (83.5%)	2484 (83.9%)	3310 (87.7%)	3592 (88.1%)	2803 (86.1%)	12821 (85.8 ± 2.1%)	<0.001
	Unsatisfactory	125 (16.5%)	478 (16.1%)	464 (12.3%)	484 (11.9%)	454 (13.9%)	2005 (13.5 ± 2.1%)	
Total Coliform ^b	Absence	736 (95.5%)	2836 (95.8%)	3629 (95.9%)	4277 (95.4%)	4285 (95.2%)	15763 (95.6 ± 0.3%)	0.541
	Presence	35 (4.5%)	125 (4.2%)	154 (4.1%)	205 (4.6%)	216 (4.8%)	735 (4.4 ± 0.3%)	
<i>Escherichia coli</i>	Satisfactory	765 (99.4%)	2946 (99.5%)	3773 (99.7%)	4465 (99.6%)	4479 (99.5%)	16428 (99.6 ± 0.1%)	0.352
	Unsatisfactory	5 (0.6%)	15 (0.5%)	10 (0.3%)	16 (0.4%)	21 (0.5%)	67 (0.4 ± 0.1%)	
Total samples (mean)		767	2963	3778	4346	4249	16104	

^aResults based on the legislations Brasil (2011) (2016 and 2017), and Brasil (2017) (2018 to 2020); results for fluoride based on the legislation SES-SP (São Paulo, 1995).

^bIn public water supply samples, the total coliform parameter is just an indicator of the treatment carried out.

^cChi-square test.

Total coliforms and *E. coli* were observed in 735 ($4.4 \pm 0.3\%$) and 67 ($0.4 \pm 0.1\%$) samples, respectively. The result was in agreement with the study carried out by Palmeira *et al.* (2019), which considered that, in general, the occurrence of these bacteria in treated water reflected the hygienic conditions of the raw waters, the efficiency of the treatment process, and the integrity of the distribution system.

The total coliforms in the water does not necessarily represent the probable presence of pathogenic bacteria, protozoa, and/ or pathogenic virus, since this group includes microorganisms that naturally occur in the ground or the vegetation (Alves *et al.*, 2017). The total coliform test is used for routine examination of public water supplies and the objective is to determine the efficiency of treatment plant operations and the integrity of the distribution system (APHA *et al.*, 2012).

Already *E. coli*, with some exceptions, generally does not survive well outside of the intestinal tract, its presence in environmental samples, food, or water usually indicates recent faecal contamination. The presence of *E. coli* in the water does not directly indicate pathogenic microorganisms in the sample, but it does indicate that there is an increased risk of the presence of other bacteria and viruses of fecal origin, such as *Salmonella spp.* or hepatitis A virus. For this reason, *E. coli* is considered a more specific indicator of faecal contamination than total coliforms (Odonkor and Ampofo, 2013). Therefore, in the legislation there is a certain tolerance for the total coliforms, but not for the *E. coli*.

Fioravanti *et al.* (2020) and Tolentino *et al.* (2019) evaluated the physicochemical and microbiological characteristics of samples of alternative water solutions from wells (non-municipal water systems) and observed the presence of apparent color in 8% and 20%, and turbidity in 11% and 4.4%, respectively, of the samples analyzed, values above the percentages determined in the current study. This difference demonstrated the effectiveness of the water treatment systems adopted in the cities of the region.

Although the presence of color is related to consumer rejection, most people can detect color above 15 true color units (TCU) in a glass of water (WHO, 2022). The study by Tolentino *et al.* (2019) observed that a significant percentage of samples with color and turbidity also showed the presence of bacteria from the coliform group, a fact explained by the values for turbidity, caused by sufficiently large suspensions of particles which can harbor microorganisms, resulting in inefficient chlorination of the water. Fioravanti *et al.* (2020) observed the presence of microorganisms, 29% of total coliforms and 9% of *E. coli*, in the total number of samples analyzed, and concluded that the results found interfered with the quality of the water offered in schools, being associated with a lack of investment in the infrastructure of the wells and the lack of water chlorination.

Table 2 presents the results found in the current study and studies carried out by other groups in the Southeast region of Brazil. The total number of samples taken in the current study is higher than the numbers taken in the other studies, evidence of the commitment of the cities and laboratories involved in the control of the water supplied to residents in the Campinas region in recent years.

For the apparent color (A.C.) and turbidity (Turb.) parameters, only data for the following regions of São Paulo state were presented: Campinas, Santos, Bauru and Ribeirão Preto. A difference between the data for Santos, which is located on the coast, and the other regions, is evident. Compared with Ribeirão Preto and Bauru, the data for the apparent color parameter in the current study (Campinas) presented a higher percentage of unsatisfactory samples, whereas for turbidity the results for the three regions were similar.

Table 2. Comparison between the current study and other studies carried out in the Southeast region of Brazil.

Article	Year	Study Region	Total Samples	Parameters: % Unsatisfactory samples						
				A. C. ¹	Turb. ²	Fluoride			T.C. ⁴	<i>E.coli</i>
						% Unsat. ³	< 0.6	> 0.8		
Current study	2016 to 2020	Campinas (SP)	16500	1.1	0.4	13.5	6.6	6.4	4.5	0.4
Freitas <i>et al.</i> (2002)	1991 to 1999	Campinas (SP)	8174	5.3	3.2	59.4	47.8	8.4		
Passos <i>et al.</i> (2012)	2007 to 2008	Santos (SP)	3094	11.8	3.7		6.0	1.0	13.9	4.7
Tavares <i>et al.</i> (2015)	2010 to 2014	Santos (SP)	9175	11.9	4.7	3.9				1.2
Romani <i>et al.</i> (2018)	2007 to 2016	Bauru (SP)	8887			31.1	22.7	8.4		
Palmeira <i>et al.</i> (2019)	2016	Bauru (SP)	2897	0.4	0.5	24.7	14.9	9.7	4.3	0.4
Dovidauskas <i>et al.</i> (2017a; 2017b)	2015 to 2016	Ribeirão Preto (SP)	4347	0.4	0.3	39.8	30.2	9.6	5.9	0.7
Faria <i>et al.</i> (2021)	2013	Rio de Janeiro (RJ)	5322						34.1	14.9
Mendonça <i>et al.</i> (2021)	2014	Espírito Santo (ES)	692			29.4	23.6	5.8		
	2017		713			14.0	13.0	1.0		

¹A.C.: apparent color; ²Turb.: turbidity; ³Unsat.: unsatisfactory fluoride, outside the 0.6 to 0.8 ppm range established by SES-SP (1995); ⁴T.C.: total coliforms.

For all studies presented in Table 2, the highest percentage of unsatisfactory samples is due to the fact that fluorine is outside the established range, especially being below the minimum of <0.6 ppm. This pattern is due to the fact that most Brazilian waters do not have fluorine naturally, being necessary to add it to the water distributed to the population, and also to the difficulties that water treatment plants have in controlling the fluoridation process. Inadequate dosage or overdose of fluoride can put public health at risk in terms of preventing tooth decay or expose the population to the risk of fluorosis, respectively, emphasizing the importance of water monitoring (Palmeira *et al.*, 2019; Romani *et al.*, 2018).

Some developed countries are removing the fluoridation system from their supply. This served as a justification for certain authors, and even for lay people to consider the method outdated and dangerous for populations. However, with regard to oral health, the Brazilian reality cannot be compared with that of developed countries, and the fluoridation of public water supplies is a safe, effective and inexpensive method that has helped humanity to control and prevent caries (Garbin *et al.*, 2017). The findings of Mendonça *et al.* (2021) reinforce the importance of maintaining public policies that guarantee the correct monitoring and maintenance of the quality of fluoridation.

The percentage of total coliforms (T.C.) and *E. coli* found in the current study are the same or below the values found in the other studies shown in Table 2, especially the data found by Faria *et al.* (2021). In general, the occurrence of total coliforms and *E. coli* in treated water reflects the hygienic conditions of the raw waters, the flaws in the treatment and/or, especially, problems with the integrity of the distribution system (Tavares *et al.*, 2015; Palmeira *et al.*, 2019). According to Brazilian legislation (Brasil, 2017), the detection of total coliforms and *E. coli* in the sample must be evaluated so that corrective actions can be taken by those responsible for the supply system and they must inform the public health authority about the measures adopted. These actions were not reported to the laboratory.

4. CONCLUSIONS

The results of this study show a prevalence of satisfactory samples in relation to the analyzed parameters; the results in greater disagreement were related to the fluoride content and the presence of total coliforms, indicating failures in fluoridation and problems in the water distribution system. Monitoring and surveillance of the quality of water supply is an important preventive measure to minimize the risks of health problems.

This study can guide future actions, informing the adoption of preventive and corrective measures, such as the need to invest in the training of health surveillance teams to carry out field analyses (chlorine and pH), training/investments to improve the water fluoridation and chlorination process, as well as investment in the distribution system to minimize the presence of microorganisms.

5. REFERENCES

- ALVES, W.; SILVA, T. I.; MARROM, D. A. S.; SANTOS, T. M. S.; SANTOS, H. R. S. Avaliação da qualidade da água do abastecimento público do Município de Juazeiro do Norte, CE. **Revista Desafios**, v. 4, n. 2, p. 112–119, 2017. <https://doi.org/10.20873/uft.23593652.2017v4n2p112>
- ANVERSA, L.; ARANTES STANCARI, R. C.; GARBELOTTI, M.; DA SILVA RUIZ, L.; PEREIRA, V. B. R.; NOGUEIRA NASCENTES, G. A. *et al.* Pseudomonas aeruginosa in public water supply. **Water Practice and Technology**, v. 14, n. 3, p. 732–737, 2019. <https://doi.org/10.2166/wpt.2019.057>
- APHA; AWWA; WEF. **Standard Methods for the examination of water and wastewater**. 22nd ed. Washington, 2012. 1496 p.
- BRASIL. Departamento de Saúde Ambiental, do Trabalhador e Vigilância das Emergências em Saúde Pública. **Indicadores institucionais do Programa Nacional de Vigilância da Qualidade da Água para consumo humano – 2019**. Brasília, DF, 2020.
- BRASIL. Departamento de Vigilância em Saúde Ambiental e Saúde do Trabalhador. **Diretriz Nacional do Plano de Amostragem da Vigilância da Qualidade da Água para Consumo Humano**. Brasília, DF, 2016.
- BRASIL. Ministério da Saúde. Portaria GM/MS nº 888, de 04 de maio de 2021. Altera o Anexo XX da Portaria de Consolidação GM/MS nº 5, de 28 de setembro de 2017, para dispor sobre os procedimentos de controle e de vigilância da qualidade da água para consumo humano e seu padrão de potabilidade. **Diário Oficial [da] União**: seção 1, Brasília, DF, n. 85, p. 127, 07 de maio 2021.

- BRASIL. Ministério da Saúde. Portaria de Consolidação nº 5, de 28 de setembro de 2017. Consolidação das normas sobre as ações e os serviços de saúde do Sistema Único de Saúde. **Diário Oficial [da] União**: seção 1, Brasília, DF, n. 190, supl., 3 de out. de 2017.
- BRASIL. Ministério da Saúde. Portaria GM/MS nº 518, de 25 de março de 2004. Estabelece os procedimentos e responsabilidades relativos ao controle e vigilância da qualidade da água para consumo humano e seu padrão de potabilidade, e dá outras providências. **Diário Oficial [da] União**: seção 1, Brasília, DF, n. 59, p. 266-270, 26 de mar. 2004.
- BRASIL. Ministério da Saúde. Portaria n. 2.914, de 12 de dezembro de 2011. Dispõe sobre os procedimentos de controle e de vigilância da qualidade da água para consumo humano e seu padrão de potabilidade. **Diário Oficial [da] União**: seção 1, Brasília, DF, p. 39, 14 de dez. de 2011.
- BRASIL. **Portal Brasileiro de Dados Abertos**. 2022. Available: <https://dados.gov.br/dataset/sisagua-tratamento-de-agua>. Access: May 16, 2022.
- DOVIDAUSKAS, S.; OKADA, I. A.; IHA, M. H.; CAVALLINI, A. G.; OKADA, M. M.; BRIGANTI, R. DE C. *et al.* Mapeamento da qualidade da água de abastecimento público no nordeste do estado de São Paulo (Brasil). **Health Surveillance under Debate: Society, Science & Technology**, v. 5, n. 2, p. 53-63, 2017a. <https://doi.org/10.22239/2317-269x.00862>
- DOVIDAUSKAS, S.; OKADA, I. A.; IHA, M. H.; CAVALLINI, A. G.; OKADA, M. M.; BRIGANTI, R. DE C. Quality Assessment of fluoridation of public water supply in 88 municipalities in the Northeast region of the state of São Paulo (Brazil). **Health Surveillance under Debate: Society, Science & Technology**, v. 5, n. 3, p. 14-23, 2017b. <https://doi.org/10.22239/2317-269X.00926>
- FARIA, C. P.; ALMENDRA, R.; DIAS, G. S.; SANTANA, P.; SOUSA, M. C.; FREITAS, M. B. Evaluation of the drinking water quality surveillance system in the metropolitan region of Rio de Janeiro. **Journal of Water and Health**, v. 19, n. 1, p. 306-321, 2021. <https://doi.org/10.2166/wh.2021.217>
- FIORAVANTI, M. I. A.; PEREIRA, P. H. L.; MARCIANO, M. A. M.; SANCHES, V. L.; FERREIRA, C. D. F.; MAZON, E. M.D. Monitoring and evaluation of alternative collective solution for water supply for public schools in Itatiba, SP. **Health Surveillance under Debate: Society, Science & Technology**, v. 8, n. 2, p. 122-133, 2020. <https://doi.org/10.22239/2317-269x.01460>
- FREITAS, V. P. S.; BRIGIDO, B. M.; BADOLATO, M. I.; ALABURDA, J. Padrão físico-químico da água de abastecimento público da região de Campinas. **Revista do Instituto Adolfo Lutz**, v. 61, n. 1, p. 51-58, 2002.
- GARBIN, C. A. S.; SANTOS, L. F. P. DOS; GARBIN, A. J. I.; MOIMAZ, S. A. S.; SALIBA, O. Fluoretação da água de abastecimento público: abordagem bioética, legal e política. **Revista Bioética**, v. 25, n. 2, p. 328-337, 2017. <https://doi.org/10.1590/1983-80422017252193>
- IBGE. **População de Cidades e Estados**. 2022. Available <https://www.ibge.gov.br/cidades-e-estados/sp>. Access: May 06, 2022.

- MENDONÇA, A.; MARTINELLI, K. G.; ESPOSTI, C. D. D.; BELOTTI, L.; PACHECO, K. T. S. Surveillance of public water supply fluoridation and municipal indicators: an analysis in the state of Espírito Santo, Brazil. **Revista Ambiente & Água**, v. 16, n. 3, 2021. <https://doi.org/10.4136/ambi-agua.2693>
- ODONKOR, S. T.; AMPOFO, J. K. Escherichia coli as an indicator of bacteriological quality of water: an overview. **Microbiology Research**, v. 4, n. 1, p. e2, 2013. <https://doi.org/10.4081/mr.2013.e2>
- PALMEIRA, A. R. O. A.; DA SILVA, V. A. T. H.; DIAS JÚNIOR, F. L.; STANCARI, R. C. A.; NASCENTES, G. A. N.; ANVERSA, L. Physicochemical and microbiological quality of the public water supply in 38 cities from the midwest region of the State of São Paulo, Brazil. **Water Environment Research**, v. 1, n. 8, p. 1/8, 2019. <https://doi.org/10.1002/wer.1124>
- PASSOS, E. C.; MELLO, A. R. P.; SOUSA, C. V.; GONZALEZ, E.; JORGE, L. I. F.; SILVA, M. L. P. *et al.* Avaliação microbiológica e físico-química da qualidade das águas para consumo humano realizada na região metropolitana da Baixada Santista, no período de 2007 a 2008. **Boletim do Instituto Adolfo Lutz**, v. 22, n. 1, p. 22-24, 2012.
- ROMANI, C. D.; STANCARI, R. C. A.; NASCENTES, G. A. N.; ANVERSA, L. Public water supply fluoridation: 10 years of monitoring in 38 municipalities of Centro-Oeste Paulista, São Paulo, Brazil. **Health Surveillance under Debate: Society, Science & Technology**, v. 6, n. 4, p. 47-55, 2018. <https://doi.org/10.22239/2317-269x.01169>
- SCALIZE, P. S.; PINHEIRO, R. V. N.; RUGGERI JUNIOR, H. C.; ALBUQUERQUE, A.; LOBÓN, G. S.; ARRUDA, P. N. Heterocontrole da fluoretação da água de abastecimento público em cidades do estado de Goiás, Brasil. **Ciência & Saúde Coletiva**, v. 23, n. 11, p. 3849–3860, 2018. <https://doi.org/10.1590/1413-812320182311.24712016>
- SÃO PAULO. Secretaria de Estado de Saúde. Resolução SS-45, de 31 de janeiro de 1992. Institui o Programa de Vigilância da Qualidade da Água para Consumo Humano-PROÁGUA e aprova diretrizes para sua implantação no âmbito da Secretaria de Saúde. **Diário Oficial [do] Estado**, São Paulo, 31 jan. 1992.
- SÃO PAULO. Secretaria de Estado de Saúde. Resolução SS-250, de 15 de agosto de 1995. Define teores de concentração do íon fluoreto nas águas para consumo humano, fornecidas por sistemas públicos de abastecimento. **Diário Oficial [do] Estado**, Seção I; São Paulo, 16 ago. 1995.
- TAVARES, M.; VIEIRA, A. H.; ALONSO, A. C. B.; MELLO, A. R. P.; SOUSA, C. V.; GONZALEZ, E. *et al.* Avaliação da qualidade microbiológica e físico-química da água para consumo humano na Região Metropolitana da Baixada Santista, Estado de São Paulo, no período de 2010-2014. **Boletim do Instituto Adolfo Lutz**, v. 25, n. 2, p. 10-13, 2015.
- TOLENTINO, F. M.; DE ALMEIDA, I. A. Z. C.; DOS SANTOS, C. C. M.; TEIXEIRA, I. S. C.; E SILVA, S. I. L.; NOGUEIRA, M. C. L. *et al.* Phenotypic and genotypic profile of the antimicrobial resistance of bacterial isolates and evaluation of physical and chemical potability indicators in groundwater in Brazil. **International Journal of Environmental Health Research**, 2019. <https://doi.org/10.1080/09603123.2019.1640354>
- WHO. **Guidelines for drinking-water quality**: fourth edition incorporating the first and second addenda. Geneva, 2022. Available in: <https://www.who.int/publications/i/item/9789241549950>. Access: May 10, 2022.



Distribution and assessment of the environmental risk of heavy metals in Aguada Blanca reservoir, Peru

ARTICLES doi:10.4136/ambi-agua.2838

Received: 22 Feb. 2022; Accepted: 06 Jun. 2022

Alfonso Torres Espirilla^{1*}; **Trinidad Betty Paredes de Gómez²**

¹Academic Department of Biology. Faculty of Biological Sciences. Universidad Nacional de San Agustín de Arequipa, Daniel Alcides Carrión, s/n, 04001, Arequipa, Peru.

²Academic Department of Chemistry. Faculty of Natural and Formal Sciences. Universidad Nacional de San Agustín de Arequipa, Avenida Independencia, s/n, 04001, Arequipa, Peru. E-mail: tparedesz@unsa.edu.pe

*Corresponding author. E-mail: atorrese@unsa.edu.pe

ABSTRACT

Sediments containing high concentrations of heavy metals in reservoirs, lakes and rivers, can resuspend into aquatic environments and negatively impact water quality. The concentrations of 10 elements were studied in surface sediments and water from the Aguada Blanca Reservoir, Peru, an important water source to 1,080,000 people in the arid province of Arequipa. Sediment and water samples were collected from nine points in 2019. The enrichment, accumulation, ecological risk and distribution of metals in sediment were determined, and the information on heavy metals in water was used to assess the quality of the aquatic system. Spatially, heavy metals showed variations throughout the study area, with an increase for most elements near the deepest part of the reservoir. The average concentration of Cd in sediment was 4 times higher than the natural background. In water, As was the only element that exceeded Peruvian regulations ($As > 10 \mu g L^{-1}$). The Enrichment Factor (EF) and Geoaccumulation Index (Igeo) of metals in sediment presented the following order: Cd > As > Pb > Zn > Cu > Ni > Cr, with Ni and Cr being the only elements that did not present enrichment. The most considerable Igeo was Cd (1.21 ± 1.45), presenting a classification of moderately to heavily contaminated. The integrated potential ecological risk (RI) of Cd presented high values in 5 points of the reservoir. The information developed will assist in establishing effective control strategies for the quality of the aquatic system.

Keywords: heavy metals, reservoir, sediments, water quality.

Distribuição e avaliação do risco ambiental de metais pesados no reservatório Aguada Blanca, Peru

RESUMO

Sedimentos contendo altas concentrações de metais pesados em reservatórios, lagos e rios, podem ressuspender no ambiente aquático e impactar negativamente na qualidade da água. A concentração de 10 elementos foi estudada em sedimentos superficiais e na água do reservatório Aguada Blanca, Peru, uma importante fonte de água para 1.080.000 pessoas na árida província de Arequipa. Foram determinados o enriquecimento, acúmulo, risco ecológico e distribuição de metais no sedimento, enquanto as informações de metais pesados na água foram utilizadas para corroborar a qualidade do sistema aquático. Amostras de sedimentos e água foram



This is an Open Access article distributed under the terms of the Creative Commons Attribution License, which permits unrestricted use, distribution, and reproduction in any medium, provided the original work is properly cited.

coletadas em nove pontos em 2019. Espacialmente, os metais pesados apresentaram variações ao longo da área de estudo com aumento para a maioria dos elementos próximos à parte mais profunda do reservatório. A concentração média de Cd no sedimento foi 4 vezes maior do que o fundo natural. Na água, o As foi o único elemento que ultrapassou as regulamentações peruanas ($As > 10 \mu g L^{-1}$). O Fator de Enriquecimento (EF) e Índice de Geoacumulação (Igeo) dos metais no sedimento apresentaram a seguinte ordem: $Cd > As > Pb > Zn > Cu > Ni > Cr$, sendo Ni e Cr os únicos elementos que não apresentaram enriquecimento. O Igeo mais expressivo foi o Cd (1.21 ± 1.45), apresentando uma classificação de moderada a fortemente contaminada. O risco ecológico potencial integrado (RI) do Cd apresentou valores elevados em 5 pontos do reservatório. Os resultados encontrados fornecem informações necessárias para estabelecer estratégias de controle sobre a qualidade do sistema aquático.

Palavras-chave: metais pesados, qualidade da água, reservatório, sedimentos.

1. INTRODUCTION

Reservoirs often present problems of heavy metal accumulation due to sediment retention behind reservoirs (Hahn *et al.*, 2018; Kondolf *et al.*, 2014; Vukovic *et al.*, 2014), which results in contamination or reduction of the quality of the water (Varol, 2013). The accumulation of heavy metals in aquatic systems can lead to human health risks and deterioration of aquatic ecology (Hahn *et al.*, 2018; Hou *et al.*, 2013). Therefore, the accumulation of metals in sediments is the subject of environmental studies in much of the world by environmental researchers (Hou *et al.*, 2013; Marziali *et al.*, 2017).

Reservoirs are of great economic importance because they supply water to the population, agricultural and industrial activities, among others (Schleiss *et al.*, 2016; Yasarer and Sturm, 2016). Therefore, water quality must be monitored because heavy metals are non-biodegradable, persistent, bio accumulative elements and with a tendency to enter the food chain (Keshavarzi and Kumar, 2019). The existence of heavy metals in water bodies is the result of anthropogenic activities and natural processes such as rock weathering and volcanic activities, with aquatic environments being the most susceptible to the negative effects of heavy metal pollution (Hahn *et al.*, 2018; Hou *et al.*, 2013; Keshavarzi and Kumar, 2019).

Sediments are important reservoirs of trace elements and could exchange cations with the aquatic environment, and over time contribute pollutants into the water column due to their constant contact (Yahaya *et al.*, 2012). Trace element concentrations in sediments become a problem when they are enriched above natural background levels due to contamination, which may create a threat to the aquatic environment (Olatunde *et al.*, 2014).

Knowing the concentrations and distribution of heavy metals are very useful to determine the degree of contamination of aquatic environments and provide the necessary information for environmental health risk assessment (Li *et al.*, 2019). The indices commonly used to assess heavy metal contamination in sediments are the Enrichment Factor (EF), the Geoaccumulation Index (I_{geo}) and Integrated Potential Ecological Risk Index (RI) (Barbieri, 2016; Decena *et al.*, 2018).

The present study was carried out in the Aguada Blanca Reservoir, located at 3650 m.a.s.l in the Arequipa region of southern Peru. An important water source to 1,080,000 people in the arid Arequipa province. This reservoir has had sediment removal problems since 1989 due to the inoperability of the discharge gate, promoting sediment accumulation until today (ANA, 2016), which could generate a problem for water quality. This research evaluated the enrichment, geoaccumulation, potential ecological risk, distribution of metals in the reservoir and the relationship between the concentration of metals in sediment and reservoir water.

2. MATERIAL AND METHODS

2.1. Study area

The Aguada Blanca Reservoir is located in the south of the Republic of Peru, in the Arequipa region (Figure 1, A-B), on the slopes of the Misti and Chachani volcanoes about 27 km from the city of Arequipa (19K, 248920 E, 820498 S and 250920 E, 8204980 S). The reservoir is 3.2 km long with an average width of 0.5 km and a maximum depth of 30 m (Figure 1, C-D). The surface of the reservoir is 1.73 km² and accumulates approximately 30 million m³ of water. The function of Aguada Blanca Reservoir is to receive, regulate and distribute the water from six other reservoirs (the Chalchuanca, the Dique de los Españoles, the Bamputañe, the El Pañe, the El Frayle and the Pillones), which feeds the Chili River Basin and supplies water to 1,080,000 people in the city of Arequipa.

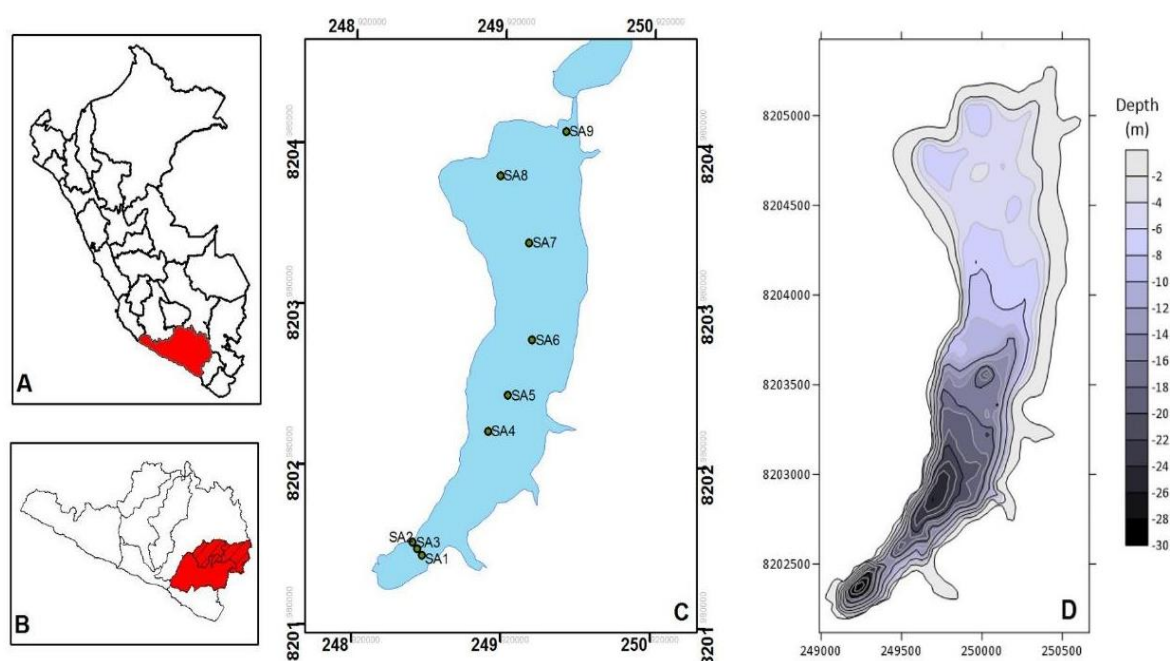


Figure 1. Study area: A). Republic of Peru, B) Arequipa Region, C) Aguada Blanca Reservoir with sampling points, D) Depth of the reservoir.

2.2. Sampling collections and analysis

Sediment and water samples were collected at 9 points in the reservoir (water entry zones, middle zone and reservoir zone), in the months of April, July and October 2019, which were averaged. The water samples were taken with a 250 mL Niskin bottle between 0.5 to 1 meter above the sediment (CCME, 2011), then surface sediment sampling was performed using a Lamotte model dredger (Cavanagh *et al.*, 1997). Sampling depth was determined using an Eagle Cuda 168 graphic echo sounder. The water samples were preserved with analytical grade nitric acid (1%) and deposited in bottles (0.25 L) and sediment samples were placed in polyethylene bags (1 Kg) to be transported to the laboratory in a cooler box with ice.

For the determination of heavy metals in sediment, we used the EPA 200.7 method (Inductively Coupled Plasma Optical Emission Spectrometry, ICP-OES, Perkin Elmer) and the EPA 200.8 method in water (Inductively Coupled Plasma Mass Spectrometry; ICP-MS, Agilent) (APHA *et al.*, 2005), for totals metals. Organic matter was determined using the ASTM D 2974-87 method (ASTM International, 2014), and the pH was determined by the APHA 4500-H + B electrometric method (APHA *et al.*, 2005) using an EXO 2 multiparameter probe (Xylem, USA).

2.3. Reagents and standards

All reagents were of analytical grade or Suprapure quality (Merck, Germany). Double deionized water was used for the preparation of all solutions. Standard solutions of elements used for calibration were prepared by diluting stock solutions of 1000 mg L⁻¹ of each element. The stock standard solutions were Merck Certificate standard. All glasswares used were cleaned by soaking in dilute nitric acid for at least 24 hours and were rinsed thoroughly in deionized water before use.

2.4. Quality control

The quality of the analytical data was assured through the application of quality methods and laboratory control. Method precision and quality control were verified by triplicate analysis of proficiency test material. Good agreement was observed between analytical results and certified values, with recovery percentages ranging from 97% (As) to 106% (Cd).

2.5. Sediment contamination assessment

2.5.1. Enrichment factor

The enrichment factor (EF) is used to determine metal enrichment factors in sediments and soils, as well as to assess the presence and intensity of anthropogenic contaminant deposition on the land surface (Barbieri, 2016). The reference values used were those defined by Turekian and Wedopohl (1961), values widely used by different researchers worldwide. The EF calculation reflects the enrichment of metals in sediments in relation to iron (Fe), which was chosen as a stationary reference element to perform this calculation (Ekenguele *et al.*, 2017), as seen in Equation 1.

$$EF = \frac{\left(\frac{M}{Fe}\right)_{sample}}{\left(\frac{M}{Fe}\right)_{Background}} \quad (1)$$

Where EF = Enrichment Factor; $\left(\frac{M}{Fe}\right)_{sample}$ Is the ratio of metal/Fe in the sample; and $\left(\frac{M}{Fe}\right)_{Background}$ is the metal/Fe ratio of the reference value. EF values are classified as follows: When EF <1 indicates no enrichment; 1 < EF <3 is low; 3 < EF <5 is moderate; 5 < EF <10 is moderately severe; 10 < EF <25 is severe; 25 < EF <50 is very serious; and EF > 50 is extremely severe (Acevedo-Figueroa *et al.*, 2006; Decena *et al.*, 2018).

2.5.2. Geoaccumulation index (I_{geo})

The geo-accumulation index (I_{geo}) was used to assess heavy metal contamination in sediments and is defined as follows (Equation 2) (Li *et al.*, 2019).

$$I_{geo} = \log_2 \frac{C}{kB} \quad (2)$$

Where: C: is the concentration of the sample; B: is the reference value; k: is the geoaccumulation constant (1.5). The I_{geo} value of each heavy metal is classified into seven classes, from uncontaminated to extremely contaminated. Classification of heavy metal contamination according to I_{geo} value: Class 0 (I_{geo} < 0), uncontaminated; Class 1 (0 < I_{geo} ≤ 1), uncontaminated to moderately contaminated; Class 2 (1 < I_{geo} ≤ 2), moderately contaminated; Class 3 (2 < I_{geo} ≤ 3), Moderately to heavily polluted; Class 4 (3 < I_{geo} ≤ 4), heavily contaminated; Class 5 (4 < I_{geo} ≤ 5), strong to extremely contaminated; Class 6 (5 < I_{geo} ≤ 10), extremely contaminated (Li *et al.*, 2019).

2.5.3. Ecological risk index

The potential ecological risk index (RI) is commonly used as a diagnostic tool to determine contamination in sediments, soils and waters due to the presence of metals in the environment. The RI is defined as the sum of the ecological risk index (RE) of each heavy metal, for which Equations 3 and 4 are shown (Hakanson, 1980; Miranzadeh Mahabadi *et al.*, 2020; Sun, 2017).

$$RE = T_r^i \times C_f^i \quad (3)$$

$$RI = \sum_{i=1}^N RE = \sum_{i=1}^N T_r^i \times C_f^i \quad (4)$$

Where: T_r^i is the toxic response factor of different heavy metals, the ecological values of Cd, Pb, Cu, Cr and Zn are 30, 5, 5, 2, 1. $C_f^i = C_i/C_r^i$: is the pollution coefficient of each heavy metal. C_r^i : is the concentration of each heavy metal. C_r^i : is the recommended value for heavy metal concentration in sediments and soils (Sun, 2017), Table 1.

Table 1. Potential ecological risk classification.

Level	Ecological Risk	
	RE	RI
Low	RE < 40	RI < 150
Moderate	40 < RE ≤ 80	150 < RI ≤ 300
Considerable	80 < RE ≤ 160	300 < RI ≤ 600
High	160 < RE ≤ 320	
Very High	RE > 320	> 600

Source: Hakanson (1980); Sun (2017).

2.6. Analysis of data

A mean and standard deviation (SD) were determined for the entire reservoir for all parameters analyzed. Statistical analyses were performed with SPSS statistics v24 software; Pearson correlation analysis ($p < 0.05$) was applied to assess the association between the concentration of metals in sediment and water. Spatial distribution graphs were made with the software Surfer Golden 16.

3. RESULTS AND DISCUSSION

3.1. Heavy metals, pH and organic matter

The heavy metal concentrations found for ten elements analyzed in sediments (mg d.w. Kg⁻¹) are shown in Table 2, where the mean concentration of Cd (1.46 ± 0.94) and the concentrations of As (12.54 ± 5.70) and Pb (16.35 ± 5.59) in some points was higher in relation to values of study by Turekian and Wedepohl (1961), while Cr (7.73 ± 2.16), Sb (1.03 ± 0.92), Ni (7.96 ± 2.86), Cu (35.02 ± 12.36), Zn (45.63 ± 13.60) and Fe (12.984 ± 4.195) presented low values. Cd is characterized by presenting high concentrations in sediments from various parts of the world (Cáceres Choque *et al.*, 2013; El-Radaideh *et al.*, 2017; Vrhovnik *et al.*, 2013; Yahaya *et al.*, 2012). A source of entry of Cd into the environment is anthropogenic; however, the study area is far from the urban area and industrial activities. These high concentrations would be attributed to the geological characteristics of the area (Vargas, 1970), volcanic material and volcanic emissions (Hutton, 1983), since the reservoir is close to two volcanoes (Misti and Chachani). Another source could be atmospheric deposition (Cai *et al.*, 2019). The dynamics of sedimentation and the entry of pollutants is little known for the reservoir.

Table 2. Concentration of heavy metals in sediment (mg d.w. Kg⁻¹), water (µg L⁻¹), pH, organic matter (%) and depth (m) in Aguada Blanca Reservoir, Peru.

Matrix	Points	As	Cr	Cd	Pb	Sb	Ni	Cu	Zn	P	Fe	pH	OM	Depth
Sediment	SA1	20.60	11.05	1.64	22.96	2.80	12.06	48.40	58.80	1773	20000	6.22	5.30	28
	SA2	10.50	6.47	2.53	18.16	1.00	6.62	35.50	43.20	1016	14104	5.96	6.30	24
	SA3	19.50	8.67	0.33	20.76	0.30	10.14	44.30	61.40	408	13289	5.95	6.27	22
	SA4	18.30	8.72	0.34	20.41	0.30	10.34	44.70	63.10	416	12514	5.90	6.15	16
	SA5	13.80	10.68	1.42	18.72	2.30	10.61	46.40	49.70	1492	18255	6.47	4.75	16
	SA6	8.20	5.93	2.20	15.00	0.70	5.73	30.20	38.60	1008	12297	6.02	5.17	10
	SA7	8.80	6.21	2.16	16.28	1.00	5.93	32.50	37.70	954	11275	6.01	5.54	5
	SA8	8.00	6.90	0.20	7.93	0.20	6.53	20.20	35.10	255	7461	5.93	3.44	5
	SA9	5.20	4.91	2.28	6.91	0.70	3.69	13.00	23.10	287	7662	5.86	-	4
	Min	5.20	4.91	0.20	6.91	0.20	3.69	13.00	23.10	255	7461	5.86	3.44	-
	Max	20.60	11.05	2.53	22.96	2.80	12.06	48.40	63.10	1733	20000	6.47	6.30	-
	Mean	12.54	7.73	1.46	16.35	1.03	7.96	35.02	45.63	841	12984	6.04	5.37	-
	SD	5.70	2.16	0.94	5.59	0.92	2.86	12.36	13.60	537	4195	0.19	2.00	-
Water	SA1	9.44	0.30	0.03	0.20	0.20	0.56	1.70	16.65	-	220.80	8.41	-	28
	SA2	11.79	LOD	0.03	0.20	0.20	0.70	2.00	9.67	-	136.10	8.23	-	24
	SA3	10.92	LOD	LOD	LOD	0.20	0.39	1.90	19.83	-	102.90	8.36	-	22
	SA4	11.21	LOD	LOD	LOD	LOD	0.43	1.80	19.12	-	139.30	7.96	-	16
	SA5	7.37	0.50	0.21	0.60	0.20	0.55	1.60	15.98	-	302.00	8.55	-	16
	SA6	12.42	LOD	0.05	0.60	0.20	0.73	2.20	9.85	-	121.70	8.53	-	10
	SA7	120.70	LOD	LOD	0.20	0.20	0.60	1.70	212.50	-	115.60	8.48	-	5
	SA8	11.30	0.20	LOD	0.30	0.20	0.45	2.70	52.29	-	128.50	8.66	-	5
	SA9	138.30	LOD	LOD	0.20	0.20	0.58	1.80	11.92	-	106.40	8.43	-	4
	Min	7.37	0.20	0.03	0.20	0.20	0.39	1.60	9.67	-	102.90	7.96	-	-
	Max	138.30	0.50	0.21	0.60	0.20	0.73	2.70	212.50	-	302.00	8.66	-	-
	Mean	37.05	0.33	0.08	0.33	0.20	0.55	1.93	40.87	-	152.60	8.40	-	-
	SD	52.62	0.18	0.07	0.22	0.07	0.12	0.34	65.65	-	66.08	0.21	-	-

LOD: Limit of Detection – in water; LOD_{Cr}=<0.20; LOD_{Cd}=<0.03; LOD_{Pb}=<0.10; LOD_{Sb}=<0.10.

The sediments had a slightly acidic to neutral pH (5.86 to 6.47). This slight acidity would be explained by the geology of the study area, which is composed of volcanic rocks (Vargas, 1970). Low pH values prevent the adsorption of metals, since under acid conditions there are enough H⁺ ions to bind to the surface of clay and organic matter (Adeniyi *et al.*, 2011), leaving metals available in the water; however, the slightly acidic to neutral pH (5.86 to 6.47) and the basic pH of the deep zone water (7.96 - 8.66) (Table 2), would promote the adsorption of metals.

Other factors influencing heavy metal adsorption are organic matter, anoxic conditions, high Fe and Mn concentrations and low temperatures (Li *et al.*, 2014). The study area presented a considerable percentage of organic matter in the sediments (3.44 - 6.30%), as well as low water temperatures of 7°C to 12°C, which makes these factors reduce the release of metals into water (Li *et al.*, 2014). The adsorption of metals by the sediment is corroborated by the low concentrations found in the water, with the exception of As (Table 2), which presents values above that established in Peruvian regulations, As > 10 µg L⁻¹ (ANA, 2016).

Heavy metal concentrations in water samples (µg L⁻¹) presented the following order: Fe (152 ± 66.08) > Zn (40.87 ± 65.65) > As (37.05 ± 52.62) > Cu (1.93 ± 0.34) > Ni (0.55 ± 0.12) > Pb (0.33 ± 0.22) > Cr (0.33 ± 0.18) > Sb (0.20 ± 0.07) > Cd (0.08 ± 0.07). The results of this study show that the concentrations are high in comparison with the study of two lakes in the central region of Peru where As values were found: 4.2±0.9 µg L⁻¹, for Lake Paca and 4.2±0.9 µg L⁻¹, for Tragadero Lake (Custodio *et al.*, 2021). While in comparison with other international studies, the values of metals were notably high for As, in the case of Cr, Cu, Ni and Pb present low concentrations, while Cd is compatible with other results (see Table 3).

The high concentration of As in the water could be due to the weathering processes of the rocks, which would incorporate As into the aquatic system. This would be reflected in the considerable concentrations of As in the Aguada Blanca Reservoir (Prieto *et al.*, 2016). The concentrations of phosphorus (P) in the sediment would have two effects: it would make As highly available in the aquatic system due to its low adsorption by the sediment (Prieto *et al.*, 2016; Zhang and Selim, 2008), and it would reduce the availability of Cd in the water, as phosphorus works as an adsorption system avoiding its release into the water (Wang and Xing, 2004). This is reflected in the values in Table 2.

Table 4 shows the analyzed data, where a significant positive correlation is observed between the As in the sediment and the other elements in the sediment: Cr, Pb, Ni, Cu, Zn, Sb, and Fe.

The strong correlation of As with the other elements explains its high content in the study area and, consequently, said element would be available in the water. Statistically, no correlation is observed between the concentration of elements in sediment and in the water, possibly the low resuspension of elements in water influences the results.

3.2. Evaluation of sediment contamination

3.2.1. Enrichment factor

The EF of each sampling point was calculated to determine the degree of enrichment in the reservoir sediment. The results are shown in Table 5. We observe that the degree of enrichment presents the following order: Cd (18.78 ± 14.89) > As (3.46 ± 1.14) > Pb (2.93 ± 0.58) > Zn (2.49 ± 0.62) > Cu (2.78 ± 0.57) > Ni (0.43 ± 0.11) > Cr (0.32 ± 0.07), where Ni and Cr, are elements that do not present enrichment, Cd presents different degrees of enrichment from moderate to very severe, while As, Pb, Zn and Cu had a low to moderate degree. An EF value between 0.5 - 1.5 (0.5 < EF < 1.5) indicate natural enrichment and values above 1.5 (EF > 1.5) are characterized by an anthropogenic enrichment (Zhang and Liu, 2002). The EF values in our study are low in relation to the EF values found by Cáceres Choque *et al.* (2013) from Lake Titicaca, which presents the following order Cd (14 - 519) > Pb (32 - 233) > Zn (10 - 162) > Co (6 - 71) > Cu (5 - 15) > Mn (3 - 10) > Ni (1 - 18), where we observe the predominance of Cd, Pb, Zn, Cu in presenting the higher enrichment values. The difference between EF values lies in low Fe values in Lake Titicaca in relation to our Fe concentration.

Table 3. Concentration of heavy metals ($\mu\text{g L}^{-1}$) in water in other studies.

		As	Cd	Cr	Cu	Fe	Ni	Pb	Zn	Reference
Aguada Blanca Reservoir, Peru	Min	7.37	0.03	0.2	1.6	102.9	0.39	0.2	9.67	Present study
	Max	138.3	0.21	0.5	2.7	302	0.73	0.6	212.5	
	Mean	37.05	0.08	0.33	1.93	152.59	0.55	0.33	40.87	
Kralkızı Dam Reservoir	Mean	2.39	0.036	20.06	2.83	58.63	15.75	2.56	5.02	(Varol, 2013)
	Median	0.70	0.018	16.77	nd	51.28	9.78	0.59	4.01	
	Max	22.61	0.25	90.12	9.18	189.24	52.12	26.48	19.6	
Dicle Dam Reservoir	Mean	1.61	0.03	18.58	2.12	62.07	15.86	1.84	4.12	(Varol, 2013)
	Median	0.40	0.014	14.27	nd	55.73	9.99	0.34	2.72	
	Max	14.14	0.322	46.63	9.63	251.62	54.23	14.73	19.32	
Batman Dam Reservoir	Mean	0.71	0.044	16.5	nd	57.66	15.96	1.56	4.09	(Karadede and Ünlü, 2000)
	Median	0.36	nd	12.11	nd	63.11	12.01	0.38	3.45	
	Max	6.11	0.428	40.89	9.08	119.12	36.46	11.12	24.57	
Atatürk Dam Reservoir, Turkey		-	nd	-	25	62	15.4	nd	64	(Karadede and Ünlü, 2000)
Tigris River, Turkey		12.32	nd	48.58	4.52	159.46	17.32	22.03	3.62	(Varol, 2013)
Danjiangkou Reservoir, China		11.08	1.17	6.29	13.32	19.14	1.73	10.59	2.02	(Li <i>et al.</i> , 2008)
Alzate Reservoir, Mexico		-	-	79	70	6923	34	61	68	(Avila-Pérez <i>et al.</i> , 1999)
Reference values		13	0.3	90	45	46700	68	20	95	(Turekian and Wedepohl, 1961)

nd: not detected.

Table 4. Pearson correlation coefficients for elements in sediment and water in Aguada Blanca Reservoir, Peru.

Elements / matrix	As_S	As_W	Cr_S	Cr_W	Cd_S	Cd_W	Pb_S	Pb_W	Sb_S	Sb_W	Ni_S	Ni_W	Cu_S	Cu_W	Zn_S	Zn_W	Fe_S	Fe_W
As_S	1																	
As_W	-0.572	1																
Cr_S	0.845**	-0.598	1															
Cr_W	0.256	-0.366	0.728*	1														
Cd_S	-0.498	0.466	-0.414	-0.156	1													
Cd_W	0.073	-0.316	0.504	0.786*	0.133	1												
Pb_S	0.864**	-0.522	0.734*	0.181	-0.112	0.225	1											
Pb_W	-0.425	-0.151	-0.002	0.513	0.37	0.725*	-0.217	1										
Sb_S	0.344	-0.141	0.663	0.741*	0.348	0.604	0.464	0.364	1									
Sb_W	-0.379	0.184	-0.172	0.227	0.447	0.196	-0.272	0.438	0.300	1								
Ni_S	0.945**	-0.654	0.968**	0.541	-0.5	0.339	0.826**	-0.177	0.512	-0.312	1							
Ni_W	-0.522	0.175	-0.411	-0.126	0.915**	0.196	-0.104	0.569	0.269	0.401	-0.482	1						
Cu_S	0.889**	-0.606	0.854**	0.372	-0.255	0.381	0.969**	-0.123	0.502	-0.294	0.915**	-0.227	1					
Cu_W	-0.403	-0.283	-0.408	-0.168	-0.32	-0.334	-0.556	0.141	-0.559	0.147	-0.382	-0.049	-0.525	1				
Zn_S	0.968**	-0.661	0.799**	0.194	-0.528	0.111	0.894**	-0.374	0.231	-0.481	0.922**	-0.485	0.924**	-0.34	1			
Zn_W	-0.261	0.55	-0.254	-0.181	0.143	-0.236	-0.085	-0.11	-0.077	0.124	-0.262	0.033	-0.13	-0.114	-0.233	1		
Fe_S	0.700*	-0.508	0.837**	0.591	0.106	0.577	0.842**	0.179	0.839**	0.042	0.796*	0.11	0.866**	-0.578	0.666	-0.233	1	
Fe_W	0.355	-0.383	0.779*	0.932**	0.007	0.873**	0.401	0.498	0.833**	0.075	0.617	0.022	0.556	-0.42	0.325	-0.226	0.767*	1

S: Sediment, W: Water.

**. The correlation is significant at the 0.01 level (bilateral); *. The correlation is significant at the 0.05 level (bilateral).

3.2.2. Geoaccumulation index evaluation (I_{geo})

I_{geo} values were calculated to determine contamination in the sediments of Aguada Blanca Reservoir. The results are shown in Table 5, where the Cd value (1.21 ± 1.45) presents values greater than 0 ($I_{geo} > 0$), and presented a degree of contamination from moderately to heavily contaminated, while As (-0.78 ± 0.69), Pb (-0.98 ± 0.62), Cu (-1.05 ± 0.64), Zn (-1.71 ± 0.47) and Cr (-4.18 ± 0.40) do not present contamination for the reservoir. The high EF and I_{geo} of Cd would be a risk in the reservoir in relation to other evaluated elements, and compared to other studies, our Cd I_{geo} would be slightly higher (Abata, 2013; Ekengele *et al.*, 2017; Li *et al.*, 2018; Marziali *et al.*, 2017; Zhang *et al.*, 2017) and less equal to studies where the concentration of Cd is described as a strong anthropogenic effect (Cáceres Choque *et al.*, 2013; Çevik *et al.*, 2009; Li, 2014; Nowrouzi and Pour Khabbaz, 2014).

3.2.3. Ecological risk index

Table 5 shows the RI values of the sediment samples, and they present the following order of risk $Cd > Cu > Pb > Zn > Cr$. The RI value of Points SA3, SA4 and SA8 were less than 150, indicating that these points present a low ecological risk (<150). While Points SA1, SA2, SA5, SA6, SA7 and SA9 presented values higher than 600, which means a high ecological risk due to the presence of heavy metals (see Table 5). The ER value of Cd is the one that most contributes to the ecological risk of the water body; an element that is characterized by increasing the risk in different investigations (Li, 2014; Mohamaden *et al.*, 2017).

3.3. Spatial distribution of metals

The Aguada Blanca Reservoir presents the highest concentrations of As, Sb, Cu, Ni, Zn, Fe, Cr and Pb in the narrow zone of the reservoir (dam - water outlet) and middle zone (Figure 2), zones characterized by greater depths and where the accumulation of sediments is greater. Therefore, there is a higher concentration of heavy metals (Colman *et al.*, 2011). High concentrations of heavy metals would be the result of deposition and low water flow velocities and where fine particles act as sinks (Palanques *et al.*, 2014). Figure 2 shows the spatial distribution of Cd, As, Pb, Cu, Ni, Zn, Cu, Fe and Sb along the Aguada Blanca Reservoir. According to the maps in Figure 2, it is observed that most of the elements present an increase in their concentrations as they approach the narrow zone of the reservoir (dam - water outlet) and the middle zone of the reservoir, with the exception of Cd, which does not present uniformity in its distribution.

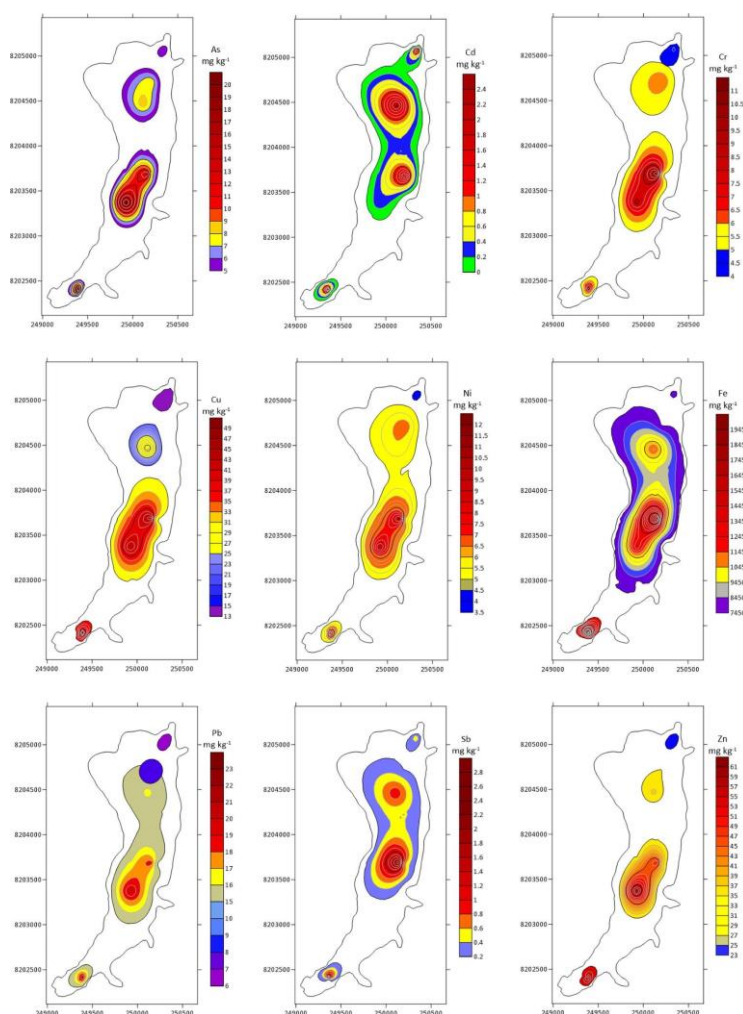


Figure 2. Spatial distribution of heavy metals in sediments of Aguada Blanca Reservoir, Peru.

Table 5. EF, I_{geo}, RE and RI values in Aguada Blanca Reservoir.

Points	EF							I _{geo}							RE					RI
	As	Cr	Cd	Pb	Ni	Cu	Zn	As	Cr	Cd	Pb	Ni	Cu	Zn	Cd	Cu	Pb	Zn	Cr	
SA1	3.7	0.29	12.76	2.68	0.41	2.51	2.02	0.08	-3.61	1.87	-0.39	-3.08	-0.48	-1.28	586	10.08	4.45	0.93	0.33	601.5
SA2	2.72	0.3	12.11	2.39	0.4	2.64	1.87	-0.89	-4.38	2.49	-0.72	-3.95	-0.93	-1.72	904	7.4	3.52	0.68	0.2	915.4
SA3	2.67	0.24	27.92	3.01	0.32	2.61	2.1	0	-3.96	-0.45	-0.53	-3.33	-0.61	-1.21	118	9.23	4.02	0.97	0.26	132.3
SA4	2.4	0.25	27.85	2.85	0.32	2.55	2.16	-0.09	-3.95	-0.4	-0.56	-3.3	-0.59	-1.18	121	9.31	3.96	0.99	0.26	136
SA5	2.8	0.29	29.82	3.37	0.36	2.99	2.3	-0.5	-3.66	1.66	-0.68	-3.27	-0.54	-1.52	507	9.67	3.63	0.78	0.32	521.5
SA6	2.44	0.33	46.32	2.11	0.33	1.76	2.07	-1.25	-4.51	2.29	-1	-4.15	-1.16	-1.88	786	6.29	2.91	0.61	0.18	795.7
SA7	5.27	0.34	3.87	3.65	0.52	3.46	3.17	-1.15	-4.44	2.26	-0.88	-4.1	-1.05	-1.92	771	6.77	3.16	0.59	0.19	782.1
SA8	5.25	0.36	4.23	3.81	0.57	3.71	3.46	-1.29	-4.29	-1.17	-1.92	-3.97	-1.74	-2.02	50	4.21	1.54	0.55	0.21	56.51
SA9	3.85	0.48	4.17	2.48	0.6	2.81	3.23	-1.91	-4.78	2.34	-2.12	-4.79	-2.38	-2.62	814	2.71	1.34	0.36	0.15	818.9
Min	2.4	0.24	3.87	2.11	0.32	1.76	1.87	-1.91	-4.78	-1.17	-2.12	-4.79	-2.38	-2.62	50	2.71	1.34	0.36	0.15	56.51
Max	5.27	0.48	46.32	3.81	0.6	3.71	3.46	0.08	-3.61	2.49	-0.39	-3.08	-0.48	-1.18	904	10.08	4.45	0.99	0.33	915.4
Mean	3.46	0.32	18.78	2.93	0.43	2.78	2.49	-0.78	-4.18	1.21	-0.98	-3.77	-1.05	-1.71	517	7.3	3.17	0.72	0.23	528.9
SD	1.14	0.07	14.89	0.58	0.11	0.57	0.62	0.69	0.4	1.45	0.62	0.56	0.64	0.47	338	2.57	1.08	0.22	0.06	337.1

4. CONCLUSIONS

Sediment quality often reflects the current state of aquatic systems. This study used sediment quality indices to characterize the status of the Aguada Blanca Reservoir in relation to heavy metal concentrations.

According to the quality indices, the reservoir sediments are enriched by Cd, As and Pb, which present concentrations higher than background concentrations and the highest concentrations are distributed in the deeper areas of the reservoir. The high EF and I_{geo} values in Cd would make it a promoter of ecological risks for the aquatic system, if appropriate conditions are given for its availability and mobilization within the system, conditions that would not be currently present due to the low concentration of Cd in the water ($0.08 \pm 0.07 \mu\text{g L}^{-1}$). As concentrations exceed Peruvian regulations and present high values in relation to other aquatic systems.

The results of this study underline that it is important to carry out further studies on the dynamics of mobilization of Cd and As to determine the possible risks to water quality under environmental and hydrological changes.

5. ACKNOWLEDGMENTS

The authors wish to thank Universidad Nacional de San Agustín de Arequipa. This research was funded by Universidad Nacional de San Agustín de Arequipa. Financing Contract N° TIM-002-2018-UNSA.

6. REFERENCES

- ABATA E. O. Assessment of Heavy Metal Contamination and Sediment Quality in the Urban River: A Case Of Ala River in Southwestern – Nigeria. **IOSR Journal of Applied Chemistry**, v. 4, n. 3, p. 56–63, 2013. <https://doi.org/10.9790/5736-0435663>
- ACEVEDO-FIGUEROA, D.; JIMÉNEZ, B. D.; RODRÍGUEZ-SIERRA, C. J. Trace metals in sediments of two estuarine lagoons from Puerto Rico. **Environmental Pollution**, v. 141, n. 2, p. 336–342, 2006. <https://doi.org/10.1016/j.envpol.2005.08.037>
- ADENIYI, A. A. *et al.* Monitoring metals pollution using water and sediments collected from Ebute Ogbo river catchments, Ojo, Lagos, Nigeria. **African Journal of Pure and Applied Chemistry**, v. 5, n. 8, p. 219–223, 2011.
- ANA (Perú). **Plan de aprovechamiento de la disponibilidad hídrica en el ámbito del consejo de recursos hídricos de la cuenca Quilca - Chili 2016 - 2017**. Lima, 2016. p. 145. <https://hdl.handle.net/20.500.12543/4430>
- APHA; AWWA; WEF. **Standard Methods for the Examination of Water and Wastewater**. 21. ed. Washington, 2005.
- ASTM INTERNATIONAL. **ASTM D 2974 - Standard test methods for moisture, ash, and organic matter of peat and other organic soils**. West Conshohocken, 2014. p. 1–4.
- AVILA-PÉREZ, P.; BALCÁZAR, M.; ZARAZÚA-ORTEGA, G.; BARCELÓ-QUINTAL, I.; DÍAZ-DELGADO, C. Heavy metal concentrations in water and bottom sediments of a Mexican reservoir. **Science of the Total Environment**, v. 234, n. 1–3, p. 185–196, 1999. [https://doi.org/10.1016/S0048-9697\(99\)00258-2](https://doi.org/10.1016/S0048-9697(99)00258-2)

- BARBIERI, M. The Importance of Enrichment Factor (EF) and Geoaccumulation Index (Igeo) to Evaluate the Soil Contamination. **Journal of Geology & Geophysics**, v. 5, n. 1, p. 1–4, 2016. <https://doi.org/10.4172/2381-8719.1000237>
- CÁCERES CHOQUE, L. F.; RAMOS RAMOS, O. E.; VALDEZ CASTRO, S. N.; CHOQUE ASPIAZU, R. R.; CHOQUE MAMANI, R. G.; FERNÁNDEZ ALCAZAR, S. G. *et al.* Fractionation of heavy metals and assessment of contamination of the sediments of Lake Titicaca. **Environmental Monitoring and Assessment**, v. 185, n. 12, p. 9979–9994, 2013. <https://doi.org/10.1007/s10661-013-3306-0>
- CAI, K.; YU, Y.; ZHANG, M.; KIM, K. Concentration, source, and total health risks of cadmium in multiple media in densely populated areas, China. **International Journal of Environmental Research and Public Health**, v. 16, n. 13, 2019. <https://doi.org/10.3390/ijerph16132269>
- CAVANAGH, N.; NORDIN, R. N.; SWAIN, L. G.; POMMEN, L. W. **Lake and Stream Bottom Sediment Sampling Manual**. Vancouver: BC, [1997].
- CCME. **Protocols Manual for Water Quality Sampling in Canada**. Winnipeg – Manitoba, 2011.
- ÇEVIK, F.; GÖKSU, M. Z. L.; DERICI, O. B.; FINDIK, Ö. An assessment of metal pollution in surface sediments of Seyhan dam by using enrichment factor, geoaccumulation index and statistical analyses. **Environmental Monitoring and Assessment**, v. 152, n. 1–4, p. 309–317, 2009. <https://doi.org/10.1007/s10661-008-0317-3>
- COLMAN, J. A.; MASSEY, A. J.; LEVIN, S. B. **Determination of Dilution Factors for Discharge of Aluminum-Containing Wastes by Public Water-Supply Treatment Facilities into Lakes and Reservoirs in Massachusetts**. Northborough: U.S. Geological Survey, 2011. (Scientific Investigations Report 2011 – 5136).
- CUSTODIO, M.; FOW, A.; CHANAMÉ, F.; ORELLANA-MENDOZA, E.; PEÑALOZA, R.; ALVARADO, J. C. *et al.* Ecological Risk Due to Heavy Metal Contamination in Sediment and Water of Natural Wetlands with Tourist Influence in the Central Region of Peru. **Water**, v. 13, n. 16, 2021. <https://doi.org/10.3390/w13162256>
- DECENA, S. C. P.; ARGUELLES, M. S.; ROBEL, L. L. Assessing heavy metal contamination in surface sediments in an urban river in the Philippines. **Polish Journal of Environmental Studies**, v. 27, n. 5, p. 1983–1995, 2018. <https://doi.org/10.15244/pjoes/75204>
- EKENGELE, L. N.; BLAISE, A.; JUNG, M. C. Accumulation of heavy metals in surface sediments of Lere Lake, Chad. **Geosciences Journal**, v. 21, n. 2, p. 305–315, 2017. <https://doi.org/10.1007/s12303-016-0047-4>
- EL-RADAIDEH, N.; AL-TAANI, A. A.; AL KHATEEB, W. M. Characteristics and quality of reservoir sediments, Mujib Dam, Central Jordan, as a case study. **Environmental Monitoring and Assessment**, v. 189, n. 4, 2017. <https://doi.org/10.1007/s10661-017-5836-3>
- HAHN, J.; OPP, C.; EVGRAFOVA, A.; GROLL, M.; ZITZER, N.; LAUFENBERG, G. Impacts of dam draining on the mobility of heavy metals and arsenic in water and basin bottom sediments of three studied dams in Germany. **Science of the Total Environment**, v. 640–641, p. 1072–1081, 2018. <https://doi.org/10.1016/j.scitotenv.2018.05.295>

- HAKANSON, L. An ecological risk index for aquatic pollution control. a sedimentological approach. **Water Research**, v. 14, n. 8, p. 975–1001, 1980. [https://doi.org/10.1016/0043-1354\(80\)90143-8](https://doi.org/10.1016/0043-1354(80)90143-8)
- HOU, D.; HE, J.; LÜ, C.; REN, L.; FAN, Q.; WANG, J. *et al.* Distribution characteristics and potential ecological risk assessment of heavy metals (Cu, Pb, Zn, Cd) in water and sediments from Lake Dalinouer, China. **Ecotoxicology and Environmental Safety**, v. 93, p. 135–144, 2013. <https://doi.org/10.1016/j.ecoenv.2013.03.012>
- HUTTON, M. Sources of cadmium in the environment. **Ecotoxicology and Environmental Safety**, v. 7, n. 1, p. 9–24, 1983. [https://doi.org/10.1016/0147-6513\(83\)90044-1](https://doi.org/10.1016/0147-6513(83)90044-1)
- KARADEDE, H.; ÜNLÜ, E. Concentrations of some heavy metals in water, sediment and fish species from the Ataturk Dam Lake (Euphrates), Turkey. **Chemosphere**, v. 41, n. 9, p. 1371–1376, 2000. [https://doi.org/10.1016/s0045-6535\(99\)00563-9](https://doi.org/10.1016/s0045-6535(99)00563-9)
- KESHAVARZI, A.; KUMAR, V. Spatial distribution and potential ecological risk assessment of heavy metals in agricultural soils of Northeastern Iran. **Geology, Ecology, and Landscapes**, v. 4, n. 2, 2019. <https://doi.org/10.1080/24749508.2019.1587588>
- KONDOLF, G. M. *et al.* Sustainable sediment management in reservoirs and regulated rivers: Experiences from five continents. **Earth's Future**, v. 2, n. 5, p. 256–280, 2014. <https://doi.org/10.1002/2013ef000184>
- LI, F.; XIAO, M.; ZHANG, J.; LIU, C.; QIU, Z.; CAI, Y. Spatial distribution, chemical fraction and fuzzy comprehensive risk assessment of heavy metals in surface sediments from the honghu lake, China. **International Journal of Environmental Research and Public Health**, v. 15, n. 2, p. 1–17, 2018. <https://doi.org/10.3390/ijerph15020207>
- LI, J. Risk assessment of heavy metals in surface sediments from the Yanghe River, China. **International Journal of Environmental Research and Public Health**, v. 11, n. 12, p. 12441–12453, 2014. <https://doi.org/10.3390/ijerph111212441>
- LI, S.; XU, Z.; CHENG, X.; ZHANG, Q. Dissolved trace elements and heavy metals in the Danjiangkou Reservoir, China. **Environmental Geology**, v. 55, p. 977–983, 2008. <https://doi.org/10.1007/s00254-007-1047-5>
- LI, X.; SHEN, H.; ZHAO, Y.; CAO, W.; HU, C.; SUN, C. Distribution and potential ecological risk of heavy metals in water, sediments, and aquatic macrophytes: A case study of the junction of four rivers in Linyi City, China. **International Journal of Environmental Research and Public Health**, v. 16, n. 16, 2019. <https://doi.org/10.3390/ijerph16162861>
- MARZIALI, L.; TARTARI, G.; SALERNO, F.; VALSECCHI, L.; BRAVI, C.; LORENZI, E. *et al.* Climate change impacts on sediment quality of Subalpine reservoirs: Implications on management. **Water (Switzerland)**, v. 9, n. 9, p. 1–18, 2017. <https://doi.org/10.3390/w9090680>
- MIRANZADEH MAHABADI, H.; RAMROUDI, M.; ASGHARIPOUR, M. R.; RAHMANI, H. R.; AFYUNI, M. Evaluation of the ecological risk index (Er) of heavy metals (HMs) pollution in urban field soils. **SN Applied Sciences**, v. 2, n. 1420, 2020. <https://doi.org/10.1007/s42452-020-03219-7>
- MOHAMADEN, M. I. I.; KHALIL, M. K.; DRAZ, S. E. O.; HAMODA, A. Z. M. Ecological risk assessment and spatial distribution of some heavy metals in surface sediments of New Valley, Western Desert, Egypt. **Egyptian Journal of Aquatic Research**, v. 43, n. 1, p. 31–43, 2017. <https://doi.org/10.1016/j.ejar.2016.12.001>

- NOWROUZI, M.; POURKHABBAZ, A. Application of geoaccumulation index and enrichment factor for assessing metal contamination in the sediments of Hara Biosphere Reserve, Iran. **Chemical Speciation and Bioavailability**, v. 26, n. 2, p. 99–105, 2014. <https://doi.org/10.3184/095422914x13951584546986>
- OLATUNDE, K. A.; AROWOLO, T. A.; BADA, B. S.; TAIWO, A. M.; OJEKUNLE, Z. O. Distribution and enrichment of metals in sediments of the Ogun River within Abeokuta, south-western Nigeria. **African Journal of Aquatic Science**, v. 39, n. 1, p. 17–22, 2014. <https://doi.org/10.2989/16085914.2014.882287>
- PALANQUES, A.; GRIMALT, J.; BELZUNCES, M.; ESTRADA, F.; PUIG, P.; GUILLÉN, J. Massive accumulation of highly polluted sedimentary deposits by river damming. **Science of the Total Environment**, v. 497–498, p. 369–381, 2014. <https://doi.org/10.1016/j.scitotenv.2014.07.091>
- PRIETO, D. M.; MARTÍN-LIÑARES, V.; PIÑEIRO, V.; BARRAL, M. T. Arsenic Transfer from As-Rich Sediments to River Water in the Presence of Biofilms. **Journal of Chemistry**, v. 2016, 2016. <https://doi.org/10.1155/2016/6092047>
- SCHLEISS, A. J.; FRANCA, M. J.; JUEZ, C.; DE CESARE, G. Reservoir sedimentation. **Journal of Hydraulic Research**, v. 54, n. 6, p. 595–614, 2016. <https://doi.org/10.1080/00221686.2016.1225320>
- SUN, Y. Ecological risk evaluation of heavy metal pollution in soil based on simulation. **Polish Journal of Environmental Studies**, v. 26, n. 4, p. 1693–1699, 2017. <https://doi.org/10.15244/pjoes/68889>
- TUREKIAN, K. K.; WEDEPOHL, K. H. Distribution of the elements in some major units of earth's crust. **Geological Society of America Bulletin**, v. 72, n. 2, p. 175–192, 1961. [https://doi.org/10.1130/0016-7606\(1961\)72\[175:DOTEIS\]2.0.CO;2](https://doi.org/10.1130/0016-7606(1961)72[175:DOTEIS]2.0.CO;2)
- VARGAS, L. Geología del cuadrángulo de Arequipa. **Boletín Ingemmet**, n. 24, 1970.
- VAROL, M. Dissolved heavy metal concentrations of the kralkizi, dicle and batman dam reservoirs in the tigris river basin, turkey. **Chemosphere**, v. 93, n. 6, p. 954–962, 2013. <https://doi.org/10.1016/j.chemosphere.2013.05.061>
- VRHOVNIK, P.; ŠMUC, N. R.; DOLENEC, T.; SERAFIMOVSKI, T.; DOLENEC, M. An evaluation of trace metal distribution and environmental risk in sediments from Lake Kalimanci (FYR Macedonia). **Environmental Earth Sciences**, v. 70, n. 2, p. 761–775, 2013. <https://doi.org/10.1007/s12665-012-2166-1>
- VUKOVIC, D.; VUKOVIC, Z.; STANKOVIC, S. The impact of the Danube Iron Gate Dam on heavy metal storage and sediment flux within the reservoir. **Catena**, v. 113, p. 18–23, 2014. <https://doi.org/10.1016/j.catena.2013.07.012>
- WANG, K.; XING, B. Mutual effects of cadmium and phosphate on their adsorption and desorption by goethite. **Environmental Pollution**, v. 127, n. 1, p. 13–20, 2004. [https://doi.org/10.1016/s0269-7491\(03\)00262-8](https://doi.org/10.1016/s0269-7491(03)00262-8)
- YAHAYA, M. I. *et al.* Seasonal potential toxic metals contents of Yauri river bottom sediments: North western Nigeria. **Journal of Environmental Chemistry and Ecotoxicology**, v. 4, n. October, p. 212–221, 2012. <https://doi.org/10.5897/jece11.080>

- YASARER, L. M. W.; STURM, B. S. M. Potential impacts of climate change on reservoir services and management approaches. **Lake and Reservoir Management**, v. 32, n. 1, p. 13–26, 2016. <https://doi.org/10.1080/10402381.2015.1107665> .
- ZHANG, H.; SELIM, H. Magdi. Competitive sorption-desorption kinetics of arsenate and phosphate in soils. **Soil Science**, v. 173, n. 1, p. 3–12, 2008. <https://doi.org/10.1097/ss.0b013e31815ce750>
- ZHANG, J.; LIU, C. L. Riverine composition and estuarine geochemistry of particulate metals in China - Weathering features, anthropogenic impact and chemical fluxes. **Estuarine, Coastal and Shelf Science**, v. 54, n. 6, p. 1051–1070, 2002. <https://doi.org/10.1006/ecss.2001.0879>
- ZHANG, Y.; LIU, S.; CHENG, F.; COXIXO, A.; HOU, X.; SHEN, Z. *et al.* Spatial Distribution of Metals and Associated Risks in Surface Sediments Along a Typical Urban River Gradient in the Beijing Region. **Archives of Environmental Contamination and Toxicology**, v. 74, n. 1, p. 80–91, 2017. <https://doi.org/10.1007/s00244-017-0462-1>



Water scarcity footprint of cocoa irrigation in Bahia

ARTICLES doi:10.4136/ambi-agua.2840

Received: 08 Mar. 2022; Accepted: 13 Jul. 2022

Kelly Félix Olegário^{1*}; **Edilene Pereira Andrade²**; **Ana Paula Coelho Sampaio³**;
Joan Sanchez Matos⁴; **Maria Cléa Brito de Figueirêdo⁵**;
José Adolfo de Almeida Neto¹

¹Programa de Pós-graduação em Desenvolvimento e Meio Ambiente. Universidade Estadual de Santa Cruz (UESC), Rodovia Ilhéus, km 16, s/n, CEP: 45662-900, Ilhéus, BA, Brazil. E-mail: jalmeida@uesc.br

²Inèdit Innovació, S.L. UAB Research Park, 08193, Bellaterra, Barcelona, Spain.

E-mail: edilene.pereira@estudiants.urv.cat

³Programa de Pós-graduação em Ciências Naturais. Universidade Estadual do Ceará (UECE), Avenida Doutor Silas Munguba, n° 1700, CEP: 60714 – 903, Campus do Itaperi, Fortaleza, CE, Brazil.

E-mail: anapaulacsampaio@gmail.com

⁴Departamento de Ingeniería. Red Peruana de Análisis de Ciclo de Vida y Ecología Industrial. Pontificia Universidad Católica del Perú, Avenida Universitaria, n° 1801, 15088, San Miguel,

Lima, Peru. E-mail: joan.s.matos@gmail.com

⁵Embrapa Agroindústria Tropical. Empresa Brasileira de Pesquisa Agropecuária (Embrapa), Rua Doutora Sara Mesquita, n° 2.270, CEP: 60511-110, Fortaleza, CE, Brazil. E-mail: clea.figueiredo@embrapa.br

*Corresponding author. E-mail: kelly_olegario@yahoo.com.br

ABSTRACT

This study simulated the water scarcity footprint (WSF) of cocoa irrigation in municipalities considered suitable for cocoa growing in the state of Bahia, according to agro climatic zoning. Irrigation demand was calculated using the model proposed by FAO (Food and Agriculture Organization of the United Nations). Subsequently, impact on water scarcity was calculated using the product of crop irrigation demand and water scarcity characterization factors of the regionalized AWARE method for Brazil. The WSF in Bahia ranged between 0.28 and 646.5 m³ of water per kilo of cocoa produced. From the defined scale, of the 417 municipalities in Bahia suitable for growing cocoa, 59% have a 'low' footprint, 18% 'medium', 10% 'high', and 12% have a 'very high' footprint. Based on these results, it is suggested that areas with lower WSF are a priority in the expansion of cocoa to avoid a possible compromise of other essential demands of the municipalities. In addition, irrigation should avoid waste, especially in regions with high levels of water scarcity. The results show that the inclusion of the WSF in agroclimatic zoning can contribute to the process of identifying potential and critical regions for new crops and the expansion of others.

Keywords: agriculture, agroclimatic zoning, AWARE, environmental indicator.

Pegada de escassez hídrica do cacau irrigado na Bahia

RESUMO

Este estudo teve como objetivo simular a pegada de escassez hídrica (PEH) da irrigação do cacau a ser produzido nos municípios considerados aptos para o cultivo de cacau no estado da Bahia, de acordo com o zoneamento agroclimático. O modelo proposto pela FAO (Organização das Nações Unidas para a Alimentação e a Agricultura), foi utilizado para calcular



This is an Open Access article distributed under the terms of the Creative Commons Attribution License, which permits unrestricted use, distribution, and reproduction in any medium, provided the original work is properly cited.

a demanda de irrigação. Posteriormente, o impacto na escassez hídrica foi calculado através do produto entre a demanda de irrigação da cultura e os fatores de caracterização da escassez hídrica do método AWARE regionalizado para o Brasil. A PEH na Bahia variou entre 0,28 e 646,5 m³-eq de água por quilo de cacau produzido. A partir da escala definida, dos 417 municípios baianos aptos para o cultivo de cacau, 59% possui uma PEH ‘baixa’, 18% ‘média’, 10% ‘alta’ e 12% possui uma pegada ‘muito alta’. Com base nestes resultados, sugere-se que as áreas com menor PEH sejam prioritárias na expansão do cacau para evitar um possível comprometimento de outras demandas essenciais dos municípios. Além disso, a irrigação deve evitar desperdícios, principalmente, em regiões com altos índices de escassez de água. Os resultados mostram que a inclusão da PEH em zoneamentos agroclimáticos pode contribuir no processo de identificação de regiões potenciais e críticas para novos cultivos e expansão de outros.

Palavras-chave: agricultura, AWARE, indicador ambiental, zoneamento agroclimático.

1. INTRODUCTION

Cocoa (*Theobroma cacao* L.) is grown in the humid tropical regions of Africa, Central and South America, and Asia. It is considered one of the most important perennial crops globally, as it is the raw material for chocolate. Brazil has been among the largest cocoa producers in the world for decades, currently occupying the sixth position in the world ranking, with almost 280 thousand tons produced per year (IBGE, 2021).

Production in southern Bahia, which has also been among the largest cocoa producers in the world (AIPC, 2021), is historic for Brazil. The region is considered a traditional cocoa growing area due to soil fertility and favorable climate conditions, contributing strongly to socioeconomic development in the region (Piasentin and Saito, 2014). The challenge for cocoa production lies in the expansion of cocoa farming to other regions, promoting irrigation systems and full-sun farming (Almeida *et al.*, 2014; Babadele, 2018; Begiato *et al.*, 2009; Sodré *et al.*, 2017; SENAR, 2018).

The critical factor in cocoa's productivity is water availability, as the cocoa tree consumes large amounts of water, and is very sensitive to water deficit in the soil (Carr and Lockwood, 2011). Precipitation for the cocoa tree must be greater than 1200 mm per year to be considered fair for production, and ideal rainfall must vary between 1800 to 2500 mm per year. In regions with precipitation below 1200 mm per year, additional irrigation is required (Carr and Lockwood, 2011; SENAR, 2018; Souza *et al.*, 2016).

Despite its importance in guaranteeing production and increasing productivity, irrigation can reduce available water resources, since irrigated agriculture is responsible for the withdrawal of 70% of the world's freshwater (FAO, 2020). In addition to competing with other environmental uses and services, irrigated agriculture is the sector that wastes the most water in Brazil. According to Olivo and Ishiki (2015), 60% of water intended for irrigation is lost due to failures in irrigation channels, application of excess water, and evapotranspiration.

In this context of global water scarcity, tools and methods are required to quantify and adequately address adverse environmental impacts (Boulay *et al.*, 2018). In 2014, the Water Scarcity Footprint (WSF) of products and organizations was recognized as an important environmental management tool, based on the ISO 14046 standard, to assess the potential impacts of products and processes throughout the life cycle in the intensification of water scarcity of a region (ISO, 2014). The assessment of the WSF provides information that can contribute to the identification of critical processes in the life cycle of a product, supporting decision-making on the performance of its processes, combining the efficient use of water, and improving water availability locally (Aldaya *et al.*, 2008).

This study therefore assesses potential water scarcity impact arising from cocoa irrigation in the Bahia region.

2. MATERIALS AND METHODS

2.1. Definition of the study area

The studied area comprises the 417 municipalities considered suitable for cocoa cultivation, according to the Agro Climatic Zoning of cocoa for the state of Bahia (Brasil, 2011).

2.2. Cocoa Irrigation Demand Calculation

Water irrigation demand (WID) for cocoa was estimated based on the FAO methodology (Allen *et al.*, 1998) and expressed considering the actual crop evapotranspiration (ET_c), the effective precipitation (P_{ef}) and the irrigation system efficiency (Equation 1). ET_c parameter indicates the amount of water (mm) needed by the plant in a given period to develop correctly. It was assumed that the irrigation requirement is equal to the crop evapotranspiration (ET_c) when the P_{ef} is zero and equal to the difference between the ET_c and the P_{ef} when the P_{ef} is different from zero. The WID was divided by the efficiency of the drip irrigation system, assumed to be 95% according to the National Water Agency (ANA) manual (ANA, 2019). Drip irrigation is the main irrigation system used in Bahia for cocoa irrigation (Brasil, 2011).

$$WID = \frac{(ET_c - P_{ef})}{Efficiency} \quad (1)$$

ET_c is obtained by the product between the reference evapotranspiration (ET_o) and the crop coefficient (k_c) (Equation 2). ET_o indicates the water requirement (mm) for a reference crop. ET_o data were obtained by the Penman-Monteith equation (Allen *et al.*, 1998), collected in the WorldClim 2 database (Fick and Hijmans, 2017). The factor k_c is related to crop characteristics and varies over the growing period (Allen *et al.*, 1998). Given the need for this coefficient and its difficult calculation, FAO provides a table of coefficients for each stage of different crops (Allen *et al.*, 1998).

$$ET_c = ET_o \times k_c \quad (2)$$

According to FAO (Allen *et al.*, 1998), the k_c coefficient for cocoa is 1 for the vegetative growth phase, formation of new shoots and leaves on the plants, and 1.05 in the second year, when the plant's vegetative development takes place. From the third year onwards, during flowering and fruit development, the value of k_c is also 1.05. To calculate the WID, the stage of total cocoa production was considered for all municipalities; therefore, k_c was equal to 1.05.

Finally, to calculate the effective precipitation for each region, the method of the United States Department of Agriculture's Soil Conservation Service (USDA, 1970), based on total precipitation (P_{total}) was used, as suggested by the FAO (Equations 3 and 4).

$$P_{ef} = \frac{(P_{total} \times (125 - 0.2))}{125}, \text{ when } P_{total} < 250 \text{ mm} \quad (3)$$

$$P_{ef} = 125 + (0.1 \times P_{total}), \text{ when } P_{total} \geq 250 \text{ mm} \quad (4)$$

2.3. Calculation of the WSF of cocoa irrigation in Bahia

An average life cycle of 25 years and average productivity of 2,500 kg ha⁻¹ was assumed to calculate the WSF. The WDI per kilogram of cocoa per month was multiplied by the monthly characterization factors (CFs, expressed in m³-eq) from Andrade *et al.* (2019). Andrade *et al.* (2019) regionalized the AWARE method (Boulay *et al.*, 2018) for Brazilian state hydrographic units (SHU) using national data from ANA. FSM results were expressed in m³-eq kg⁻¹ of cocoa.

The AWARE method was recommended by the United Nations Environment Program (UNEP) and the Society for Environmental Toxicology and Chemistry (SETAC) to assess impacts related to water scarcity in Life Cycle Assessment (LCA) studies of products and processes (UNEP/SETAC, 2016). AWARE assesses the potential for water deprivation for humans and aquatic ecosystems, considering that the lower the availability of water in a given region, the greater the likelihood of water scarcity (Boulay *et al.*, 2018).

AWARE provides characterization factors (CFs) - a ratio applied to translate water consumption to a potential impact on water scarcity - from 0.1 (assumed as very low water scarcity potential) to 100 (very high water scarcity potential). A qualitative assessment of CFs was proposed by Andrade *et al.* (2019) to better guide users from recommendations (Table 1).

Table 1. Definition of ranges for qualitative assessment of water scarcity characterization factors.

Range	Definition	Qualitative potential impact on the watershed's water scarcity
= 0.1	Minimum CF value defined by the method	Very low
0.02 – 33.3	Linear distribution of CFs between minimum and maximum values of the method.	Low
33.4 – 66.6		Medium
66.7 – 99.9		High
= 100	Maximum CF value defined by the method	Very high

There is currently no scale to qualitatively define the calculated WSF. However, it is important to consider presenting the results at this scale to facilitate the identification of less and more critical regions in Bahia when installing a new cocoa orchard. In the present work, a scale from 'Low WSF' to 'Very high WSF' was adopted, considering a linear division of the WSF values of the municipalities. Thus, the scale between 0 (minimum WSF found in the present study) and 700 (maximum value found in the present study) for WSF was considered (Table 2).

Table 2. Definition of ranges for qualitative assessment of water scarcity footprint (WSF).

WSF ($\text{m}^3\text{-eq kg}^{-1}$ of cacao)	WSF qualitative classification
0 – 165	Low WSF
165.1 – 330	Medium WSF
330.1 – 495	High WSF
495.1 – 700	Very High WSF

3. RESULTS AND DISCUSSION

3.1. Water demand for cocoa irrigation in Bahia

The precipitation in Bahia municipalities varies from 299.5 mm (in Sobradinho) to 1707.3 mm (in Cairu on the coast). A total of 50 municipalities in the state have precipitation equal to or greater than 1200 mm. The average annual reference evapotranspiration of the municipalities ranges from 1356.6 to 1980.3 mm. The west, south, and southwest regions of Bahia are the most favorable for cultivation, as they have the best precipitation values, potential lower irrigation demands, and SHUs with low scarcity impact.

The demand for irrigation in the state ranged from 1.26 to 7.1 $\text{m}^3 \text{kg}^{-1}$. Naranjo-Merino *et al.* (2018) accounted for the irrigation water consumption of cocoa production in Colombia and

presented an average of $18.876 \text{ m}^3 \text{ kg}^{-1}$. The demand for irrigation in the municipalities was below the average (up to 93.3%) found by the authors mentioned above due to the favorable weather conditions in Bahia.

3.2. Water scarcity footprint of irrigated cocoa in Bahia

The annual WSF for irrigation of cocoa produced in Bahia ranged from 0.28 to $646.5 \text{ m}^3\text{-eq kg}^{-1}$ of cocoa (Figure 1).

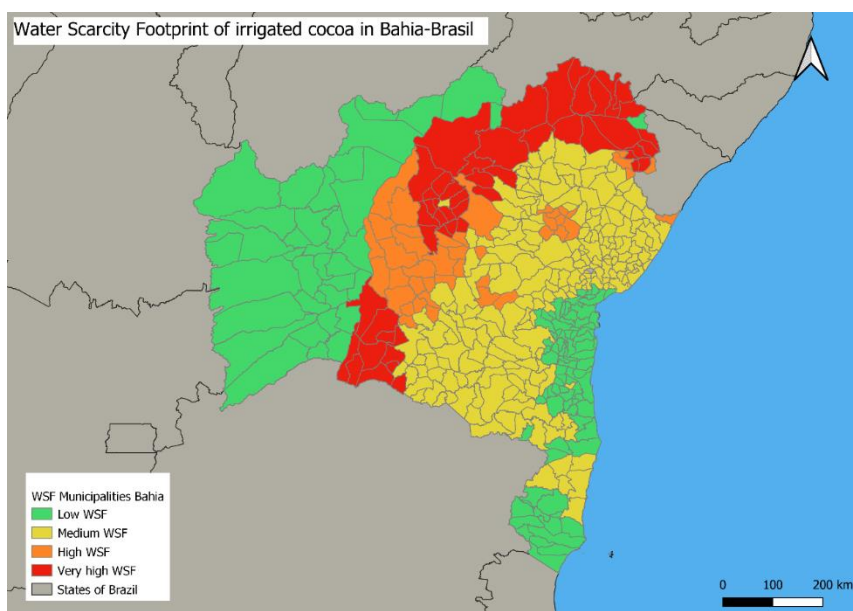


Figure 1. Water Scarcity Footprint of cocoa irrigation in the municipalities of Bahia.

According to the range established, of the 417 municipalities in the state, 28% have a 'Low WSF'; 50%, 'Medium WSF'; 10%, 'High WSF'; and 12%, 'Very high WSF'.

Irrigation of cacao in six SHUs would have the greatest impact on water scarcity: Macururé and Curaçá, Carnaíba de Dentro, Salitre, Vaza-Barris, Verde and Jacaré and Verde Grande. These SHUs have characterization factors (CFs) equivalent to $100 \text{ m}^3\text{-eq}$ for at least seven months of the year and have the potential to compromise essential local demands.

A total of 40 (9.6%) municipalities in Bahia have CF equal to $100 \text{ m}^3\text{-eq}$ in at least one month of the year. On the other hand, 42 municipalities (10%) have CF equivalent to $100 \text{ m}^3\text{-eq}$ in the whole year, meaning they have a very high water scarcity potential throughout the year.

The largest WSF is cocoa production in the municipality of Juazeiro ($646.5 \text{ m}^3\text{-eq kg}^{-1}$), located in the SHU of Macururé and Curaçá. In Juazeiro, the average annual demand for irrigation was estimated to be $6.74 \text{ m}^3 \text{ kg}^{-1}$. However, this municipality has 11 months with CFs of $100 \text{ m}^3\text{-eq}$, except in March, when the CF is $39.5 \text{ m}^3\text{-eq}$.

The monthly demand for irrigation in SHU of Macururé and Curaçá ranged from 1.26 to $7.10 \text{ m}^3 \text{ kg}^{-1}$. Although the highest WSF was in the municipality of Juazeiro, the highest demand for irrigation was in the municipality of Sobradinho ($7.10 \text{ m}^3 \text{ kg}^{-1}$).

The municipality of Sobradinho is part of the SHU Lago de Sobradinho whose CFs vary from 0.2 to 0.7, provoking a very low impact on water scarcity. Thus, the WSF of cocoa produced in Sobradinho was only $3.13 \text{ m}^3\text{-eq kg}^{-1}$, 99.5% smaller than Juazeiro's WSF. This fact highlights that a larger footprint does not indicate a greater water demand. Otherwise, the WSF is more affected by the water stress, and related CF, attributed to the SHU in which the municipality is located.

The municipalities with the smallest WSF (between 0 and $165 \text{ m}^3\text{-eq kg}^{-1}$) were inserted in the west, south coast, and extreme south of Bahia. However, according to Oliveira *et al.* (2019), the west region of Bahia is the largest agribusiness area in the state and has faced pressure on water resources, mainly due to irrigation, causing conflicts between water users.

The ten leading cocoa-producing municipalities are in southern Bahia, and they have low WSFs, ranging from 9.73 to $24.13 \text{ m}^3\text{-eq kg}^{-1}$. These municipalities are located in the SHUs Leste, Recôncavo Sul and De Contas. The municipalities located in these SHUs demand between 0 to $0.44 \text{ m}^3 \text{ kg}\cdot\text{month}^{-1}$.

3.3. Comparison with other studies for agricultural products

Few previous studies assessed the WSF of tropical irrigated fruits applying the AWARE method (Boulay *et al.*, 2018). Those studies considered the WSF of irrigation as well as the production of inputs used in the cropping systems in the study of Brazilian mango (Carneiro *et al.*, 2019), Peruvian and Italian grapes (Vázquez-Rowe *et al.*, 2017; Borsato *et al.*, 2019), Brazilian green coconut (Sampaio *et al.*, 2021) and Argentine lemon (Ferrero *et al.*, 2022). Although only the WSF of the cocoa irrigation process was accounted for in this study, comparing results with the WSF of these other fruits is essential to understand their magnitude.

Irrigation was the process that most contributed to crop WSF, although different irrigation systems were applied (micro sprinkler and drip), each with different efficiencies. Furthermore, the applied irrigation water in these studies was often higher (Carneiro *et al.*, 2019) or lower (Sampaio *et al.*, 2021) than the crop irrigation water demand. Carneiro *et al.* (2019) found an average footprint of $0.93 \text{ m}^3\text{-eq kg}^{-1}$. Sampaio *et al.* (2021) evaluated the WSF of green coconut in the main regions of Northeast Brazil, in the states of Alagoas, Bahia, Ceará, and Sergipe. Coconut WSF ranged from 0.332 to $0.758 \text{ m}^3\text{-eq kg}^{-1}$. As in the present study, the state of Ceará had the worst performance compared to the other regions analyzed, consuming a greater volume of water for irrigation and presenting the largest footprints.

Vázquez-Rowe *et al.* (2017) obtained an average irrigation WSF of $210 \text{ m}^3\text{-eq kg}^{-1}$. This value was due to the region's high CFs values, ranging from 61 to 100. In comparison, Borsato *et al.* (2019) found an irrigation WSF of $0.243 \text{ m}^3\text{-eq kg}^{-1}$, and Ferrero *et al.* (2022) obtained $0.102 \text{ m}^3\text{-eq kg}^{-1}$ for fresh lemon.

3.4. Uncertainties in the study

The uncertainties of the study are related mainly to the uncertainties of the CFs. Alves *et al.* (2020) have shown that the greater the temporal variation, the greater the uncertainty of CFs, such as in the Brazilian semiarid region. Another point of uncertainty is regarding kc; applying specific kcs to the different stages and locations can provoke different irrigation demands, contributing to reducing uncertainties in footprint calculation.

4. CONCLUSIONS

The coastal region of Bahia is the most favorable for cacao cultivation (or expansion) considering potential WSFs for the municipalities, as it has the smallest WSF (from 0.28 to $159.62 \text{ m}^3\text{-eq kg}^{-1}$). In the interior of the state, where cocoa irrigation is still a prospective activity, the WSF increases up to $646.5 \text{ m}^3\text{-eq kg}^{-1}$, indicating that irrigated cocoa cultivation could conflict with other essential local demands. Furthermore, this study showed that increased demand for cocoa irrigation does not necessarily correspond with an increase in the water scarcity footprint, as the impact is related to the water stress of the local water source. Thus, it is possible to infer that including WSF and CFs could improve agroclimatic zoning studies by adding new parameters to assess the potential water scarcity of the locals. Finally, the results of this study could be used as a baseline in the future for more specific WSFs for cocoa in Bahia.

5. REFERENCES

- AIPC. **Plan for the growth of cocoa culture in Brazil**. Available: <http://www.aipc.com.br/>. Access: Aug. 6, 2020.
- ALDAYA, M. M.; HOEKSTRA, A. Y.; ALLAN, J. A. **Strategic importance of green water in international crop trade**. (Value of Water Research Report Series, 25). Delft: UNESCO, 2008.
- ALLEN, R. G.; PEREIRA, L. S.; RAES, D.; SMITH, M. **Crop evapotranspiration: guidelines for computing crop water requirements**. Rome: FAO, 1998. 301 p.
- ALMEIDA, R. L. S.; CHAVES, L. H. G.; BONOMO, P.; ALMEIDA JUNIOR, R. L. S.; FERNANDES, J. D. Production of cocoa under different irrigation depths and nitrogen rates. **Caatinga Magazine**, v. 27, n. 4, p. 171–182, 2014.
- ALVES, K. F.; ANDRADE, E. P.; SAVIOLI, J. P.; PASTOR, A. V.; FIGUEIRÊDO, M. C. B.; UGAYA, C. M. L. Water scarcity in Brazil: part 2—uncertainty assessment in regionalized characterization factors. **The International Journal of Life Cycle Assessment**, v. 25, n. 12, p. 2359–2379, 2020. <https://doi.org/10.1007/s11367-020-01739-3>
- ANA (Brasil). **Situation of water resources in Brazil 2019**: annual report. Brasília, 2019.
- ANDRADE, E. P.; DE ARAÚJO NUNES, A. B.; DE FREITAS ALVES, K.; UGAYA, C. M. L.; DA COSTA ALENCAR, M.; DE LIMA SANTOS, T. *et al.* Water scarcity in Brazil: part 1—regionalization of the AWARE model characterization factors. **The International Journal of Life Cycle Assessment**, v. 25, p. 2342–2358, 2019. <https://doi.org/10.1007/s11367-019-01643-5>
- BABADELE, F. I. Effects of Shade Regimes and Varying Seasons of Irrigation on Survival, Developmental Pattern and Yield of Field Grown Cacao (*Theobroma cacao*). **International Journal of Plant & Soil Science**, v. 22, n. 3, p. 1–12, 2018. <https://doi.org/10.9734/IJPSS/2018/37339>
- BEGIATO, G. F.; SPERS, E.; NEVES, M. F.; CASTRO, L. T. Analysis of the agro-industrial system and the attractiveness of the São Francisco Valleys for irrigated cacao. **Costs and @gribusiness Online**, v. 5, 55–87, 2009.
- BORSATO, E.; GIUBILATO, E.; ZABEO, A.; LAMASTRA, L.; CRISCIONE, P.; TAROLLI, P. *et al.* Comparison of water-focused life cycle assessment and water footprint assessment: the case of an Italian wine. **Science of the Total Environment**, v. 666, p. 1220–1231, 2019. <https://doi.org/10.1016/j.scitotenv.2019.02.331>
- BOULAY, A. M.; BARE, J.; BENINI, L.; BERGER, M.; LATHUILLIÈRE, M. J.; MANZARDO, A. *et al.* The WULCA consensus characterization model for water scarcity footprints: Assessing impacts of water consumption based on available water remaining (AWARE). **The International Journal of Life Cycle Assessment**, v. 23, p. 368–378, 2018. <https://doi.org/10.1007/s11367-017-1333-8>
- BRASIL. Ministério da Fazenda; Ministério da Agricultura, Pecuária e Abastecimento. Portaria interministerial MF/MAPA nº 254, de 17 de maio de 2011. **Diário Oficial [da] União**, seção 1, Brasília, DF, 19 maio 2011.

- CARNEIRO, J. M.; DIAS, A. F.; BARROS, V. S.; GIONGO, V.; MATSUURA, M. I. S. F.; FIGUEIRÊDO, M. C. B. Carbon and water footprints of Brazilian mango produced in the semiarid region. **The International Journal of Life Cycle Assessment**, v. 24, n. 4, p. 735-752, 2019. <https://doi.org/10.1007/s11367-018-1527-8>
- CARR, M. K. V.; LOCKWOOD, G. The water relations and irrigation requirements of cocoa (*Theobroma cacao* L.): a review. **Experimental Agriculture**, v. 47, n. 4, p. 653-676, 2011. <https://doi.org/10.1017/S0014479711000421>
- FAO. **2050**: Water scarcity in many parts of the world threatens food security and livelihoods. 2020. Available: <http://www.fao.org/news/story/pt/item/283456/icode/>. Access: Jan. 6, 2022.
- FERRERO, L. M. M.; WHEELER, J.; MELE, F. D. Life cycle assessment of the Argentine lemon and its derivatives in a circular economy context. **Sustainable Production and Consumption**, v. 29, p. 672-684, 2022. <https://doi.org/10.1016/j.spc.2021.11.014>
- FICK, S. E.; HIJMANS R. J. WorldClim 2: new 1 km spatial resolution weather surfaces for global land areas. **International Journal of Climatology**, v. 37, n. 12, p. 4302-4315, 2017. <https://doi.org/10.1002/joc.5086>
- IBGE. **Systematic Survey of Agricultural Production**. 2021. Available at: <https://sidra.ibge.gov.br/home/lspa/brasil>. Access: Jan 6, 2022.
- ISO. **ISO 14046**: Environmental management – Water footprint – Principles, requirements and guidelines. Geneva, 2014.
- NARANJO-MERINO, C. A.; ORTÍZ-RODRIGUEZ, O. O.; VILLAMIZAR-G, R. A. Assessing green and blue water footprints in the cocoa production supply chain: a case study in northeastern Colombia. **Sustainability**, v. 10, n. 38, 2018. <https://doi.org/10.3390/su10010038>
- OLIVEIRA, L. T.; KLAMMLER, H.; LEAL, R. B.; GRISSOLIA, L. E. Analysis of the long-term effects of groundwater extraction on the water balance in part of the Urucuia Aquifer System in Bahia - Brazil. **Revista Ambiente & Água**, v. 14, n. 6, 2019. <https://doi.org/10.4136/ambi-agua.2390>
- OLIVO, A. M.; ISHIKI, H. M. Brazil facing water scarcity. **Colloquium Humanarum**, v. 11, n. 3, p. 41–48, 2015.
- PIASENTIN, F. B.; SAITO, C. H. Different methods of cocoa cultivation in southeastern Bahia, Brazil: historical aspects and perceptions. **Bulletin of the Museu Paraense Emílio Goeldi. Human Sciences**, v. 9, n. 1, p. 61-78, 2014. <https://doi.org/10.1590/S1981-81222014000100005>
- SAMPAIO, A. P. C.; SILVA, A. K. P.; DE AMORIM, J. R. A.; SANTIAGO, A. D.; DE MIRANDA, F. R.; BARROS, V. S. *et al.* Reducing the carbon and water footprints of Brazilian green coconut. **The International Journal of Life Cycle Assessment**, v. 26, n. 4, p. 707-723, 2021. <https://doi.org/10.1007/s11367-021-01871-8>
- SENAR. **Cocoa**: production, management and harvest. Brasília, 2018. 145 p.
- SODRÉ, G. A.; MARROCOS, P. C. L.; SARMENTO, D. A. **Cocoa cultivation in the state of Ceará**. Ilhéus: CEPLAC/CEPEC, 2017. (Technical Bulletin, 209). 34p.

- SOUZA, C. A. S.; AGUILAR, M. A. G.; DIAS, L. A. S.; SIQUEIRA, P. R. Water relations and irrigation. *In: SOUZA, C. A. S. et al. (ed.). Cacao from planting to harvest*. Viçosa, MG: Editora da UFV, 2016. p. 178-199.
- UNEP/SETAC. **Global Guidance for Life Cycle Impact Assessment Indicators Volume 1**. Paris, 2016.
- USDA. Department of Agriculture. **Irrigation water requirements**. Washington, DC, 1970. (USDA. Technical Release, 21).
- VÁZQUEZ-ROWE, I.; TORRES-GARCÍA, J.R.; CÁCERES, A.L.; LARREA-GALLEGOS, G.; QUISPE, I.; KAHHAT, R. Assessing the magnitude of potential environmental impacts related to water and toxicity in the Peruvian hyper-arid coast: A case study for the cultivation of grapes for pisco production. **Science of the Total Environment**, v. 601–602, p. 532–542, 2017. <https://doi.org/10.1016/j.scitotenv.2017.05.221>



Analyzing the impact of agricultural water-demand management on water availability in the Urubu River basin – Tocantins, Brazil

ARTICLES doi:[10.4136/ambi-agua.2847](https://doi.org/10.4136/ambi-agua.2847)

Received: 12 Apr. 2022; Accepted: 27 Jun. 2022

**Nicole John Volken^{1*} ; Ricardo Tezini Minoti² ;
Conceição Maria de Albuquerque Alves¹ ; Fernán Enrique Vergara³ **

¹Faculdade de Tecnologia. Programa de Pós-graduação em Tecnologia Ambiental e Recursos Hídricos. Universidade de Brasília (UnB), Campus Universitário Darcy Ribeiro, Asa Norte, CEP: 70919-900, Brasília, DF, Brazil. E-mail: cmaalves@gmail.com

²Faculdade de Tecnologia. Departamento de Engenharia Civil e Ambiental. Universidade de Brasília (UnB), Campus Universitário Darcy Ribeiro, CEP: 70919-900, Brasília, DF, Brazil. E-mail: rtminoti@gmail.com

³Departamento de Engenharia Ambiental. Universidade Federal do Tocantins (UFT), Quadra ARNO 14, Avenida NS 15, CEP: 77001-090, Palmas, TO, Brazil. E-mail: vergara@mail.uft.edu.br

*Corresponding author. E-mail: nicolejvolken@gmail.com

ABSTRACT

The Urubu River is part of the Formoso River Basin located in Tocantins State in northern Brazil. It is an important agricultural region where irrigation has an important role in rice and soybean crops, cultivated during the rainy and the dry seasons, respectively. The high levels of irrigation associated with below-average precipitation in 2016 and in the following years resulted in a water crisis in the Urubu Basin, with serious consequences to the environment and the economy of the region. This work evaluated the impact of reducing irrigation on environmental flows in the Urubu River Basin using hydrological modeling in WEAP. Irrigation water demand scenarios were simulated and analyzed from July 2018 through June 2019. Results indicated the need to reduce 35% of all water withdrawals in order to avoid the interruption of flow in the Urubu River Basin. This percentage was even greater when only some of the farmers cooperated. The paper emphasized that it is important that all farmers be involved and cooperate to reduce their water withdrawal by any means, including improving their irrigation system efficiency. The water regulator may also motivate water withdrawal reduction by modifying water permits and applying water withdrawal restrictions during the dry season.

Keywords: hydrological modeling, scenario analysis, water balance.

Análise da influência da gestão de demanda agrícola na disponibilidade hídrica da bacia hidrográfica do Rio Urubu – Tocantins, Brasil

RESUMO

O rio Urubu faz parte da bacia hidrográfica do rio Formoso, localizado no estado do Tocantins na região Norte do Brasil, sendo uma importante região agrícola e com forte utilização da irrigação para fortalecer a produção de arroz, cultivado na estação chuvosa, e em especial da soja para semente, durante a estação seca. A elevada dependência da irrigação



This is an Open Access article distributed under the terms of the Creative Commons Attribution License, which permits unrestricted use, distribution, and reproduction in any medium, provided the original work is properly cited.

associada a uma pluviosidade abaixo da média registrada no ano de 2016 que se estendeu pelos anos seguintes, ocasionou um período de escassez hídrica com impactos ambientais severos na bacia do rio Urubu. A disponibilidade hídrica na Bacia foi modelada com uso da ferramenta WEAP, com o objetivo de avaliar a necessidade de alteração das demandas de água para irrigação, buscando manter uma mínima vazão remanescente no rio Urubu. Para isso foram simulados cenários de redução percentual da vazão captada pelas bombas hidráulicas de irrigação. O período de análise foi de julho 2018 a junho de 2019 devido à restrição de disponibilidade de dados. Os resultados dos cenários indicam a necessidade de redução de 35% da demanda de referência para evitar uma interrupção na vazão do rio, sendo esse valor ainda maior na quando uma parcela dos agricultores não reduza o consumo. Para mudança da gestão dos recursos hídricos na bacia do rio Urubu, a participação dos diversos agentes se mostra fundamental, onde é preciso aumentar a eficiência na irrigação aliando alterações nos limites de outorgas de uso da água e aplicação de restrições de captação na estação seca.

Palavras-chave: análise de cenários, balanço hidrológico, modelo hidrológico.

1. INTRODUCTION

The planning and management of water resources aim to ensure access to water in adequate quantity and quality for a variety of water users while alleviating possible conflicts among them. The management structure focuses not only on meeting the water demand related to human activities, such as drinking water, sanitation and hygiene, industries, and irrigation but also on defining alternatives that allow the protection of environmental quality, including the groundwater and its ecology (Tundisi, 2013). According to Bernardi *et al.* (2012) the management of the water resources on the geographic limits of the watershed makes it possible to evaluate the singularities associated with each of the sub-basins, taking into account the stakeholders (social and economic aspects) and the physical and climatic characteristics, together with the available alternatives of policies and solutions.

Understanding the water balance of a river basin thus proves to be an important first step for the water-resource planning and management and can assist in the decision-making process, strengthening environmental protection and water security in the river basin. Considering that the greatest water user in Brazil is the irrigation sector, approaching almost 50% of the total water demand (ANA, 2020), many studies have focused on advancing the knowledge of water balance in different river basins and enhancing the water-resource management in these areas (Mendes *et al.*, 2021; Albuquerque *et al.*, 2019; Abreu and Tonello, 2018). Many efforts have also been developed to incorporate water demand management as an important step to reduce water shortage and improve production in agricultural river basins. Water demand management in the agriculture sector focuses on changes in crop and irrigation techniques, intensification of data monitoring and optimization of irrigation methods (Almeida *et al.*, 2021; Beltrão Júnior, 2017; Nikoo *et al.*, 2022; Srinivasan *et al.*, 2022).

The State of Tocantins (TO) has a flat landscape, fertile soils in excellent condition, a tropical climate, good water availability and suitable road infrastructures. All of these are important advantages for agricultural production, allowing the development of agriculture and livestock as the most significant economic sectors in the state (Tocantins, 2016). Tocantins State is a highlight in the Brazilian scenario as an agricultural power in expansion with an arable area that corresponds to half of the total area of the state, reaching 13.8 million hectares. In 2021, according to the Ministry of Agriculture, Livestock, and Supply (Brasil, 2021), the State reached the mark of US\$3.36 billion in Gross Value of Agricultural Production (GVP), consolidating itself as the third state in the Northern Region and in the eleventh state in Brazil, summing a total of US\$ 202.2 billion in GVP amounts converted on 12/31/2021 according to

Banco Central do Brasil registration. According to the Systematic Survey of Agricultural Production, the 2021 highlights in agricultural production in the Tocantins were soybeans (9.8 million tons), corn (1.5 million tons), and rice (1.2 million tons), which reached the third position in the country's production ranking, following the states of Rio Grande do Sul (13.6 million tons) and Santa Catarina (1.9 million tons) (IBGE, 2022; Brasil, 2022).

The Formoso River Basin is in the area of the PRODOESTE state program that encourages the development of irrigated agriculture. Its flat and naturally flooded topography favors the production of rice on its floodplains during the rainy season. During the dry season (May through November), other crops are cultivated, such as beans, watermelon and especially soybean seeds (Tocantins, 2016; Santos and Rabelo, 2008; Faria *et al.*, 2018; Vergara *et al.*, 2013).

Irrigation is especially important during the dry season, between May and November, resulting in the issuance of 99% of water grants to irrigators (Vergara *et al.*, 2013; Magalhães Filho *et al.*, 2015). The agricultural water withdrawal in the Formoso River is carried out by 98 hydraulic pumps with an average capacity of 1,620 L s⁻¹, adding up to 158,100 L s⁻¹ if they are all turned on at the same time. These pumps are located along the main rivers in the region, the Formoso, the Urubu, the Dueré, and the Xavante, but most of them are installed near the mouth of the Formoso (IAC, 2017; 2018; Faria *et al.*, 2018).

In 2016, the Formoso River Basin faced a water crisis due to a drought event combined with anthropic actions (Fleischmann *et al.*, 2017). However, a set of components were considered the drivers of the high risk of the environmental impact registered in the region, such as high level of water demand for irrigation, lack of water levels monitoring, lack of supervision and application of water policies aimed to preserve the availability of water resources (NATURATINS, 2016; IAC, 2018).

With the purpose of informing the management of water resources and preventing water shortage, an increase in the application of socio hydrological models capable of simulating the impact of human decisions in the hydrological processes has been observed all over the world. These modeling tools can help the management of water resources, increasing the understanding of hydrological, economic, and social dynamics at a watershed scale (Magalhães and Barp, 2014). In addition, these models allow the evaluation of alternative scenarios, simulating the performance of policies and management measures through these scenarios. This process has been proved to favor the implementation of effective policies and management actions building flexibility, robustness and resilience to the system. (McPhail *et al.*, 2018; Ermolieva *et al.*, 2022; Narita *et al.*, 2022).

The “scenario discovery” methodology has emerged as an alternative to the traditional approach of “predict and act” analysis. The process consists of building a set of scenarios showing slight variations from a baseline or reference scenario, similar to a sensitivity analysis. In many cases, this reference scenario represents the current situation in a watershed. For the other scenarios, variations of some specific group of parameters or characteristics are built in a set of other scenarios and the performance of the policies is tested under this new set of scenarios (Silva *et al.*, 2017; Mhiribidi *et al.*, 2018; Gorgoglione *et al.*; 2019).

The *Water Evaluation and Planning System* (WEAP) developed by the Stockholm Environmental Institute and later improved by the *Hydrologic Engineering Center* (HEC) of the US Army Corps of Engineers (USACE - US Army Corps of Engineers), is a computational tool capable of modeling hydrological systems. WEAP is based on mass balance principles applied to a net of nodes and links, which represents the water-resource system to be modeled. Some of these elements of the system are reservoirs, rivers, water demand points, water and sewage treatment plants and urban centers (SEI, 2016).

WEAP allows the comparison of water availability and the demand required between the reference scenario and any alternative scenarios in a simplified and visually accessible way. It

shows graphs and tables that facilitate the decision-making process. Alternative scenarios can incorporate the most variable scenario changes, such as increased efficiency in the pumping system, evaluation of water management actions and policies, changing crop selection and production practices, population increase and other characteristics of the water system. (SEI, 2016).

The WEAP model has been applied in many studies to evaluate the reliability of irrigation systems in regions that intend to expand the agricultural area, to evaluate best management practices and their impact on the irrigation system efficiency, to assess the impact on water supply due to increase in wastewater discharge from industries and to analyze public policies and development plans. In addition, the WEAP model has been widely applied to assess future scenarios of climate change and its possible consequences on water balance, agricultural productivity and the future need to expand water supply to meet drought events (Gao *et al.*, 2017; Mirdashtvan *et al.*, 2021; Layani and Bakhshoodeh, 2021; Asitatie and Gebeyehu, 2021; Noon *et al.*, 2022).

The hydrological and human system combined in the Formoso River Basin requires efforts to improve knowledge concerning the dynamics of interaction among social, hydrological and economic systems in the region. The Formoso River simulation model may give insights on water policies that could enhance the reliability of the irrigation system together with the protection of environmental flows in the basin that is an important area of grain production in the country, with a great impact on the regional economy (Magalhães Filho *et al.*, 2015, IAC, 2018).

In this sense, the objective of this study was to carry out a scenario-based analysis to assess water balance in the Urubu River, given the need to reduce the demand for water for irrigation as a way of preserving the local ecosystem. The study is a pioneering analysis of the hydrological system in the Urubu/TO River Basin. The basin encompasses extensive agricultural areas of rice and soybean for seeds crops with many water pumps that in 2016 motivated the interruption of the river flow during a drought that hit the region.

The work is an effort of research that has been developed in the Formoso River Basin and uses monitoring data from the High-Level Management (GAN) research project, a pioneer in Brazil to use technology to register real-time data of flows and water withdrawals for irrigation, contributing to more efficient management and inspection actions (IAC, 2018). The study evaluated alternatives to water demand management to avoid future water crises and conflicts in the Urubu River Basin, and illustrates how demand management arrangements and high technology applied to data monitoring can increase the efficiency of irrigation systems and water use in agriculture, avoiding water shortage. The analysis illustrated the importance of cooperation among farmers, favoring possible collective benefits in the river basin while at the same time protecting environmental flows and general conditions.

2. METHODOLOGY

The selected study area is the Urubu River Basin, which represents 29% of the total area of the Formoso River Basin covering a total of 6,183 km² in the State of Tocantins (TO) in the northern region of the country, as presented in Figure 1. The Dueré River Basin covers 3,553 km² converges to the mouth of the Urubu Basin, influencing the availability of water in the last two water pumps installed in the Urubu River.

The basin is located in the Cerrado biome, presenting a dry and humid tropical climate and a defined rainy season between December and April, and a dry season between May and November. The precipitation regime presents great variability between the dry and the rainy seasons. Although the annual average of precipitation is considered high, around 1579.6 mm, the average precipitation during the most critical months, from June to August, is only 6 mm

(Valente *et al.*, 2013; Alvez *et al.*, 2014; 2016).

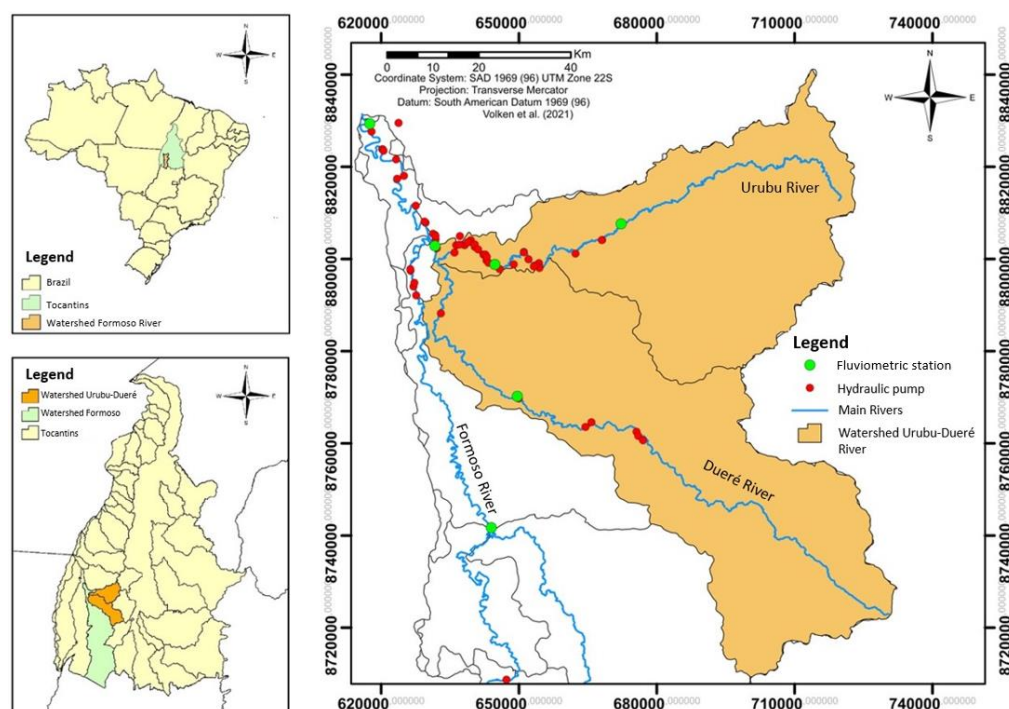


Figure 1. Location of the Urubu and Dueré River Basins (tributaries), in the State of Tocantins.

Although there are three discharge stations in the Urubu River Basin, Foz Rio Urubu (26798500), Fazenda Fortaleza (26795700), and Fazenda São Bento (26795100), and one in the Dueré River Basin, Foz Rio Dueré (26792000), the historical series of flow data start in 2017 and have many missing values, resulting in low confidence in the records. Thus, the methodology applied in this work and presented in Figure 2 sought to propose a framework to contribute to the understanding of the water balance in the study area. The flows in the Urubu and Dueré Rivers were simulated to build the reference scenario, where the water demands for agriculture were evaluated in order to define water resource allocation scenarios.

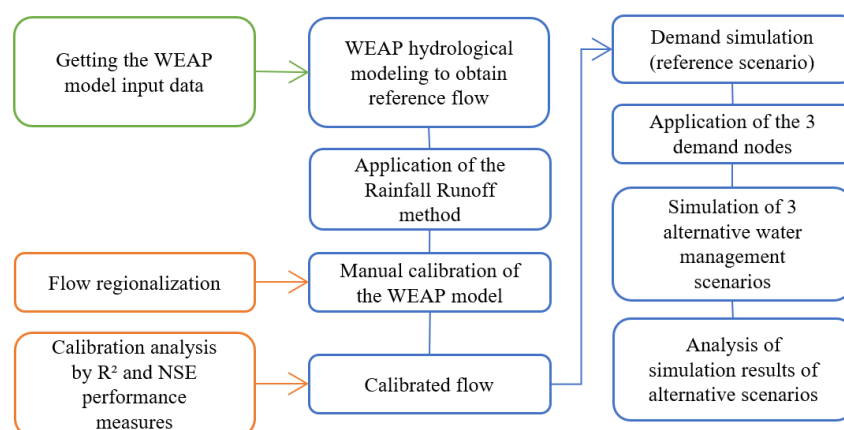


Figure 2. Methodological flowchart applied in the study of water balance analysis in the Urubu and Dueré River Basins.

Reference flow and water balance in the Urubu River Basin, including the Dueré Sub-basin, was modeled using the *Water Evaluation And Planning System* (WEAP), as illustrated in Figure 3. The simulation period encompassed July 2018 to June 2019, given the best

availability of data in a daily time step. The Urubu River Basin and the Dueré River Basin were represented in the WEAP model by two basin nodes. Three nodes, D1, D2 and D3 represented the set of water demand sites along the Urubu River.

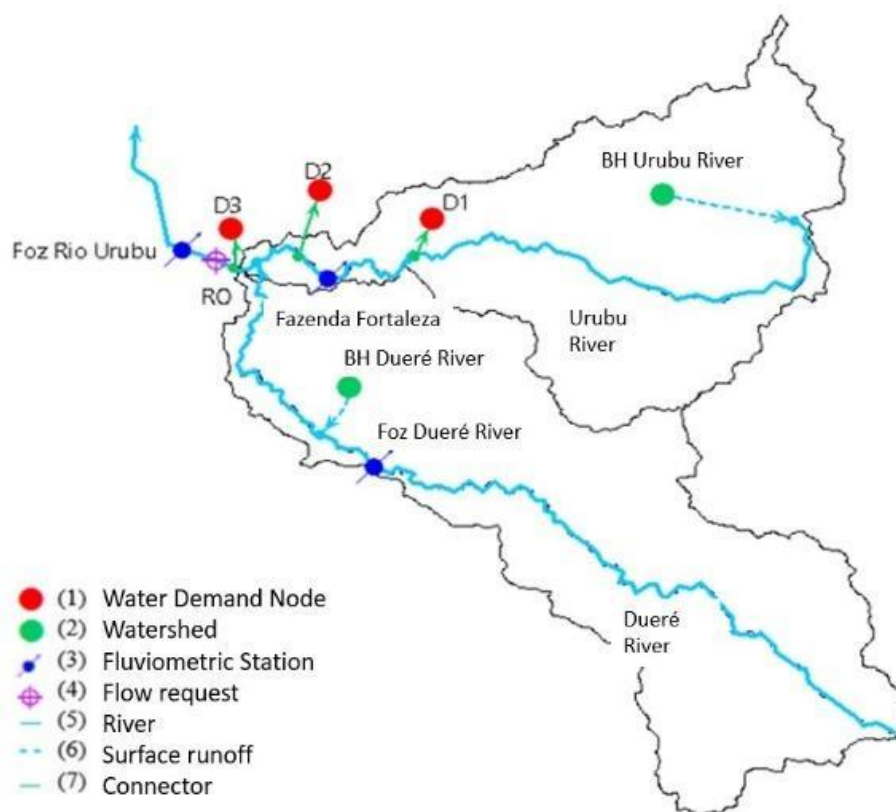


Figure 3. Water resource network in WEAP representation. (Urubu and Dueré River Basins – Tocantins).

The streamflow in the node representing the Urubu River was simulated using the Rainfall Runoff (Soil Moisture Method) Module in the WEAP. The method considers two one-dimensional layers of soil, surface and deep. The following processes are simulated in the upper soil layer (surface): evapotranspiration, surface runoff, soil moisture and percolation into the lower soil layer. The base flow, the deep soil moisture changes and the water flow into the aquifers are simulated in the deep soil layer module. The input data for the Rainfall Runoff method are climate data, soil type and land-use data, spatially distributed in the sub-basins defined by the users. This method is considered the most complete in all hydrologic models in WEAP (SEI, 2016).

The streamflow simulation was performed using the *Rainfall-Runoff (Soil blend Method)* module considering the parameters and configuration presented in Table 1 and Figure 4. The climate data used in this research is presented in Table 2. The average daily rainfall over the areas of the Urubu and Dueré River Basins was the result of the application of the Thiessen method using the rainfall stations in Table 3.

The streamflow modeling calibration was based on graph comparisons using three streamflow gauges in the basin, the Urubu River outlet (code 26798500), the Fortaleza Farm (code 26798500) and the Praia Alta (code 26720000). All three streamflow gauges are in the Formoso River Basin. Initially, the author analyzed the environmental characteristics of the basin, such as area, perimeter, main channel length, drainage density, compactness coefficient, circulatory ratio and factor form in order to perform the regionalization of flows among these gauges using the linear interpolation method.

Table 1. Input data in the method Rainfall-Runoff in the WEAP model to obtain the streamflow of the Urubu and Dueré Rivers. *WEAP (suggested system data) **GIS (Geographic Information System).

Land use	Category	Value	Unit	Source	Resolution
Area	BH Urubu River	2640	km ²	Magalhães Filho <i>et al.</i> (2013)	
Area	BH Dueré River	1054	km ²		
BH Urubu River Contribution Area (A)	Cerrado	63.51		GIS functions **	Sub-basin
	Agriculture	4.17	%		
	Pasture	31.7			
BH Dueré River Contribution Area (A)	Cerrado	59.6		GIS functions **	
	Agriculture	3.44	%		
	Pasture	36.8			
Culture Coefficient (Kc)	Cerrado	1		Olivos (2017)	Use of the soil
	Agriculture	Figure 4	-	Monteiro (2009); Faria <i>et al.</i> (2018)	
	Pasture	0.9		Olivos (2017)	
Yield Resistance Factor (RRF)	Cerrado	6		Olivos (2017)	
	Agriculture	2	-		
	Pasture	4			
Top layer field capability (SMax1)	Plintossolo	1000	mm	WEAP*	Soil type
Conductivity in the root zone (Ks)	Plintossolo	1350	mm day ⁻¹	Reis <i>et al.</i> (2018)	
The preferred direction of flow (f)	Plintossolo	0.15	-	WEAP*	
Relative soil humidity (Z1)	Plintossolo	7	%	Quintino <i>et al.</i> (2015)	
Bottom layer capacity (SMax2)	-	1000	mm	WEAP*	Hydrographic basin
Deep layer conductivity rate (Ks2)	-	160	mm day ⁻¹	Reis <i>et al.</i> (2018)	
Deep layer storage (Z2)	-	54	%	Silva <i>et al.</i> (2003)	

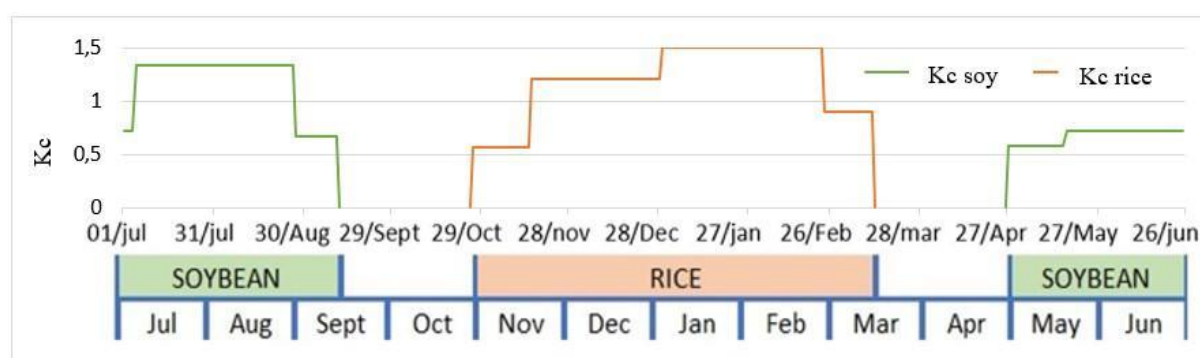
**Figure 4.** Soybean and rice Crop coefficient (Kc) in the Urubu/TO River Basin.

Table 2. Climate data source used in the streamflow simulation for the reference scenario in the Urubu and Dueré River Basins.

Climate	Unit	Station	Code
Temperature	°C	Lagoa da Confusão	A055
Relative humidity	%	Lagoa da Confusão	A055
Average wind speed	m s ⁻¹	Lagoa da Confusão	A055
Fraction of clear sky	%	Porto Nacional	83064

Table 3. Weather stations in the Urubu/TO River basin area.

Station	Code	Responsible	Operator
Lagoa da Confusão	1049003	ANA	CPRM
Dueré	1149000	ANA	CPRM
Poço da Pedra	1149003	ANA	A-N-A
Rio Dueré outlet	26792000	SEMARH-TO	SEMARH-TO
Rio Urubu outlet	26798500	SEMARH-TO	SEMARH-TO
Rio Urubu Fazenda Fortaleza	26795700	SEMARH-TO	SEMARH-TO
Fátima	1048000	ANA	CPRM
Pium	1049001	ANA	CPRM

Calibration performance was evaluated using metrics based on Moriasi *et al.* (2015), defined as the coefficient of determination (R^2), and the Nash-Sutcliffe (NSE) coefficient, both suitable for the daily time scale and the spatial scale of the Formoso River Basin.

After determining the reference flow, the demand impact on the flow of the Urubu River was simulated. Table 4 shows the identification of each irrigation demand hydraulic pump organized in a set of water demand in each water demand node. There were 15 and 16 hydraulic pumps in nodes D1 and D2, respectively, while node D3 represented only 2 pumps, totaling 33 hydraulic pumps. The water withdrawal in this pump was recorded from July 2018 to June 2019. This division was established to represent the withdrawal above the Fazenda Fortaleza fluviometric station (D1), after the station, but before the entrance of the Dueré River to the Urubu River (D2), and after the confluence near the mouth of the Urubu River (D3). Hydraulic pumps belonging to the same farmer received the same identification number, and farms may have abstractions in different stretches of the Urubu River. The irrigation demand data in the model comes from the High-Level Management System (GAN) <https://gan.iacuft.org.br/>, and so does the daily flow data. The abstractions belong to 21 farmers, some of which have more than one hydraulic pump represented by letters in the identification number (a, b, c and so on).

Table 4. Identification of hydraulic pumps in the Urubu River Basin (TO) WEAP model.

Demand node	Hydraulic pump identification																
D1	1	2	3a	3b	4	5a	5b	6	7a	7b	8	9	10	11	12	-	
D2	13a	13b	13c	13d	14a	14b	15	16	17a	17b	18	19a	19b	20a	20b	21a	
D3	21b	20c								-							

The daily irrigation demand data in each water pump were input to the WEAP model in the reference (baseline) scenario. Records from 18 water pumps showing less than 10% of failures were averaged to substitute for other missing data in water pumps with flaws in the records. This process separated the whole simulation in three periods as shown in Figure 5 and calculated the average water demand for each of the 18 selected pumps in each period. These values filled in the missing data in all pumps. For the period between harvests, it was considered that there was no water withdrawal, and the gaps were filled with zero. The whole process also observed the schedule defined in the Biennium Plan (IAC, 2018) for water withdrawal in the basin. The total water demand at each node during the simulation period is shown in Figure 6.

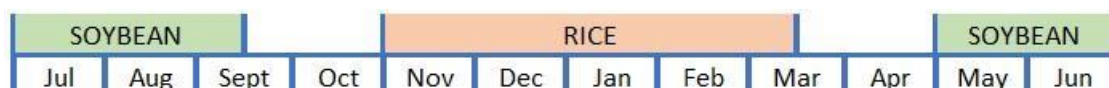


Figure 5. Soybean seed and rice cultivation period considered in this study in the Urubu River Basin/TO.

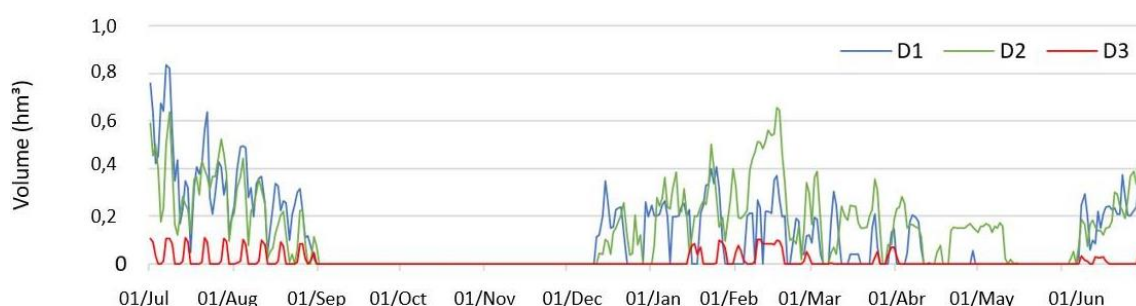


Figure 6. Total irrigation water demand node during the modeling simulation in WEAP (Urubu River Basin/TO).

The WEAP model considers that there may be losses in the water collection and distribution system and that part of this water may be reused internally in the system (SEI, 2016). Thus, Equation 1 computes the flow required for crop irrigation at each water demand node, taking into account losses in the system, internal reuse of water to supply part of the demand, and any technology to use water more efficiently in the system. To consider the actual water demand in the basin, all these parameters and the return flow were set to zero in the Urubu River Basin simulation. The return flow is represented by a percentage of the amount of water that, after being made available for irrigation and not being absorbed by the plants, returns to the river, increasing the availability of water. In this sense, we sought to simulate the most conservative reference scenario.

$$Required = \frac{(Daily\ Demand) * (1 - \%Reuse) * (1 - \%Economy)}{(1 - \%Loss)} \quad (1)$$

The reference or baseline scenario consists of simulated streamflow minus the irrigation water withdrawn from the water demand nodes along the Urubu River, considering both the soybean and rice crops. Based on the reference scenario, three alternative scenarios of demand management were considered and evaluated in terms of the objective to maintain an environmental flow (minimum) in the Urubu River. The study analyzed the reduction of environmental impacts due to high levels of irrigation water demands added to drought events.

The work considered that the alternative scenarios of demand management could result from either the enhancement in the irrigation management practices, the modification of irrigation practices, or the reductions in irrigation network losses, or the selection of alternative crops in the region, especially during the dry season or by anticipating demand through early planting, as long as the sanitary intervals are respected to protect the crops. This study did not

focus on proposing the technical solution to be implemented, but on evaluating the required demand reduction to guarantee an environmental flow to protect the ecology and aquatic life in the Urubu River Basin area.

Alternative scenarios were evaluated during the entire year, but since the most critical situation happened between July and August, the analysis concentrated on these months and considered the flows at three sites right after the demand nodes (D1, D2 and D3) in the water resource network built-in WEAP, as shown in Figure 7. The parameters evaluated were the remaining flow after the water demand nodes, the required percentage of demand reduction in order not to interrupt the flow and also to guarantee a minimum flow ($1.245 \text{ m}^3 \text{ s}^{-1}$, as indicated in the Report of Phase B of the Diagnosis of Water Demand (IAC, 2017), carried out by the GAN Project team, as possible Q_{90} for the Urubu River in the dry season).



Figure 7. Single-line diagram of demand nodes and analysis points simulated in WEAP (Urubu River Basin/TO).

Scenario 1 considered that all farmers would be able to reduce their water demand by changing the irrigation methods to more efficient and rational choices. Thus, in this scenario, what would be this reduction percentage was evaluated to the point that the Urubu River did not suffer any interruption in its flow and that later it was possible to maintain the flow used as a reference throughout the year. The work evaluated the stream flows in the Urubu River as a result of intervals of a 5% reduction in the water withdraws in all farms. The reduction percentage was applied equally to all water pumps.

Scenario 2 considered the water demand reduction in 90%, 80% and 70% of the water pumps that presented the highest water withdraws aiming in preserving a minimum flow of $1,265 \text{ m}^3 \text{ s}^{-1}$. For this, the percentage of water demand in each farm was calculated as a portion of the total irrigated water demand in the Urubu River. The assessment included all hydraulic pumps belonging to the same property. The division of catchment groups into 90%, 80%, and 70% considered that the farm as a whole would apply measures to increase efficiency. In this way, all pumps on the farm would apply the same percentage reduction in the water volume withdrawal. Table 5 summarizes the water demand management procedures in Scenario 2. The reduction was evaluated every 5% and all demand nodes had hydraulic pumps that reduced demand.

Scenario 3 assesses the impact of anticipating water demand in time. This scenario took into account soybeans for the seed crop period in which there is a sudden decrease in water availability given the beginning of the dry season. The scenario was built on the assumption that anticipating the crop sowing would coincide with a high level of flows in the river, reducing the impact of water withdrawals requiring smaller reductions using efficient practices.

According to farmers in the Urubu River Basin, the starting date to plant soybean crops for seeds occurs on May 1st (IAC, 2017). So this study considered this date as a reference. The Agricultural Defense Agency of Tocantins (ADAPEC) determines that the sowing of soybeans in the lowland regions of Tocantins can only take place from April 20 onwards (ADAPEC, 2016). Thus, Scenario 3 considered the impact of the anticipation of planting by 5 and 10 days. The anticipations were also applied to the period of irrigated rice cultivation. As in Scenario 1, the percentage of water demand reduction was applied to all hydraulic pumps at intervals of 5% reduction.

Table 5. Water demand reduction in Scenario 2 of the Urubu River simulation model in WEAP.

Demand node	Pump ID			Demand representation (%)
	90% of pumps	80% of pumps	70% of pumps	
D2	13a; 13b; 13c; 13d	13a; 13b; 13c; 13d	13a; 13b; 13c; 13d	17.40%
D2	14a; 14b	14a; 14b	14a; 14b	9.40%
D1	7a; 7b	7a; 7b	7a; 7b	8.80%
D2	17a; 17b	17a; 17b	17a; 17b	8.20%
D2/D3	20a; 20b; 20c	20a; 20b; 20c	20a; 20b; 20c	6.60%
D1	10	10	10	5.30%
D2/D3	21a; 21b	21a; 21b	21a; 21b	4.40%
D1	9	9	9	4.30%
D1	6	6	6	4.30%
D1	8	8	8	3.80%
D2	16	16	16	3.60%
D2	19a; 19b	19a; 19b	19a; 19b	3.10%
D1	4	4	4	2.80%
D1	2	2	-	2.70%
D1	1	1	-	2.60%
D2	18	18	-	2.50%
D1	12	12	-	2.50%
D1	5a; 5b	-	-	2.30%

3. RESULTS AND DISCUSSIONS

Table 6 presents the comparison of river basins' morphometric characteristics considered in the streamflow simulation in WEAP. All sub-basins presented regular drainage density, except the Dueré River Basin. The Compactness Coefficient, the Circulatory Ratio and the Form Factor indicate that all sub-basins tend to present elongated shapes instead of circular preventing floods due to climate extreme events. The drainage density in the Dueré River Basin indicates that this basin is prone to generating quick surface runoff.

Table 6. Morphometric characteristics in the sub-basins.

Sub basins	Urubu River	Dueré River downstream	Fortaleza Farm	Dueré River outlet	Praia Alta
Area (km ²)	2630.45	1050.70	2545.90	2502.14	6000.70
Catchment perimeter (km)	319.23	196.61	371.13	383.65	642.21
Main channel (km)	175.70	63.72	144.90	134.11	439.84
All channels (km)	3370.50	926.70	3209.90	4819.60	8793.50
Drainage density	1.28	0.88	1.26	1.93	1.47
Compactness coefficient	1.74	1.70	2.06	2.15	2.32
Circulatory Ratio	0.32	0.34	0.23	0.21	0.18
Form Factor	0.09	0.26	0.12	0.14	0.03

The Plintossolo is the predominant soil type in the area, adding up to the following percentages in the sub-basins: Urubu River (85.2%), Dueré downstream (98.9%), Fortaleza Farm (84.8%), Dueré River outlet (92.2%). This type of soil presents a high probability to generate temporarily flooded areas, especially in plain relief areas that are frequent in the basins. The predominant soil type in the Praia Alta sub-basin is the Latossolo covering 73.3% of the area, indicating better infiltration capacity and faster soil drainage when compared to other basins. Slight portions of Gleissolo, Argissolo and Neossolos of type Quartzarenico and

Litólico are also present in the basin, the two last cited are found only in the Praia Alta Basin.

The study area is predominantly agricultural as shown in the following percentage of agriculture areas in each sub-basin, Urubu River (31.7%), Dueré River downstream (36.8%), Fortaleza Farm (28.6%), Dueré River outlet (40.1%) and Praia Alta (49.6%). The remaining areas in the basins are covered by natural vegetation characteristic of the Cerrado Biome. The predominant slope is classified as plain or slightly undulating, favoring the formation of flooded areas, which is frequent in the Formoso River Basin. The streamflow simulation in WEAP was calibrated using the land use and soil type parameters presented in Table 7.

Table 7. Land use and soil type parameters were considered for the WEAP streamflow calibration.

Parameters	Category	Valor	Unit
Crop coefficient (Kc)	Cerrado	10	-
Root zone Conductivity (Ks)	Plintossolo	100	mm/dia
Runoff resistance factor (RRF)	Cerrado	8	-
	Pastagem	6	
Storage Capacity of the lower layer (SMax2)	-	500	mm

Figure 8 presents the WEAP streamflow calibrated with a good approximation to the regionalized flows. Although the simulated streamflows seemed overestimated at the beginning of the period from September to March, for the rest of the simulation period the calibrated streamflows were close to the regionalized observed data.

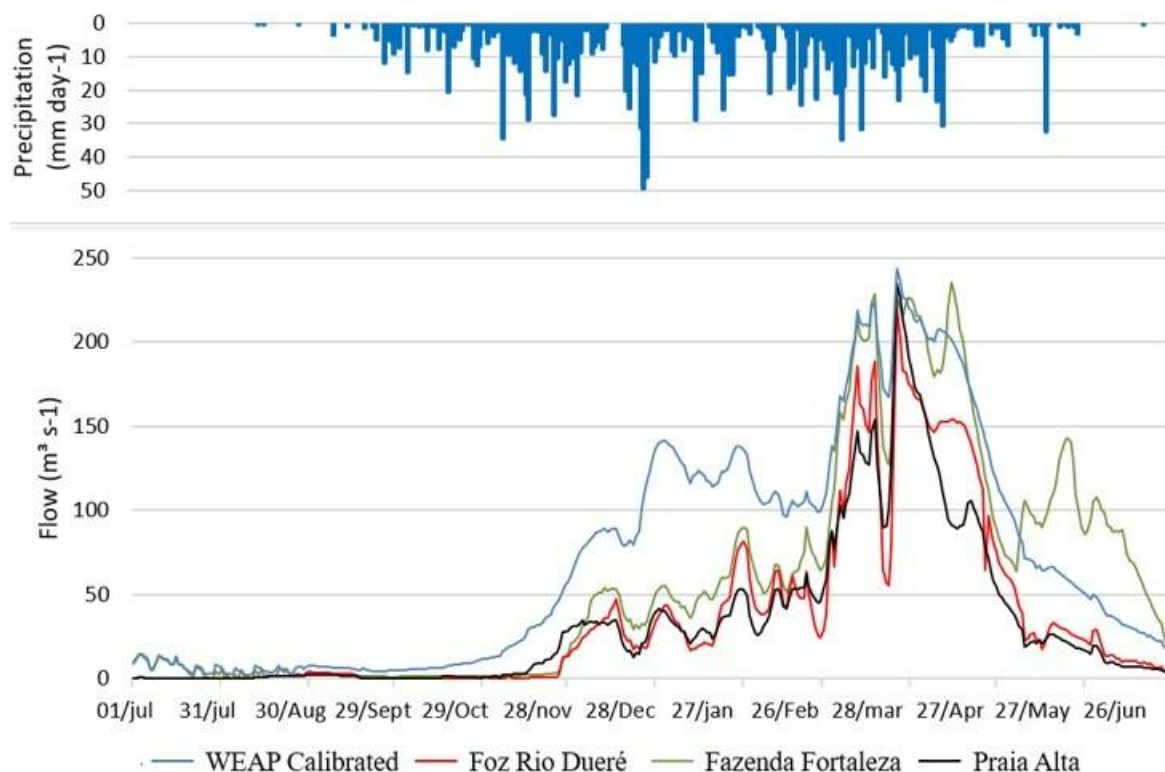


Figure 8. Calibrated Streamflow simulation in WEAP.

Table 8 presents the simulation modeling performance metrics, the coefficient of determination (R^2) and the Nash-Sutcliffe coefficient (NSE). When visually analyzing the flows in Figure 8, it can be seen that they all follow a similar trend despite presenting values in general

below the simulated flow, especially for the Praia Alta streamflow gauge in the period from November to February. Since the NSE coefficient is sensitive to extreme values, this may be the reason why the result of the coefficient remains unsatisfactory even after calibration. However, as the other analyses showed improvements and the calibration visibly brought the simulated flow closer to the regionalized ones, the result was considered satisfactory for use as a reference flow in this study.

Table 8. Result of the statistical performance of the flow simulation in the WEAP model compared to regionalized flows.

Streamflow Gauge Stations	R ²				NSE			
	Not Calibrated		Calibrated		Not Calibrated		Calibrated	
Fortaleza Farm	0.63	Satisfactory	0.81	Well	-3.96	Unsatisfactory	0.79	Well
Dueré River outlet	0.65	Satisfactory	0.84	Well	-9.28	Unsatisfactory	0.55	Satisfactory
Praia Alta	0.76	Well	0.89	Very Good	-11.76	Unsatisfactory	0.31	Unsatisfactory

Figure 9 presents the simulation of flows right after the nodes D1, D2 and D3 for the reference scenario and the specific growing season of each of the crops, rice and soybean seed. One can observe that the low flows are critical during the dry season in the Urubu River Basin. Irrigation in this period is mainly associated with soybean for seeds crops sown beginning in May and requires high amounts of water. The high volumes of water demand are not only linked to the plant needs, but also to the predominant irrigation technique applied in the basin, the sub-irrigation by raising the water table. This technique uses large volumes of water, has a low capacity for process optimization, and generates high losses related to water infiltration into the soil. Evaporation in the irrigation channels also influences the water demand, resulting in low irrigation efficiency.

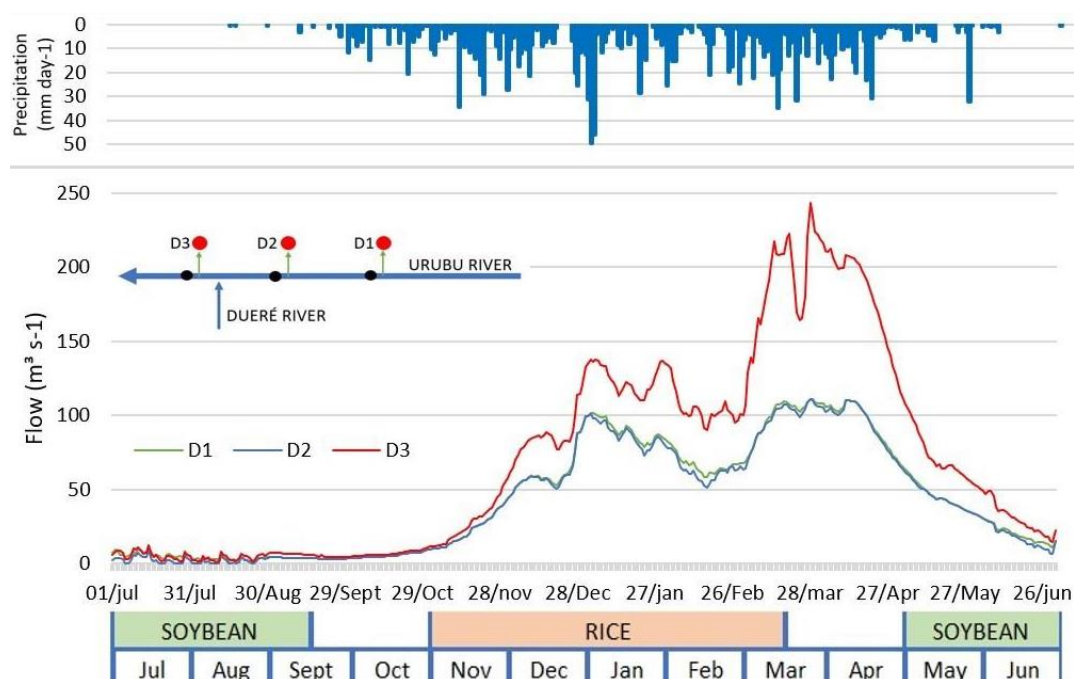


Figure 9. Streamflow simulation after the demand nodes considering the reference scenario (Urubu River Basin/TO).

Figure 9 shows that streamflow volumes after node D3 are higher than the flows after

nodes D1 and D2, due to the Dueré River that joins as tributary inflow into the Urubu River, increasing the water availability near its mouth, which is especially relevant in the dry season when soybeans are planted.

Results in the period of rice crop in Figure 9 also showed that, despite the high volume of water withdrawn for irrigation, it does not result in critical flows at any of the analysis points. The greater availability of water during the rice season meant that the impact of water demand was not so significant, especially when compared to the season of soybeans seeds.

Given these initial results, this paper investigated the impact of water demand during part of the dry season, especially between July and August. Figure 10 shows the simulated remaining flows after the demand nodes D1, D2 and D3. Note that flow values after D1 (in the green curve) are already very low, reaching a minimum of $1.67 \text{ m}^3 \text{ s}^{-1}$. This point of analysis is important considering that demand points D2 and D3 will withdraw a high volume of water and the lower the availability observed after node D1, the greater the chances of points D2 and D3 not receiving enough water, triggering water-use conflicts in the region near the basin outlet.

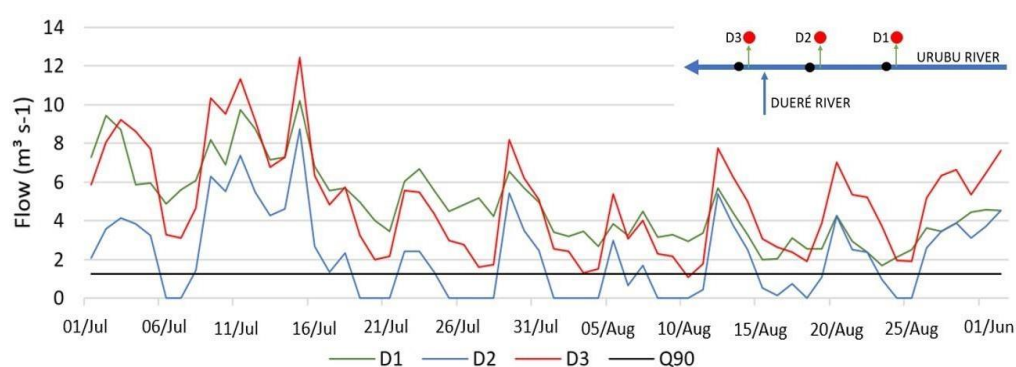


Figure 10. Streamflow during the dry season (July and August) in the Urubu River (TO) after the simulation of demand nodes in WEAP in the reference scenario.

Flows after node D2 were the most critical, as illustrated in Figure 10 in the blue line. At this point, most of the water withdrawals have already taken place and the flow of the Dueré River tributary has not yet been added to the Urubu River. The flows in several points after D2 are down to zero resulting in severe environmental impacts for the region, causing an imbalance to the local ecosystem damaging the biota, making it difficult to return the system to a regular equilibrium. In addition, there are also social and economic damages in the basin, which in turn reflect crop losses due to the lack of water for irrigation.

Also in Figure 10, one can observe that the flow condition after node D3 is much better than in node D2, given the flows coming from the Dueré tributary. However, low flow values are still noted. The analysis at this point is important, considering that the remaining flow will be the inflow to the Formoso River and if this flow is very low or considered insignificant, the crops downstream of the Urubu Basin will also be jeopardized due to propagated impacts in the lower Formoso River Basin.

Given the required reduction in the irrigation water withdrawal observed in the reference scenario of the Urubu River Basin, this research tried to define a minimum percentage of reduction in irrigation water demand that could preserve environmental flows and promote the rational use of water for irrigation in the region. The research evaluated alternative percentages through the simulation of alternative scenarios of irrigation water demands. The focus was to guarantee a minimum flow of $1.245 \text{ m}^3 \text{ s}^{-1}$ (IAC, 2017) in the Urubu River and to avoid the interruption of flow at any point of time during the simulation.

The first alternative scenario took into account that all the irrigators in the basin would apply measures to promote the reduction of water abstraction and, with that, they contributed

equally, reaching the same percentage of reduction. Figure 11 shows the remaining flow in the Urubu River after the demand nodes with the application of a 35% reduction in demand, which is the minimum value to guarantee the flows in the river during the simulation period along the main channel. This value was defined by trials adding intervals of 5% reduction until there was no longer a remaining flow equal to zero after the demand nodes.

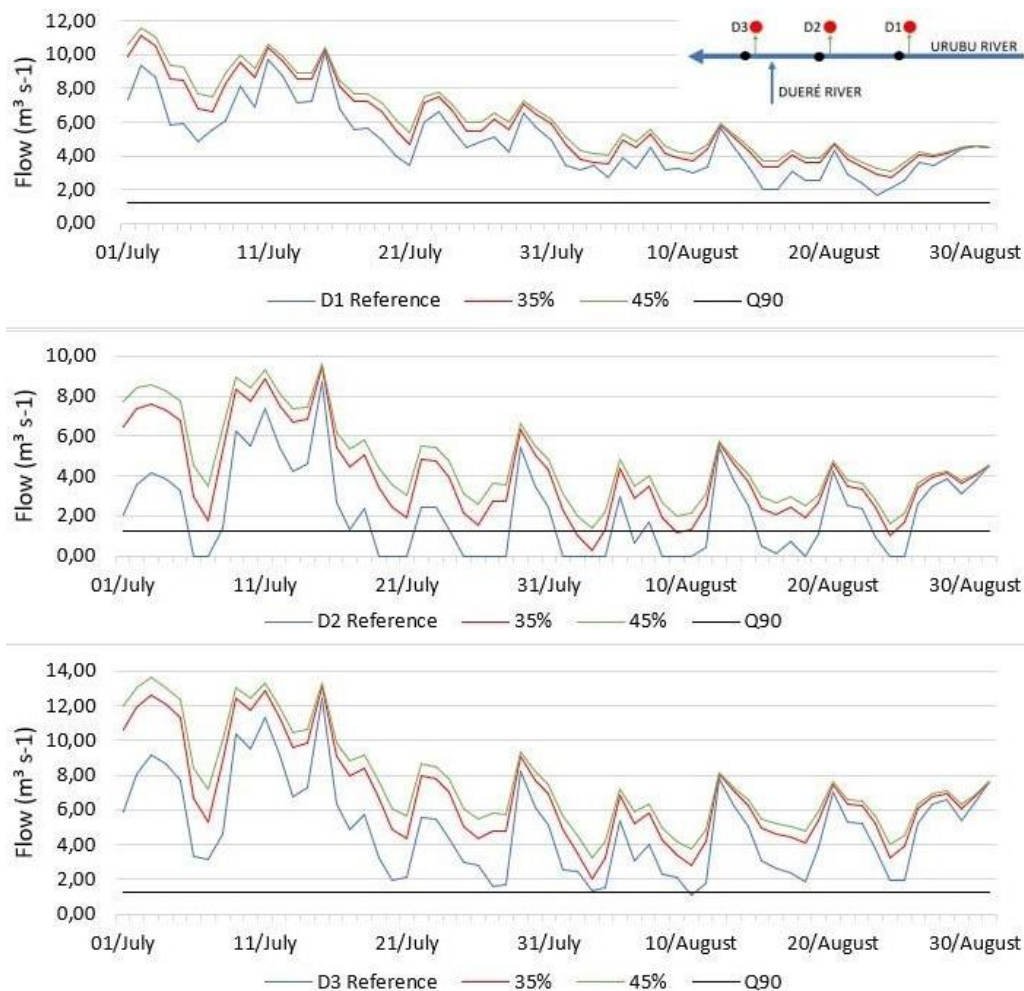


Figure 11. The remaining flow in the Urubu River (TO) after reductions of 35% and 45% was applied to all WEAP simulated abstractions for Scenario 1.

The percentage of 35% reduction is high and difficult to achieve by means of demand management measures or even by increasing the efficiency of the system. Reducing 35% of the water demand in some cases represents reducing a large volume of water and requires high values of investments. On the other hand, the small farmers find it very hard to reduce their demand even more approaching a value that could be harmful to their crops.

It is noteworthy that the reduction aimed at lowering the peaks of flow at the most critical moments, especially after the demand node D2, and that the flow demanded in the analysis period was occurring according to demand rotation rules (IAC, 2018). Thus, peaks in demand could be even more expressive in years when this measure was not applied, resulting in even greater reductions.

With a 35% reduction in demand, despite no interruption in the flow of the Urubu River, the minimum value recorded after node D2 was still very low. In this sense, it was also verified what would be the required reduction so that a minimum flow of $1.245 \text{ m}^3 \text{s}^{-1}$ in the Urubu River could be guaranteed throughout the simulation period. This water demand reduction should be 45%, as seen in Figure 11, representing a very expressive reduction and, probably,

very difficult for farmers to internalize. Considering that the reduction was mainly necessary during the soybean crop, especially from July through August, the demand reduction could actually be applied only during the soybean irrigation, from May through September, maintaining the same values of water demand, without reduction, during the rice season. However, the scenario considered the reduction throughout the simulation period.

The demand reduction established in Scenario 1 demonstrates that the preservation of environmental flows in the Urubu River Basin cannot be based solely on reducing the volumes of irrigation water withdraws according to efforts supported by the farmers themselves. This solution should come from a shared vision among users and public managers. Water-resource managers need to define policies and programs that could benefit the environmental conditions of the drainage system in the basin, protecting the ecosystem services and the economy in the region. Studies that evaluate measures of more sudden changes, revision of the minimum flow values, suspension of grants, or economic evaluation of the benefit/cost ratio of current grants can be carried out to demonstrate the applicability together with the efforts of farmers to achieve environmental conservation in the basin.

The second alternative scenario evaluated the need to reduce the irrigation water demand in the reference scenario so that there would be no interruptions in the flow imposing demand management measures only for users (farmers) of large volumes of water. Figure 12 shows the remaining flow in the Urubu River after the reduction in water demand by 90%, 80%, and 70% of the water pumps. The lowest value of water demand reduction to maintain a minimum flow after irrigation water withdrawals must be 40% for 90% and 80% of the pumps. In this condition, the minimum flow in the Urubu River in the most critical section, located after the demand node D2, would be $0.51 \text{ m}^3 \text{ s}^{-1}$. The additional 5% reduction of flows compared to Scenario 1 represents an additional pressure on farmers to commit to improving their irrigation system.

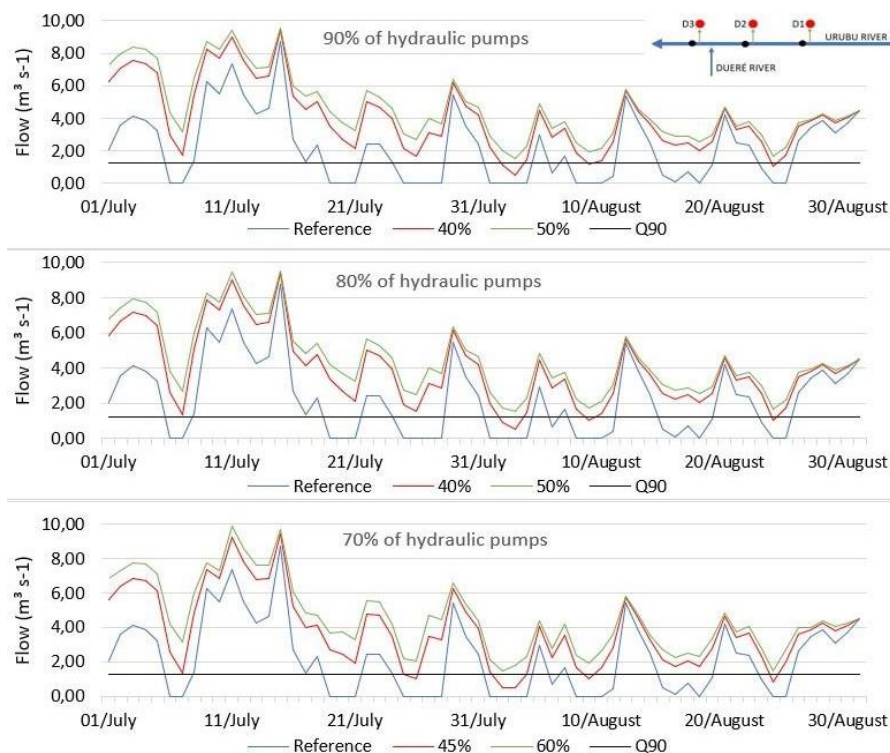


Figure 12. Remaining flow in the Urubu River (TO) after node D2, with an application of demand reduction to 90%, 80%, and 70% of the hydraulic pumps in the WEAP simulations for Scenario 2.

In the most critical situation simulated in the second scenario, in which only 70% of the pumps collecting water for irrigation would reduce the water demand, it would be necessary for them to reach a percentage reduction of at least 45% to avoid the interruption of the water supply, as shown in Figure 12. In this condition, the minimum flow was $0.47 \text{ m}^3 \text{ s}^{-1}$. This reduction is 10% greater than the reduction in Scenario 1.

Maintaining a minimum flow in the Urubu River that is at least equal to $1.245 \text{ m}^3 \text{ s}^{-1}$, the associated effort is very high, reaching a reduction of 50%, equivalent to a remaining flow of $1.52 \text{ m}^3 \text{ s}^{-1}$ when 90% and 80% of irrigators commit to applying demand reduction measures. The simulated situation is even worse, with the participation of 70% of the irrigators, reaching a reduction of 60% of the reference demand, with a minimum remaining flow equal to $1.46 \text{ m}^3 \text{ s}^{-1}$. These values are unrealistic and will hardly be reached. Furthermore, these values can even discourage a change in irrigation techniques and implementation of more effective methods, as it becomes so complex and costly, in addition to perhaps fostering greater conflicts in the basin, given the non-participation behavior of some irrigators in the face of excessive cost.

The results of Scenario 2, which considered the reduction of irrigation demand is only part of the users ended up overloading them. Thus, the percentage value necessary to maintain a minimum flow in the Urubu River would be even higher than in the first alternative scenario and could be even more expressive, if the irrigators who capture larger volumes of water for irrigation did not apply any demand reduction. The simulation could therefore show an impractical situation with a very relevant socio economic impact, where the other farmers could even have to completely stop water abstraction to maintain the minimum flow in the Urubu River.

Alternative Scenario 3 proposed a combined approach that considers both the planting anticipation and the demand reduction addressed in previous scenarios. This combination proved to be especially advantageous during the dry season when the farmers grow soybeans seeds. The anticipation of demand meant that water withdrawal took place in a period when there was greater availability of water in the Urubu River due to the rainy season or the beginning of the dry season, reducing the impacts of water withdrawal on the remaining flow. This situation was observed in the anticipation of 5 and 10 days, shown in Figure 13. This anticipation had no effect on the rice plantation, given it coincides with the rainy season in the basin.

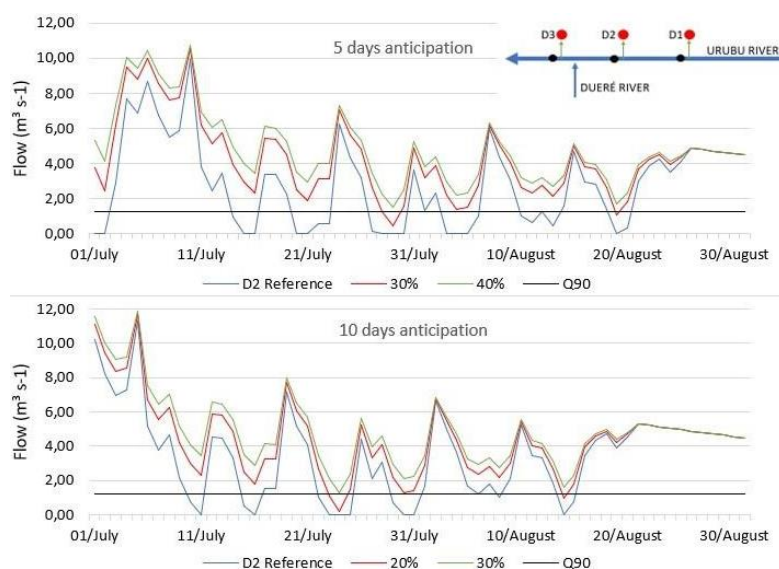


Figure 13. WEAP simulation of the remaining flow in the Urubu River (TO) after node D2 for anticipation of irrigation by 5 and 10 days in Scenario 3.

Figure 13 shows the flows after the demand node D2 and the anticipation of irrigation by 5 days. To avoid the interruption of flow in the Urubu River, it was necessary to apply a 30% reduction in the flow captured in all hydraulic pumps. This reduction made it possible for the lowest remaining flow to be $0.44 \text{ m}^3 \text{ s}^{-1}$, after node D2 at the end of July. Considering the requirement of minimum flow in the Urubu River, the percentage of reduction rose to 40%. In comparison with the first scenario, the reduction associated with the application of more sustainable water management practices decreased by 5%, which favors the farmers and improves this scenario as a possible solution for water-demand management in the Urubu River Basin.

Figure 13 also shows the remaining flow of the Urubu River after node D2 for the anticipation of 10 days and a 20% reduction in the flow captured by all irrigators, so that there would be no interruption in the remaining flow. Despite not interrupting the flow, the minimum value observed was only $0.18 \text{ m}^3 \text{ s}^{-1}$, requiring a reduction rate of 30% to maintain a minimum flow throughout the analysis period. In both cases, the value is 15% lower than in the first scenario, which highlights the importance of all farmers working together, combined with a planting practice that is aligned with the natural cycle of water availability. The combination of these two demand management measures can increase the performance of local agriculture, reducing socio-environmental conflicts and environmental and economic damage caused by water shortage.

Table 9 summarizes the minimum water demand reductions required in all scenarios in order to preserve the streamflow in the Urubu River and also the minimum water demand reduction in order to maintain the environmental streamflow defined as $1.245 \text{ m}^3 \text{ s}^{-1}$.

Table 9. Necessary demand reduction results for each alternative scenario simulated.

Scenario	Scenario Condition	Minimum Demand Reduction	Minimum Demand Reduction to Maintain $1.245 \text{ m}^3 \text{ s}^{-1}$
Scenario 1	All hydraulic pumps	35%	45%
Scenario 2	90% of hydraulic pumps	40%	50%
	80% of hydraulic pumps	40%	50%
	70% of hydraulic pumps	45%	60%
Scenario 3	Demand anticipation in 5 days	30%	40%
	Demand anticipation in 10 days	20%	30%

The results in the simulation show the importance of water demand management measures to irrigation efficiency in the Urubu River Basin. These efforts also reduce the environmental impacts associated with ecological systems. Water demand reduction may be achieved by means of controlling water losses in the transport channels to the plantation areas, changing the method of sub-irrigation by technologies that promote rational water use, selecting crops that may be less water-demanding or be more adapted to dry seasons. According to the results of the alternative scenarios, it is important that all farmers in the basin cooperate actively and contribute to these efforts.

One should not forget the important role of water institutions and managers in the region once they could enhance monitoring, regulation and enforcement contributing to the security of water systems in the basin especially during droughts. Thus, measures such as modifying water permits during droughts events, planning and scheduling water-use restriction when necessary, and considering the application of a collective permit can help in the management of water resources in the Urubu River Basin. The High-Level Management Project (GAN) has also proved to be extremely important to increase knowledge about water availability and

demand in the region of the river basin of the Formoso River. The project allowed the installation of flow meters in all hydraulic pumps in the basin contributing to enhancing the water regulation and monitoring in the region, allowing the selection of management measures and practices to improve the water resources security in the Formoso River Basin.

4. CONCLUSIONS

The Urubu River Basin is an important agricultural area for the state of the Tocantins, North of Brazil. The basin has faced water shortage due to a combination of factors, years of low levels of rainfall and high irrigation water demand, especially associated with soybean crops during the dry season (July and August). First, the work evaluated the WEAP hydrological modeling to obtain a reference flow for the Urubu River and part of the Dueré River, using the Rainfall Runoff method in WEAP. The analysis of the statistical performance results for the calibrated flows was Very Good (R^2) and Good (NSE).

The second stage of this work simulated the water balance in the Urubu River Basin using the WEAP model for a reference scenario including all of the irrigation water demand sites and evaluated the effect of alternative irrigation water demand management scenarios in the Urubu River Basin. The alternative scenarios were analyzed considering the objective to avoid environmental and economic impacts due to low levels of flow in the main channel. The unsustainable irrigation water demand in the region has proved to be a reflection of an inefficient irrigation system that jeopardizes aquatic life and economic activities in the Urubu River Basin.

In an ideal situation in where all farmers contribute and modernize their irrigation system, resulting in lower irrigation water demand (Scenario 1 - equal percentage reduction for all), the required demand reduction would be 35%, so that the river did not suffer any interruption of the flow rate and 45% to maintain at least $1,245\text{m}^3\text{ s}^{-1}$ at all times. The reduction is even greater when compared to Scenario 2, in which the simulation considered that part of the farmers did not contribute to the irrigation water demand reduction. For this condition, reductions of 40% and 45% were necessary, when 10% and 30%, respectively of the irrigators did not contribute to the demand management measures.

Finally, Scenario 3 illustrates that combining water demand reduction with anticipation of crop sowing (10 and 5 days) and observing agriculture sanitary regulations could be a good strategy for streamflow conservation in the Urubu River Basin. The alternative scenarios also showed that the active participation of all irrigators is essential to reduce conflicts and environmental impacts in the basin. It is also important to emphasize that the application of hydrological models to expand the knowledge of the water balance in a basin and analyze different scenarios, proved to be an important tool enabling the illustration of benefits from robust water demand policies and management in the basin.

The analysis highlighted the importance of water demand management practices in the Urubu River Basin, such as efficient and rational irrigation techniques, reduction of water losses in the irrigation network and channels, and selection of crops more adapted to the dry season. These practices should be adopted by all irrigators so that they do not overload only part of the farmers in the region, reducing the emergence of conflicts and making it possible to implement adequate water demand management in the region.

The simulation of the water balance in the Urubu River Basin presented challenges regarding the availability of data. Thus, the importance of hydrological monitoring and its expansion in the Formoso River Basin is also emphasized showing the benefits of research projects, such as the High-Level Management Project (GAN). The future use of these historical series with greater consistency may contribute to better management of water resources, strengthening the balance between environment and economic activities. It is also noteworthy

that with the greater availability of data in the future, the results of the present research should be reevaluated to confirm and evolve the water management practices in the basin.

5. ACKNOWLEDGEMENTS

Thanks to the "Rede de Pesquisa para Gestão de Alto Nível dos Recursos Hídricos na Bacia do Rio Formoso -TO", funded by CAPES-ANA, Programa de Apoio ao Ensino e à Pesquisa Científica e Tecnológica em Regulação e Gestão de Recursos Hídricos – Pró-Recursos Hídricos, call nº. 16/2017.

6. REFERENCES

- ABREU, M. C.; TONELLO, K. C. Disponibilidade e demanda hídrica na bacia do rio Sorocaba, Brasil: um alerta à gestão dos recursos hídricos. **Sociedade & Natureza**, v. 30, n. 3, p. 209-232, 2018. <https://doi.org/10.14393/SN-v30n3-2018-11>
- ADAPEC (Tocantins). Portaria nº 164 de 02/05/2016. **Diário Oficial [do] Estado TO**, Palmas, 5 maio 2016.
- ALBUQUERQUE, A. M.; FERREIRA, Y. B.; SILVA, S. B.; SALES, M. C. L. Balanço hídrico como ferramenta de gerenciamento de recursos hídricos: aplicação na área de influência direta do açude Castanhão – CE. **Revista da Casa da Geografia de Sobral**, v. 21, n. 2, p. 454-466, 2019. <https://doi.org/10.35701/rcgs.v21n2.601>
- ALMEIDA, A. H. B.; ALMEIDA, H. S. A.; OLIVEIRA, M. K. T. Perspectivas da gestão hídrica no semiárido brasileiro para irrigação. **Disciplinarum Scientia. Série: Naturais e Tecnológicas**, v. 22, n. 2, p. 119-132, 2021. <https://doi.org/10.37779/nt.v22i2.3489>
- ALVEZ, K. C. C. L. F.; VIOLA, M. R.; MELLO, C. R.; GIONGO, M.; COELHO, G. Precipitação provável na bacia hidrográfica do rio Formoso, Tocantins. **Water Resources and Irrigation Management**, v. 3, n. 2, p. 65-78, 2014.
- ALVEZ, K. C. C. L. F.; VIOLA, M. R.; MELLO, C. R.; GIONGO, M.; COELHO, G.; SANTOS, A. F. Distribuição da precipitação mensal, anual e máxima diária anual na bacia hidrográfica do rio Formoso, Tocantins. **Ambiência Guarapuava**, v. 12, n. 1, p. 49-70, 2016.
- ANA (Brasil). **Conjuntura dos recursos hídricos no Brasil 2020**: informe anual. Brasília, 2020. p. 118.
- ASITATIKIE, A. N.; GEBEYEHU, W. Z. Assessment of hydrology and optimal water allocation under changing climate conditions: the case of Megech river sub-basin reservoir, Upper Blue Nile Basin, Ethiopia. **Modeling Earth Systems and Environment**, v. 7, p. 2629-2642, 2021. <https://doi.org/10.1007/s40808-020-01024-0>
- BELTRÃO JÚNIOR, J. A.; COSTA, R. N. T.; LIMA, S. C. R. V.; IÑGUEZ, L. M.; SOUSA, P. G. R. Fornecimento relativo de irrigação como estratégia de gestão do distrito de irrigação. **Revista Brasileira de Agricultura Irrigada**, v. 11, n. 5, p. 1756–1762, 2017. <https://doi.org/10.7127/rbai.v11n500801>
- BERNARDI, E. C. S.; PANZIERA, A. G.; BURIOL, G. A.; SWAROWSKY, A. Bacia hidrográfica como unidade de gestão ambiental. **Disciplinarum Scientia, Ciências Naturais e Tecnológicas**, v. 13, n. 2, p. 159-168, 2012.

- BRASIL. Ministério da Agricultura, Pecuária e Abastecimento. **Valor Bruto de Produção Agropecuária**. Levantamento Sistemático da Produção Agrícola – LSPA. Brasília, Janeiro 2021.
- BRASIL. Ministério da Agricultura, Pecuária e Abastecimento. **Valor Bruto de Produção Agropecuária**. Levantamento Sistemático da Produção Agrícola – LSPA. Brasília, Janeiro 2022.
- ERMOLIEVA, T.; HAVLIK, P.; FRANK, S.; KAHIL, T.; BALKOVIC, J.; SKALSKY, R. *et al.* A Risk-Informed Decision-Making Framework for Climate Change Adaptation through Robust Land Use and Irrigation Planning. **Sustainability**, v. 14, p. 1430, 2022.
- FARIA, L. A.; PELÚZIO, J. M.; SANTOS, W. F.; SOUZA, C. M.; COLOMBO, G. A.; AFFÉRI, F. S. Características agronômicas de soja cultivadas na região central do Tocantins em diferentes épocas de semeadura. **Journal of Bioenergy and Food Science**, v. 5, n. 3, p. 85- 96, 2018. <https://doi.org/10.18067/jbfs.v5i3.192>
- FLEISCHMANN, A. S.; MATTIUZI, C. D. P.; KICH, E. M.; GONDIM, G.; PAIVA, A. R. R. Avaliação da seca de 2016 do Rio Javaés (bacia do Rio Araguaia) com uso de dados de múltiplos satélites. Anais. In: SIMPÓSIO BRASILEIRO DE SENSORIAMENTO REMOTO -SBSR, 18., 28-31 maio 2017, Santos, SP. **Anais[...]** São José dos Campos: INPE, 2017
- GAO, J.; CHRISTENSEN, P.; LI, W. Application of the WEAP model in strategic environmental assessment: Experiences from a case study in an arid/semi-arid area in China. **Journal of Environmental Management**, v. 198, Part 1, p. 363-371, 2017. <https://doi.org/10.1016/j.jenvman.2017.04.068>
- GORGOGNONE, A.; CRISCI, M.; KAYSER, R. H.; CHRETIES, C.; COLLISCHONN, W. A New Scenario-Based Framework for Conflict Resolution in Water Allocation in Transboundary Watersheds. **Water**, v. 11, p. 1174, 2019. <https://doi.org/10.3390/w11061174>
- IAC. **Relatório Fase B**. Palmas: Universidade Federal do Tocantins, 2017.
- IAC. **Gestão de Alto Nível**. Plano do Biênio 2018 -2019. Palmas: Universidade Federal do Tocantins, 2018.
- IBGE. **Indicadores IBGE**. Levantamento Sistemático da Produção Agrícola Estatística da Produção Agrícola. Rio de Janeiro, 2022.
- LAYANI, G; BAKHSHOODEH, M. Effects of climate change on the agricultural sector in the Kheirabad River Basin. **Journal of Agricultural Economics Research**, v. 13, n. 4, p. 208-223, 2021. <https://dx.doi.org/10.30495/jae.2021.21701.2030>
- MAGALHÃES, R. C.; BARP, A. R. B. Inovações metodológicas para construção de cenários estratégicos em bacias hidrográficas. **Revista de Administração e Inovação**, v. 11, n. 3, p. 200-226, 2014. <https://doi.org/10.11606/rai.v11i3.100221>
- MAGALHÃES FILHO, L. N. L.; MARINHO FILHO, G. M.; MACIEL, G. F.; DIAS, R. R.; REZENDE, C. S. A.; FIGUEROA, F. E. V. *et al.* Avaliação de Características Morfométricas da Bacia Hidrográfica do Rio Formoso - TO. **Revista de Ciências Ambientais**, v. 7, 2013. <http://dx.doi.org/10.18316/578>
- MAGALHÃES FILHO, L. N. L.; VERGARA, F. E.; RODRIGUES W. Cobrança pelo uso da água na bacia hidrográfica do rio Formoso - TO: Estudo de Viabilidade Financeira. **REGA**, v. 12, n. 1, p. 53-61, 2015. <http://dx.doi.org/10.18316/578>

- MCPHAIL, C.; MAIER H. R.; KWAKKEL, J. H.; GIULIANI, M.; CASTELLETTI, A.; WESTRA, S. Robustness Metrics: How Are They Calculated, When Should They Be Used and Why Do They Give Different Results? **Earth's Future**, v. 6, p. 169-191, 2018. <https://doi.org/10.1002/2017EF000649>
- MENDES, L. S. A. S.; SILVA NETO, T. A.; SOUSA, J. S. F. O.; SILVA NETO, C. A. S.; VASCONCELOS, M. B.; SALGUEIRO, A. R. G. N. L. *et al.* Diagnóstico da oferta hídrica do município de Russas – CE: Uma análise descritiva como subsídio à gestão sustentável dos recursos hídricos. **Revista Brasileira de Geografia Física**, v. 14, n. 3, p. 1612-1625, 2021.
- MHIRIBIDI, D.; NOBERT, J.; GUMINDOGA, W.; RWASOKA, D. T. Optimal water resource allocation modeling in the Lowveld of Zimbabwe. **Proceedings of IAHS**, v. 378, p. 67-72, 2018. <https://doi.org/10.5194/piahs-378-67-2018>
- MIRDASHTVAN, M.; NAJAFINEJAD, A.; MALEKIAN, A.; SA'DODDIN, A. Sustainable Water Supply and Demand Management in Semi-arid Regions: Optimizing Water Resources Allocation Based on RCPs Scenarios. **Water Resources Management**, v. 35, p. 5307-5324, 2021. <https://doi.org/10.1007/s11269-021-03004-0>
- MONTEIRO, J. E. B. A. **Agrometeorologia dos cultivos**: o fator meteorológico na produção agrícola. Brasília: INMET, 2009. p. 530.
- MORIASI, D. N.; GITAU, M. W.; PAI, N.; DAGGUPATI, P. Hydrologic and Water Quality Models: Performance Measures and Evaluation Criteria. **Transactions of the ASABE**, v. 58, n. 6, p. 1763-1785, 2015. <https://doi.org/10.13031/trans.58.10715>
- NARITA, D.; SATO, I.; OGAWADA, D.; MATSUMURA, A. Evaluating the Robustness of Project Performance under Deep Uncertainty of Climate Change: A Case Study of Irrigation Development in Kenya. **Climate Risk Management**, v. 36, 2022. <https://doi.org/10.1016/j.crm.2022.100426>
- NATURATINS. Portaria nº 300, de 12 de agosto de 2016. Dispõe sobre a suspensão de outorgas de recursos hídricos. Palmas, 2016. **Diário Oficial [do] Estado TO**, Palmas, n. 4689, 22 ago. 2016.
- NIKOO, M. R.; IZADY, A.; SALMAN, R.; AL-MAKTOUMI, A.; CHEN, M.; AL-ISMAILI, A. *et al.* A coupled water allocation simulation – optimization model to advance agricultural water management. **Arabian Journal of Geosciences**, n. 15, p. 397, 2022. <https://doi.org/10.1007/s12517-022-09692-1>
- NOON, A. M.; IBRAHIM, H. G.; SULAIMAN, S. O. Application of water evaluation and planning (WEAP) model for reuse of urban wastewater in Western Iraq. **AIP Conference Proceedings**, v. 2386, n. 1, 2022. <https://doi.org/10.1063/5.0067164>
- OLIVOS, L. M. O. **Sustentabilidade do uso dos recursos hídricos superficiais e subterrâneos no município de São Carlos-SP**. 2017. Dissertação (Mestrado) - Escola Politécnica, Universidade de São Paulo, São Paulo, 2017.
- QUINTINO, A. C.; ANDRADE, P. J.; SILVA, T. J.; CANEPPELE, M. A.; ABREU, J. G. Métodos de determinação de umidade nos solos de cerrado. **Enciclopédia Biosfera**, v. 11, n. 22, 2015. http://dx.doi.org/10.18677/Enciclopedia_Biosfera_2015_193

- REIS, A. F. de B; ALMEIDA, R. E. M.; LAGO, B. C.; TRIVELIN, P.C.; LINQUIST, B.; FAVARIN, J. L. Aerobic rice system improves water productivity, nitrogen recovery and crop performance in Brazilian weathered lowland soil. **Field Crops Research**, v. 218, p. 59-68, 2018. <https://doi.org/10.1016/j.fcr.2018.01.002>
- SANTOS, A. B.; RABELO, R. R. **Informações técnicas para a cultura do arroz irrigado no Estado do Tocantins**. Santo Antônio de Goiás: Embrapa Arroz e Feijão, 2008. 136 p. Available at: <http://www.infoteca.cnptia.embrapa.br/infoteca/bitstream/doc/216530/1/doc218.pdf>. Access May 4, 2019.
- STOCKHOLM ENVIRONMENT INSTITUTE. **Tutorial**: a collection of stand-alone modules to aid in learning the WEAP software. Stockholm, 2016. 286p.
- SILVA, E. M. da; AZEVEDO, J. A.; RAUBER, J. C.; REATTO, A. **Caracterização físico-hídrica e hidráulica de solos do bioma cerrado submetidos a diferentes sistemas de preparo**. Planaltina, DF: Embrapa Cerrados, 2003. 22p. (Embrapa Cerrados. Boletim de Pesquisa e Desenvolvimento, 101).
- SILVA, S. M.; SOUZA FILHO, F. A.; AQUINO, S. H. S. Avaliação do risco da alocação de água em período de escassez hídrica: o caso do Sistema Jaguaribe–Metropolitano. **Revista Engenharia Sanitária e Ambiental**, v. 22, n. 4, 2017. <https://doi.org/10.1590/S1413-41522017161303>
- SRINIVASAN, E.; MEDIDAS, R.; FEAR, A. ELLEY, G. Making the invisible visible: Co-learning guided the development of an operational tool for irrigation management. **Agriculture Water Management**, v. 264, n. 107492, 2022. <https://doi.org/10.1016/j.agwat.2022.107492>
- TOCANTINS. SEPLAN. **Perfil do Agronegócio Tocantinense**. Relatório Final. Palmas: FAPTO, 2016. p. 145.
- TUNDISI, J. G. Governança da água. **Revista UFMG**, v. 20, n. 2, p. 222-235, 2013. <https://doi.org/10.35699/2316-770X.2013.2698>
- VALENTE, C. R.; LATRUBESSE, E. M.; FERREIRA, L. G. Relationships among vegetation, geomorphology and hydrology in the Bananal Island tropical wetlands, Araguaia River basin, Central Brazil. **Journal of South American Earth Sciences**, v. 46, p. 15, 2013. <https://doi.org/10.1016/j.jsames.2012.12.003>
- VERGARA, H. F; REIS, F. C; MAGALHÃES FILHO, L. N. L; REZENDE, C. S. A. Proposta de vazão de referência Q90 para o Rio Formoso na bacia do Araguaia. **Engenharia Ambiental**, v. 10, n. 1, p. 84-102, 2013.